

**Identification of the causal agent, epidemiology and forecast
of purple spot (*Stemphylium vesicarium*) on asparagus
(*Asparagus officinalis* L.)**

Von der Naturwissenschaftlichen Fakultät der
Gottfried Wilhelm Leibniz Universität Hannover

zur Erlangung des Grades

Doktor der Gartenbauwissenschaften (Dr. rer. hort.)

genehmigte Dissertation

von

Henrik Enno Bohlen-Janßen, M. Sc.

2018

Referent: Prof. Dr. Bernhard Hau

Korreferent: Prof. Dr. Hartmut Stützel

Tag der Promotion: 01.03.2018

Meinen Lieben

Abstract

The aim of this thesis is to analyse the asparagus disease “purple spot” and to develop a forecasting model, called SIMSTEM (**S**imulation of *Stemphylium*), to be used as a tool in integrated pest management. For this purpose, the exact identification of the pathogen at an early stage is essential.

Although the fungal species *Stemphylium vesicarium* has been identified as the causal pathogen of purple spot worldwide, the closely related species *Stemphylium botryosum* has also been detected in Germany, Japan, and Greece. Due to phenotypical similarities, morphological differentiation between the species is very difficult, and therefore a suitable alternative method to distinguish these species was needed. A molecular- and genetics-based method to differentiate *S. vesicarium* and *S. botryosum* was developed to identify the causal agent of purple spot in Germany. The most significant difference between the species was a 3 kb intron present in the cytochrome b region of *S. botryosum* that was absent in *S. vesicarium*. Besides qualitative analysis by the PCR reaction, the frequencies of the species were directly detected from infected asparagus samples via qPCR. In all 232 German samples collected between 2010 and 2014, only *S. vesicarium* was identified. The life cycle of *S. vesicarium* can be divided into the monocyclic (ascospores) and polycyclic (conidia) phases, which were both modelled using biological data from field and laboratory trials. Spore flight, germination, and germ tube length were measured separately for both phases. In addition, we modelled the number of lesions formed by conidia, as a measure of disease efficiency, and the mycelium growth.

Yearly ascospore flight was monitored by spore traps. In 2014 to 2016, ascospores flew from March to July, but were mostly released in early May. The cumulative percentage of trapped ascospores was modelled by a logistic, Gompertz and Chapman Richards function depending on the daily temperature sum (base 5 °C) and daily rain amount ($RA > 0.0$ and 0.2 mm). The best fit was obtained for the Chapman Richards function with $RA > 0.0$ mm. Yearly conidial flight was also measured with spore traps. In the years 2013 to 2015, conidial flight began in mid-July, but only after mid-August to early September the number of trapped conidia was very pronounced. The cumulative percentage of trapped conidia was modelled by a logistic function depending on the daily temperature sum (base 0 °C) and daily rain amount ($RA > 0.2$ mm). When both phases were compared, a gap from June to July was observed, during which the fungus released no or very few spores.

The germination of ascospores, depending on leaf wetness duration and temperature, was investigated in trials on water agar. A fitted Chapman Richards function with a temperature-dependent capacity and rate described germination adequately with an optimal temperature of 31.04 °C. The conidial germination data were modelled by a generalised beta-modified Chapman Richards function with a clearly lower optimum temperature of 23.3 °C. Considering the rapid germination rate and the wide temperature range of both phases, germ tube length was introduced as an additional factor for lesion development, resulting in a more specific growth-limiting factor for forecasting. The optimal temperature of germ tube length for ascospores (30.4 °C) was modelled by a generalised beta-linear function while that for conidia (28.7 °C) was modelled by a generalised beta-power function.

To include the factor host plant, the number of lesions was recorded on green asparagus spears after inoculation of conidia from two strains. This measure of disease efficiency was modelled by a generalised beta function with an optimum temperature of 21.9 °C and the narrowest optimum temperature range of all model parts. After a lesion is formed, the spread of the fungus in plant tissue depend on mycelium growth. The mycelium growth of four strains in a petri dish experiment was modelled by a generalised beta function with an optimum temperature of 24.7 °C.

All modelled aspects of both phases were combined in the algorithm of SIMSTEM, which is currently in the testing phase (2018). The model algorithm was developed by the Central Institute for Decision Support Systems in Crop Protection (ZEPP) and integrated into the agricultural internet platform for the integrated plant production ISIP (www.isip.de). The model can be used flexibly, because it can forecast the beginning of the epidemic, the time of the first treatment, and the disease progression (as a proportion of the diseased leaf area), and can signal periods with high disease pressure via a traffic light system. SIMSTEM uses area-specific weather data, and all model rates are calculated using hourly weather parameters of temperature (in °C), relative humidity (in %), and rainfall (in mm). In Germany, the later-occurring polycyclic phase has emerged as clearly more important for forecasting and control. Ascospore flight is often completed before the end of harvest, and treatment with fungicides against the monocyclic phase may be irrelevant in many production sites in Germany. However, the monocyclic phase may also be a critical factor in some seasons, such as in the cases of earlier harvest ends and non-harvested young plants.

Keywords: Asparagus, Forecast, SIMSTEM, Purple spot, *Stemphylium vesicarium*

Zusammenfassung

Ziel dieser Arbeit ist die Beschreibung und Modellierung der Spargellaubkrankheit ‘Purple Spot‘ zur Neuentwicklung eines Prognosemodells, Simulation von *Stemphylium* (SIMSTEM), als Werkzeug des integrierten Pflanzenschutzes. Zu diesem Zweck ist zudem die Identifizierung des Erregers im Vorfeld wesentlich.

Obwohl weltweit der Pilz *Stemphylium vesicarium* als Erreger identifiziert wurde, ist in Deutschland, Japan und Griechenland die eng verwandte Art *S. botryosum* beschrieben worden. Die morphologische Differenzierung dieser Arten ist aufgrund phänotypischer Ähnlichkeiten sehr schwierig und die Entwicklung einer geeigneten Alternative zur Unterscheidung war wesentlich. Um den in Deutschland vorherrschenden Erreger der Spargellaubkrankheit zu identifizieren, wurde zunächst eine molekulargenetische Differenzierungsmethode entwickelt. Der bedeutendste Unterschied war ein 3 kb Intron in der Cytochrom b Region, welches in *S. botryosum* jedoch nicht in *S. vesicarium* nachgewiesen werden konnte. Neben der qualitativen Analyse (PCR-Reaktion) wurde zudem die Häufigkeit beider Arten mit Hilfe einer qPCR direkt aus infizierten Spargelproben ermittelt. In allen 232 deutschen Proben, die von 2010 bis 2014 gesammelt wurden, konnte dabei ausschließlich *S. vesicarium* identifiziert werden.

Der Lebenszyklus von *S. vesicarium* ist in die mono- (Askosporen) und die polyzyklische (Konidien) Phase geteilt, welche mittels biologischer Daten aus Feld- und Laborversuchen modelliert werden konnten. Sporenflug, Keimung und Keimschlauchlänge wurden für beide Phasen separat gemessen. Modelliert wurden zudem die von Konidien gebildete Läsionensanzahl als Maß für die Krankheitseffizienz und das Myzelwachstum.

Der jährliche Askosporenflug wurde durch Sporenfallen ermittelt. Askosporen flogen in 2014 - 2016 von März bis Juli, die meisten waren bereits bis Anfang Mai freigesetzt. Der kumulative Prozentsatz wurde in Abhängigkeit der täglichen Temperatursumme (Basis 5 °C) und der täglichen Regenmenge ($RA > 0,0$ und $0,2$ mm) durch die logistische, Gompertz und Chapman Richards Funktion modelliert. Die beste Anpassung gelang mittels Chapman Richards Funktion bei $RA > 0,0$ mm. Der Konidienflug wurde mit Sporenfallen ermittelt. In 2013 - 2015 begannen Flugereignisse ab Mitte Juli, aber erst nach Mitte August Anfang September, war der Konidienflug ausgeprägt. Der kumulative Prozentsatz gefangener Konidien wurde, abhängig von täglicher Temperatur- (Basis 0 °C) und Regenmenge ($RA > 0,2$ mm), mit einer logistischen Funktion modelliert. Zwischen den

Flugperioden, von Juni bis Juli, bestand eine Lücke, in der der Pilz keine bis wenig Sporen freisetzte.

Die Keimung von Ascosporen wurde, abhängig von der Blattnässedauer und der Temperatur, in Versuchen auf Wasser-Agar untersucht. Eine Chapman Richards Funktion mit temperaturabhängiger Kapazität und Rate beschreibt die Keimung adäquat, mit einem Temperaturoptimum von 31,04 °C. Die Keimungsdaten der Konidien wurden dagegen mit einer verallgemeinerten Beta-modifizierten Chapman Richards Funktion modelliert, mit einem Optimum von 23,3 °C. Aufgrund der rapiden Keimung und des weiten Temperaturbereichs in beiden Phasen, wurde die Keimschlauchlänge als zusätzlicher Faktor für die Läsionsentwicklung herangezogen, was in einem spezifischeren, wachstumsbegrenzenden Faktor für die Prognose resultierte. Die optimale Temperatur der Keimschlauchlänge für Ascosporen (30,4 °C), wurde durch eine verallgemeinerte Beta-linear Funktion und für Konidien (28,7 °C) durch eine Beta-Power Funktion ermittelt.

Um den Faktor Wirtspflanze einzuschließen, wurde als Maß für die Krankheitseffizienz die Anzahl der Läsionen von Konidien für zwei Stämme an grünen Spargelstangen untersucht und durch eine verallgemeinerte Beta Funktion mit einem Optimum bei 21,9 °C beschrieben. Das Ergebnis zeigte das engste Temperaturoptimum aller Modellteile. Im Pflanzengewebe ist die Ausbreitung des Pilzes vom Myzelwachstum abhängig. Das Myzelwachstum von 4 Stämmen wurde durch eine verallgemeinerte Beta Funktion mit Daten aus einem Petrischalen-Experiment modelliert und hat sein Optimum bei 24,7 °C.

Alle Aspekte beider Phasen sind im SIMSTEM Algorithmus enthalten. Dieser wurde von der Zentralstelle der Länder für EDV-gestützte Entscheidungshilfen und Programme im Pflanzenschutz (ZEPP) entwickelt und im Internetauftritt des Informationssystems für Integrierte Pflanzenproduktion (www.isip.de) integriert. Das Modell ist flexibel nutzbar, da Epidemiebeginn, Erstbehandlung und Krankheitsfortschritt prognostiziert werden können und die Signalisierung von Perioden mit hohem Krankheitsdruck über ein Ampelsystem möglich sind. SIMSTEM nutzt standortspezifische Wetterdaten und die Modelraten werden mit den stündlichen Werten der Temperatur (in °C), relativer Feuchte (in %) und Niederschlag (in mm) berechnet. Die spätere polyzyklische Phase ist in Deutschland für die Prognose und Kontrolle weitaus bedeutender. Der Askosporenflug ist oft bereits vor dem Ernteende abgeschlossen und Fungizidbehandlungen gegen die monocyclische Phase können irrelevant sein. Diese Phase kann jedoch in einigen Jahren bedeutend sein, zum Beispiel bei früherem Ernteende und in nicht geernteten Jungpflanzenanlagen.

Schlagwörter: Prognose, Purple spot, SIMSTEM, Spargel, *Stemphylium vesicarium*

Statement of contributions

Graf, S., Bohlen-Janssen, H., Miessner, S., Wichura, A. and Stammler, G. (2016) Differentiation of *Stemphylium vesicarium* from *Stemphylium botryosum* as causal agent of the purple spot disease on asparagus in Germany. *Eur. J. Plant. Pathol.*, 144 (2), 411-418. doi.org/10.1007/s10658-015-0777-6

Contribution:

Graf, S.: Molecular work, data collection and analysis, manuscript preparation

Bohlen-Janssen, H.: Sample collection and critical revision of the manuscript

Miessner, S.: Experimental design

Wichura, A.: Critical revision of the manuscript

Stammler, G.: Experimental design and critical revision of the manuscript

Status: published in the European Journal of Plant Pathology

Presented in Chapter 2

Bohlen-Janssen, H., Racca, P., Hau, B. and Wichura, A. (2018) Modelling some aspects of the monocyclic phase of *Stemphylium vesicarium*, the pathogen causing purple spot on asparagus (*Asparagus officinalis* L.). *Eur. J. Plant. Pathol.*, doi.org/10.1007/s10658-018-1455-2

Contribution:

Bohlen-Janssen, H.: Experimental design, data collection and analysis, modelling and manuscript preparation

Racca, P.: Experimental design, modelling and critical revision of data and manuscript

Hau, B.: Experimental design, modelling and critical revision of data and manuscript

Wichura, A.: Experimental design and critical revision of data and manuscript

Status: published in the European Journal of Plant Pathology

Presented in Chapter 3

Bohlen-Janssen, H., Racca, P., Hau, B. and Wichura, A. (2018) Modelling the effects of temperature and wetness on the polycyclic phase of *Stemphylium vesicarium*, the pathogen causing purple spot on asparagus (*Asparagus officinalis* L.) *J. Phytopathol.*, doi.org/10.1111/jph.12691

Contribution:

Bohlen-Janssen, H.: Experimental design, data collection and analysis, modelling and manuscript preparation

Racca, P.: Experimental design, modelling and critical revision of data and manuscript

Hau, B.: Experimental design, modelling and critical revision of data and manuscript

Wichura, A.: Experimental design and critical revision of data and manuscript

Status: published in the Journal of Phytopathology

Presented in Chapter 4

Racca, P., Bohlen-Janssen, H., Hau, B. and Wichura, A. (2018) SIMSTEM - a model to forecast the epidemic of purple spot (*Stemphylium vesicarium*) on asparagus (*Asparagus officinalis* L.).

Contribution:

Racca, P.: Development of the SIMSTEM algorithm, validation and manuscript preparation

Bohlen-Janssen, H.: Data collection, modelling and manuscript preparation

Hau, B.: Modelling, critical revision of data and manuscript

Wichura, A.: Critical revision of data and manuscript

Status: submission planned in the EPPO Bulletin

Presented in Chapter 5

Table of content

Abstract	I
Zusammenfassung	IV
Statement of contributions.....	VII
Table of content	IX
List of figures	XII
List of tables	XVI
1. Introduction	1
2. Differentiation of <i>Stemphylium vesicarium</i> from <i>Stemphylium botryosum</i> as causal agent of the purple spot disease on asparagus in Germany	6
2.1. Abstract	6
2.2. Introduction.....	6
2.3. Materials and methods	8
2.3.1. Origin of isolates	8
2.3.2. Analyses of the DNA marker regions.....	9
2.3.3. Molecular genetic species identification	9
2.3.4. Species-specific identification of <i>Stemphylium</i> spp.	10
2.3.5. qPCR based differentiation of <i>S. vesicarium</i> and <i>S. botryosum</i>	11
2.3.6. Validation of the developed differentiation methods	11
2.3.7. Monitoring of Asparagus fields.....	11
2.4. Results.....	12
2.4.1. Species identification.....	12
2.4.2. Cyt b of <i>S. vesicarium</i> and <i>S. botryosum</i>	12
2.4.3. Differentiation of <i>S. vesicarium</i> from <i>S. botryosum</i>	12
2.4.4. Analysed asparagus samples	14
2.5. Discussion.....	14

3. Modelling some aspects of the monocyclic phase of <i>Stemphylium vesicarium</i>, the pathogen causing purple spot on asparagus (<i>Asparagus officinalis</i> L.)	17
3.1. Abstract	17
3.2. Introduction.....	17
3.3. Materials and methods	19
3.3.1. Effects of temperature and rain amount on ascospore flight	19
3.3.2. Effects of temperature and wetness duration on germination and germ tube length	21
3.3.3. Statistical software.....	23
3.4. Results.....	23
3.4.1. Effects of temperature and rain amount on ascospore flight.....	23
3.4.2. Effects of temperature and wetness duration on germination	26
3.4.3. Effects of temperature and wetness duration on germ tube length.....	29
3.5. Discussion.....	32
4. Modelling the effects of temperature and wetness on the polycyclic phase of <i>Stemphylium vesicarium</i>, the pathogen causing purple spot on asparagus (<i>Asparagus officinalis</i> L.).....	38
4.1. Abstract	38
4.2. Introduction.....	38
4.3. Materials and methods	40
4.3.1. Spore traps and cumulative percentage of trapped conidia	40
4.3.2. Germination and germ tube length	42
4.3.3. Number of lesions as a measure for disease efficiency	44
4.3.4. Mycelium growth	44
4.3.5. Statistical software.....	45
4.4. Results.....	45
4.4.1. Spore traps and cumulative percentage of trapped conidia	45
4.4.2. Germination	48

4.4.3. Germ tube length	51
4.4.4. Number of lesions as a measure for disease efficiency	54
4.4.5. Mycelium growth	55
4.5. Discussion and conclusions	57
5. SIMSTEM - a model to forecast the epidemic of purple spot (<i>Stemphylium vesicarium</i>) on asparagus (<i>Asparagus officinalis</i> L.).....	62
5.1. Abstract	62
5.2. Introduction.....	62
5.3. Materials and methods	64
5.3.1. Model description	64
5.3.2. Model validation.....	70
5.3.3. Weather data	70
5.3.4. Statistical software.....	71
5.4. Results.....	71
5.4.1. Model output	71
5.4.2. Subjective validation	72
5.4.3. Statistical validation	76
5.4.4. Applying SIMSTEM in practice.....	77
5.5. Discussion	82
6. General discussion.....	85
7. References	92
Acknowledgement.....	XIX

List of figures

Figure 2.1 Intron-exon organization of the <i>cyt b</i> gene (partial) of <i>S. vesicarium</i> and <i>S. botryosum</i>	14
Figure 2.2 Principle of the qualitative differentiation of the <i>Stemphylium spp.</i> . 1: <i>S. vesicarium</i> , 2: <i>S. botryosum</i> , 3: 1:1 Mixture of <i>S. vesicarium</i> and <i>S. botryosum</i> , 4: <i>A. alternata</i> , 5: <i>B. cinerea</i> , 6: <i>P. triticina</i> , 7: NTC, M: 1 kb DNA Ladder	15
Figure 2.3 Distribution of analysed asparagus samples and <i>Stemphylium</i> -isolates.....	16
Figure 3.1 Weekly trapped ascospores [per 0.42 cm ²] of <i>S. vesicarium</i> with daily mean temperature [in °C] and daily rainfall [in mm] from March 1 st at (a) Hannover-Ahlem 2014, (b) Hannover-Ahlem 2015, (c) Fuhrberg 2015 and (d) Schifferstadt 2016 ..	24
Figure 3.2 Cumulative percentage of trapped ascospores of <i>S. vesicarium</i> [in %] that is modelled by a Chapman Richards function (Eq. 3.3) depending on <i>SumT</i> (Base 5 °C and <i>RA</i> > 0.0) from February 1 st (points = data, line = fitted Eq. 3.3 with parameter values from Table 3.1 and dotted line = lower and upper confidence limit (95 %))	26
Figure 3.3 Germination of ascospores of <i>S. vesicarium</i> <i>GA</i> [in %] depending on the leaf wetness duration <i>WD</i> for different temperature levels (points = data, line = fitted Eq. 3.4 with parameter values from Table 3.2)	27
Figure 3.4 Modelled germination of ascospores of <i>S. vesicarium</i> <i>GA</i> [in %] depending on temperature <i>T</i> and the leaf wetness duration <i>WD</i> (points = data, surface = fitted Eq. 3.5 with parameter values of Table 3.3).....	29
Figure 3.5 Germ tube length of ascospores of <i>S. vesicarium</i> <i>LA</i> [in µm] depending on the leaf wetness duration <i>WD</i> for temperature levels of 5, 10, 15, 20, 25 and 30 °C (points = data and line = fitted linear Eq. 3.6 with parameter values of Table 3.4).....	30
Figure 3.6 Modelled $b_{LA}(T)$ of the germ tube length of ascospores of <i>S. vesicarium</i> depending on temperature <i>T</i> (points = estimated data for b_{LA} from Table 3.4 and line = fitted Eq. 3.7 with parameter values from Table 3.5)	31

Figure 3.7 Modelled germ tube length of ascospores of <i>S. vesicarium</i> LA [in μm] depending on temperature T and the leaf wetness duration WD (points = data and surface = fitted Eq. 3.8 with parameter values from Table 3.6)	32
Figure 3.8 Conidia of <i>S. vesicarium</i> formed directly on pseudothecia on plant debris..	35
Figure 4.1 Weekly trapped <i>S. vesicarium</i> conidia [per 0.42 cm^2] illustrated with daily temperature [in $^{\circ}\text{C}$], daily rainfall [in mm], and irrigation amount [in mm] at Fuhrberg 2013 (a), Fuhrberg 2014 (b), Hannover-Ahlem 2014 (c), Fuhrberg 2015 (d) and Hannover-Ahlem 2015 (e).....	46
Figure 4.2 Cumulative percentage of trapped <i>S. vesicarium</i> conidia [in %] depending on $\text{Sum}T$ (base 0 $^{\circ}\text{C}$ and $RA > 0.2$ mm) starting on 1 st May (points = data; line = fitted Eq. 4.1 with parameter values from Table 4.1; dotted line = lower and upper confidence limits (95 %)).....	48
Figure 4.3 Germination of conidia of <i>S. vesicarium</i> GC [in %] depending on leaf wetness duration WD at temperature levels of 5 $^{\circ}\text{C}$, 10 $^{\circ}\text{C}$, 15 $^{\circ}\text{C}$, 20 $^{\circ}\text{C}$, 25 $^{\circ}\text{C}$, and 30 $^{\circ}\text{C}$ (triangles = data of St.sp.25.9.13.A; points = data of St.sp.25.9.13.F; line = fitted Eq. 4.4 with parameter values from Table 4.2)	50
Figure 4.4 Modelled germination of conidia of <i>S. vesicarium</i> GC [in %] depending on temperature T and leaf wetness duration WD (points = mean value of two strains; surface = fitted Eq. 4.6 with parameter values from Table 4.3)	51
Figure 4.5 Germ tube length of conidia of <i>S. vesicarium</i> LC [in μm] depending on leaf wetness duration WD for temperature levels of 15 $^{\circ}\text{C}$, 20 $^{\circ}\text{C}$, 25 $^{\circ}\text{C}$, and 30 $^{\circ}\text{C}$ (triangles = data of St.sp.25.9.13.A; points = data of St.sp.25.9.13.F; line = fitted Eq. 4.7 with parameter values from Table 4.4)	53
Figure 4.6 Modelled germ tube length of conidia of <i>S. vesicarium</i> LC [in μm] depending on temperature T and leaf wetness duration WD (points = mean value of two strains; surface = fitted Eq. 4.8 with parameter values from Table 4.5)	54
Figure 4.7 Effect of temperature T on the number of lesions L [in % of the maximum number at 20 $^{\circ}\text{C}$] counted 5 d after the inoculation of conidia of two different <i>S. vesicarium</i> strains on green asparagus spears (points = data; line = fitted Eq. 4.5 with parameter values from Table 4.6; MV = mean value)	55

Figure 4.8 Modelled mycelium growth MG of four different <i>S. vesicarium</i> strains [in %] depending on temperature T (points = data; line = fitted Eq. 4.5 with parameter values from Table 4.7; MV = mean value)	56
Figure 4.9 Comparison of the effect of temperature T on the four observed parts of the polycyclic phase of <i>S. vesicarium</i>	59
Figure 5.1 Values of infection probabilities β_A and β_C for the weather station Hannover in the period between 1 st of June and 31 st of October, 2014	71
Figure 5.2 SIMSTEM model output of the different disease categories. Weather station Hannover, 2014, period between the 1 st of June and the 31 st of October. L = latent disease proportion; I = infectious disease proportion; R = removed disease proportion; Y = total disease proportion; V = visible disease proportion	72
Figure 5.3 Assessed disease severity (DS) compared with visible disease proportion simulated by the SIMSTEM model (line = simulated V , point = assessed DS value with 95 % confidence interval). See Table 5.1 for the location A, B, C and years	73
Figure 5.4 Assessed disease severity (DS) compared with visible disease proportion simulated by the SIMSTEM model (line = simulated V , point = assessed DS value with 95 % confidence interval). See Table 5.1 for the location D, E, F and years .	74
Figure 5.5 Assessed disease severity (DS) compared with visible disease proportion simulated by the SIMSTEM model (line = simulated V , point = assessed DS value with 95 % confidence interval). See Table 5.1 for the location G1, G2, G3 and years	75
Figure 5.6 Validation of the SIMSTEM model using regression analysis	76
Figure 5.7 Hypothetical threshold for the simulation of the disease appearance in the fields, comparison of assessed DS data (0-0.05 DS) with simulated V	78
Figure 5.8 Hypothetical threshold for the simulation of the date of the first treatment, comparison of assessed DS data (0.05-0.1 DS) with simulated V	78
Figure 5.9 Boxplot analysis of the relative disease increase r_L data to determine two risk thresholds for the traffic light system based on the median and the upper quartile	79

Figure 5.10 Simulation of disease proportion V and relative disease increase r_L for the weather station Bergen, year 2006.....	80
Figure 5.11 Simulation of disease proportion V and relative disease increase r_L for the weather station Bergen, year 2008.....	80
Figure 5.12 Simulation of disease proportion V and relative disease increase r_L for the weather station Hannover, year 2009.....	81
Figure 5.13 Simulation of disease proportion V and relative disease increase r_L for the weather station Hannover, year 2014.....	81

List of tables

Table 2.1 <i>Stemphylium</i> Isolates investigated in this study	10
Table 3.1 Estimated parameter values for the logistic, Gompertz, and Chapman Richards functions (Eq. 3.1-3.3) for the cumulative percentage of trapped ascospores of <i>S. vesicarium</i> (r_{LA} , r_{GA} , and r_{CA} = rate parameters for the logistic, Gompertz, and Chapman Richards function, respectively; y_0 = y-intercept; m = shape parameter of the Chapman Richards function; $n = 81$).	25
Table 3.2 Estimated parameter values for the Chapman Richards function (Eq. 3.4) for the germination of ascospores of <i>S. vesicarium</i> GA (in %) depending on leaf wetness duration WD for temperatures of 5, 10, 15, 20, 25, and 30 °C (GA_{max} = maximum germination of ascospores (in %); r_{GA} = rate parameter (h^{-1}); m = shape parameter).	28
Table 3.3 Estimated parameter values for the modified function (Eq. 3.5) for the germination of ascospores of <i>S. vesicarium</i> GA (in %) depending on the temperature T and leaf wetness duration WD (a_k and b_k = parameters of the linear temperature function $GA_{max}(T)$; b_r = proportionality factor for the temperature function $r_{GA}(T)$; a_m = shape parameter of the Chapman Richards function).	28
Table 3.4 Estimated slope b_{LA} parameter values (in $\mu m h^{-1}$) for the linear function (Eq. 3.6) for the germ tube length of ascospores of <i>S. vesicarium</i> depending on the leaf wetness duration WD at temperatures 5 °C, 10 °C, 15 °C, 20 °C, 25 °C, and 30 °C	31
Table 3.5 Estimated parameter values for the generalized beta function (Eq. 3.7)* for the slope b_{LA} of the germ tube length (in $\mu m h^{-1}$) of ascospores of <i>S. vesicarium</i> depending on the temperature T (b_{LAopt} = slope of germ tube length at T_{opt} ; T_{opt} = optimal temperature (in °C); n = shape parameter).	31
Table 3.6 Estimated parameter values for the generalized beta-linear function (Eq. 3.8)* for the germ tube length of ascospores of <i>S. vesicarium</i> LA (in $\mu m h^{-1}$) depending on the temperature T and leaf wetness WD (b_{LAopt} = slope of germ tube length (in μm) at T_{opt} ; T_{opt} = optimal temperature (in °C); n = shape parameter).	32

Table 4.1 Estimated parameter values of the logistic function (Eq. 4.1) for the cumulative percentage of trapped <i>S. vesicarium</i> conidia (in %) (y_0 = y-intercept; r_{LC} = rate parameter of the logistic function, $n = 82$).....	47
Table 4.2 Estimated parameter values of the Chapman Richards function (Eq. 4.4) of the mean germination value of conidia of two <i>S. vesicarium</i> strains GC (in %) depending on leaf wetness duration WD at temperature levels of 5 °C, 10 °C, 15 °C, 20 °C, 25 °C and 30 °C (GC_{max} = maximum germination (in %); r_{GC} = rate parameter; m = shape parameter)	49
Table 4.3 Estimated parameter values of the modified generalized beta-Chapman Richards function (Eq. 4.6)* for the mean germination value of conidia of two <i>S. vesicarium</i> strains GC (in %) depending on temperature T and leaf wetness duration WD (T_{opt} = optimal temperature (in °C); n = shape parameter of the beta function; a_r = intercept of the linear temperature function of $r_{GC}(T)$; b_r = slope parameter of the linear temperature function of $r_{GC}(T)$; m = shape parameter of the Chapman Richards function).....	51
Table 4.4 Estimated parameter values of a power function (Eq. 4.7) of the mean germ tube length value of conidia of two <i>S. vesicarium</i> strains LC (in μm) depending on leaf wetness duration WD for temperature levels of 15 °C, 20 °C, 25 °C and 30 °C (a = scaling factor of the power function; d = exponent)	52
Table 4.5 Estimated parameter values of the generalized beta-power function (Eq. 4.8)* for the mean germ tube length value of conidia of two <i>S. vesicarium</i> strains LC (in μm) depending on temperature T and leaf wetness duration WD (a_{opt} = scaling factor of the power function at T_{opt} ; T_{opt} = optimal temperature (in °C); n = shape parameter of the generalized beta function; d = exponent of the power function)	53
Table 4.6 Estimated parameter values of the generalized beta function (Eq. 4.5)* for number of lesions L (in %) of 2 different <i>S. vesicarium</i> strains depending on temperature T (T_{opt} = optimal temperature (in °C); n = shape parameter).....	55
Table 4.7 Estimated parameter values of the generalized beta function (Eq. 4.5)* for the mycelium growth MG of 4 different <i>S. vesicarium</i> strains relative to the maximum (in %) depending on temperature T (T_{opt} = optimal temperature (in °C); n = shape parameter)	56

Table 5.1 Locations, years, varieties and weather stations used for the model validation	70
Table 5.2 Validation of the SIMSTEM model. Hypotheses test of regression parameters: For the intercept, the hypotheses are H_0 , that the intercept = 0 and H_1 , that the intercept $\neq 0$. For the slope, the hypotheses are H_0 , that the slope = 1 and H_1 , that the slope $\neq 1$ (Teng 1981)	77
Table 5.3 Validation of the SIMSTEM model with non-parametric Kolmogorov-Smirnov test, shares (in %) of the significance ($p < 0.05$)	77

1. Introduction

The genus *Asparagus* includes 300 species distributed over three subgenera, *Asparagus*, *Protasparagus*, and *Myrsiphyllum* (Clifford and Conran 1987; Tomassoli et al. 2012). Modern taxonomic studies classify the genus *Asparagus* into the family Asparagaceae and the order Asparagales (Chase et al. 2009). *Asparagus officinalis* L. is economically the most important species worldwide (Tomassoli et al. 2012). It is perennial, dioecious, and occasionally occurs as hermaphrodite individuals (Lee et al. 1996; Ainsworth 2000). In 2009, asparagus was reported to be cultivated in 62 countries with a yield of 760,000 t per year. The total cropland area devoted to asparagus is 195,000 ha, 35.5 % of which is in Asia, 34 % in North and South America, and 29 % in Europe (Benson 2009). In 2014, the German crop area was reported to be 25,335.7 ha (20,122 ha in yield) with a harvest volume of 114,090.1 t (StBA (Statistisches Bundesamt) 2015). Asparagus was initially used for medical purposes before it was eaten as food; today, it is recognized for its wealth of vitamins, minerals, and fibre content (Amaro-López et al. 1998; Sun and Powers 2007). While green asparagus is highly popular in the USA, white asparagus is in demand in Western Europe (Benson 2009). White and green asparagus can be obtained from the same plant, although some varieties are more suited to specific cultivation methods (Feller et al. 2012).

Asparagus presents four plant parts: the storage roots, the fibrous roots, the rhizome, and the shoots. If the shoots are not cut after harvest, they form lateral shoots from which phylloclades emerge (Weinheimer 2008). During the summer, the phylloclades produce assimilates, which are moved to subterranean storage organs. Under German cultivation conditions, the shoots begin to mature in the autumn. Maturation induction is triggered under Central European conditions by a temperature impulse and under tropical conditions by water deficiency (Krug 1996; 1998; 1999a; 1999b). After the winter repose, the buds begin to sprout once more. Shoot growth begins on a larger scale when the threshold temperature of 12 °C is exceeded near the crown (Hartmann 1989; Vogel 1996).

In asparagus production, yield quantity and quality determine economic success. The highest revenues can be achieved in Germany with a quality grade of 16-26 mm in diameter (Weinheimer 2008). Wilson et al. (2008) explained that asparagus yield is the result of a complex sequence of physiological processes influenced by the environment and management in both the current and previous years. Yield depends on the ability of the

storage roots to accumulate carbohydrates, which are produced by fern activity in the season before spear harvest and, possibly, the preceding years (Paschold et al. 2002). Studies on asparagus physiology have shown a close relationship between the amount of root-stored carbohydrates and spear yield (Robb 1984; Wilson et al. 1999). The capacity for aged fern to produce carbohydrates is severely reduced (Dufault 1995; 1999; Dufault and Ward 2005). Premature defoliation of fern also decreases the photosynthetic potential of the crop (Cunnington and Irvine 2005).

Alleopathic residues (Yang 1982), acidic soils (Hodupp 1983), soil compaction, winter crown injury (Putnam and Lacy 1977), and excessive spear cutting pressure (Shelton and Lacy 1980) can contribute to asparagus decline. Biotic factors, such as insects and weeds, can also lead to poor stand and decline (Damicone et al. 1987; Putnam and Lacy 1977). The common asparagus beetle *Crioceris asparagi* (Linnaeus) and the twelve-spotted asparagus beetle *Crioceris duodecimpunctata* (Linnaeus) are leaf beetles that feed exclusively on asparagus (LeSage et al. 2008). The asparagus fly (*Platyparea poeciloptera*), along with the asparagus beetle, is the most important insect pest of asparagus in Germany (Crüger 1991). The asparagus miner (*Ophiomyia simplex* Loew), a putative vector of pathogenic *Fusarium* spp, may also occur (Bishop et al. 2004). In addition, the aphid *Brachycorynella asparagi* (Mordvilko) causes a characteristic severe distortion of the terminal bud of asparagus ferns called rosetting, which shortens internodes and leaves and turns the latter blue-green (Stoetzel 1990). Aphids are also able to spread viruses in asparagus (Hein 1969; Greiner 1980).

To date, nine viruses have been associated with asparagus (Tomassoli et al. 2012). The two most important viruses, which were first described in Germany, asparagus virus 1 (AV1) (Hein 1960) and asparagus virus 2 (AV2) (Hein 1963), occur only in asparagus, as does asparagus virus 3 (AV3) (Fujisawa 1986). Tobacco streak virus (Paludan 1964), cucumber mosaic virus (Weissenfels and Schmelzer 1976), tobacco mosaic virus (Faccioli 1965), and three nepoviruses (Posnette 1969) are also associated with asparagus.

Besides insects and viruses, diseases are predominantly responsible for damage to asparagus (Elmer 1996). Grey mould (*Botrytis cinerea*) can infect shoot tissue and, if not controlled, cause considerable losses by instigating premature shoot death. Grey mould can also be isolated from stem bases (Blok and Bollen 1995). Asparagus rust, which is caused by *Puccinia asparagi* DC., in Lam. & DC., was originally described in France in 1805 and appeared in New Jersey, North America, in 1896 (Halstead 1898). The symptoms of

this disease in mature stems are elongated lesions that contain small, orange-red pustules arranged in concentric rings (Cheah and Davis 2002). *Fusarium* stem and crown rot (Johnston et al. 1979) was first noted in 1908 (Stone and Chapman 1908). Over the years, this disease has been termed dwarf asparagus (Cook 1923), wilt and root rot (Cohen and Heald 1941), seedling blight (Grogan and Kimble 1959), and crown rot complex (Endo and Burkholder 1971). Depending on the respective site conditions, *Fusarium oxysporum* (Schlecht) f. sp. *asparagi* (S. I. Cohen) and *Fusarium proliferatum* (Matsushima) Nirenberg could occur frequently (Cohen and Heald 1941; Blok and Bollen 1995; Elmer 1996; Gossmann et al. 2001; 2005; 2008; Logrieco et al. 1998; Weber et al. 2006). Numerous fungi of the genus *Fusarium* are able to form mycotoxins from type B fumonisins, which, in addition to a reduction in yield, cause a qualitative impairment in the crop (Logrieco et al. 1998; Seefelder et al. 2002).

Purple spot or *Stemphylium* leaf spot is a significant disease in all asparagus-growing regions worldwide (Suzui 1973; Menzies 1980; Lacy 1982; Blancard et al. 1984; Falloon et al. 1984; Gindrat et al. 1984) and a serious problem in Germany (Menzinger and Weber 1990). Due to the premature defoliation of fern in the autumn and the resulting reduction in photosynthetic potential, significant yield loss may result from purple spot (Menzies et al. 1992).

The genus *Stemphylium* was described for the first time in asparagus with the type species ‘*Stemphylium botryosum* W. ad *Asparagum*’ in 1833 (Wallroth 1833). It has since been morphologically analysed and described in detail by Wiltshire (1938) and Simmons (1967; 1969). The teleomorph form of *S. botryosum* was later taxonomically rewritten and altered from *Pleospora herbarum* (Pers) Rabenhorst to *Pleospora tarda* (Simmons 1985). The fungus described as *Helmisporium vesicarium* (Wallroth 1833) is now known as *S. vesicarium* and has been supplemented by the teleomorphic form *Pleospora allii* (Simmons 1969). According to the Amsterdam Declaration on Fungal Nomenclature (Hawksworth et al. 2011), the dual nomenclature was changed to ‘one fungus, one name’. The name of the anamorph is applicable for species belonging to the genus *Stemphylium*, whereas the name of the teleomorph *Pleospora* is suppressed (Wijayawardene et al. 2014; Rossman et al. 2015). Following these conventions, *S. vesicarium* is used for each form of the fungus in this study.

Stemphylium is a genus of plant pathogens and saprophytes in the Ascomycota family of Pleosporaceae (Inderbitzin et al. 2009). *Stemphylium* species are dematiaceous hyphomycetes with muriform, septate, and usually pigmented conidia produced by conidiophores, which proliferate percurrently. The percurrently proliferating conidiophore is the key morphological feature that distinguishes this genus from other genera with muriform conidia, such as *Ulocladium* and *Alternaria* (Simmons 1967). Unlike *Alternaria* sp., the conidia of *Stemphylium* are not formed in chains (Inderbitzin et al. 2009). About 30-110 species are known to belong to the genus *Stemphylium* (Câmara et al. 2002; Inderbitzin et al. 2009; Farr and Rossman 2015). Most of these species are saprophytes that grow on cellulose materials and dead plants (Simmons 1969; Ellis 1971). Fifteen genera and 24 species have been described as host plants for *Stemphylium* species (Farr and Rossman 2015).

Resistance and environmental problems caused by the massive use of chemicals to maintain crops resulted in sharp criticism in the 1960s (Carson 1962) and led to the promotion and development of alternative pest control strategies (Perkins 1982). The integrated pest management (IPM) concept is based on the economical use of plant protection products, the benefits of utilising natural enemies, and their threat by plant protection measures. IPM includes a wide range of alternative pest control measures, such as crop rotation, undersowing, planting of resistant varieties, adjustment of cultivation times to the infestation pressure, and mechanical methods (Dent and Elliott 1995; Burth and Freier 1996). An alternative approach to reduce fungicides treatments is the use of forecasting models. In other arable and fruit tree cultures, beneficial experiences have been achieved by adopting computer-assisted decision support systems (Kleinhenz and Jörg 1998; Jörg et al. 1999). In the former German Democratic Republic, simulation models were used to control plant diseases, for instance, to regulate the nationwide use of fungicides (Gutsche and Kluge 1983). Decision support systems can be useful for forecasting the date of exceeding control thresholds and, thus, the date of fungicide application. Using mathematical models, the time requirement for field evaluations can be minimised (Racca et al. 2002). The effects of temperature and leaf wetness duration on the infection and growth of fungal plant diseases can be modelled to forecast infection periods (Lalancette et al. 1988; Carisse and Kushalappa 1990; Montesinos and Vilardell 1992; Montesinos et al. 1995b; Broome et al. 1996). The model Forecasting *Alternaria solani* on Tomatoes (FAST), for instance, was developed to identify favourable environment conditions for early blight

and to provide a schedule for efficient fungicide applications (Madden et al. 1978). Brown spot of pear forecasting (BSPcast) was subsequently derived from FAST by adapting the model to the aetiology and epidemiology of *S. vesicarium* on pear (Montesinos and Villarrell 1992; Montesinos et al. 1995a; Montesinos et al. 1995b; Llorente et al. 2000; Llorente et al. 2011). The tomato disease forecasting (TOM-CAST) model was also derived from FAST as a weather-timed fungicide spray forecasting model for tomato anthracnose, *Septoria* leaf spot, and late blight (Pitblado 1992). TOM-CAST was later tested in order to reduce fungicide spray application in the control of purple spot in asparagus (Meyer et al. 2000; Eichhorn et al. 2010); however, BSPcast and TOM-CAST are not sufficiently adapted to the pathogen *S. vesicarium* or the host asparagus. Furthermore, the number of fungicide applications administered in practice is currently lower than that recommended by these two models.

The integrated control of purple spot by a new forecast model, called SIMSTEM (Simulation of *Stemphylium*), requires the exact identification of the pathogen and more detailed information regarding the pathogen's biology in asparagus.

The objectives of this study, therefore, are:

- (i) to develop a molecular- and genetics-based method to distinguish *S. vesicarium* from *S. botryosum*;
- (ii) to analyse infected German asparagus samples to identify the prevalent causal agent of purple spot in Germany;
- (iii) to describe and model the monocyclic phase of *S. vesicarium* in asparagus based on biological data from ascospores collected in laboratory and field trials;
- (iv) to describe and model the polycyclic phase of *S. vesicarium* in asparagus based on biological data from conidia gathered in laboratory and field trials; and
- (v) to relate the monocyclic and polycyclic phases in the revised forecasting model SIMSTEM and complete its implementation in www.isip.de.

2. Differentiation of *Stemphylium vesicarium* from *Stemphylium botryosum* as causal agent of the purple spot disease on asparagus in Germany

2.1. Abstract

The purple spot disease of asparagus is the most important disease in German asparagus growing regions. Two different *Stemphylium* species, *S. vesicarium* and the closely related species *S. botryosum*, are described as causal pathogens. Because of the strong phenotypical similarities, the morphological differentiation is very difficult. Therefore, the development of a suitable alternative to distinguish these species is an important need. The aim of this study was to develop a molecular and genetic based differentiation method for *S. vesicarium* and *S. botryosum*, and to analyze asparagus samples from Germany with this method to identify the prevalent causal agent of the purple spot disease in Germany. The sequences of three different DNA-markers were compared to get the most appropriate basis. Additionally, to the commonly used ITS regions, parts of the protein-coding genes *gapdh* (glyceraldehyde-3-phosphate-dehydrogenase) and cytochrome b were analysed. The most significant difference between the two species was a 3 kb intron present in the *S. botryosum* cytochrome b region but not in *S. vesicarium*. This difference showed to be suitable for the distinction of these two *Stemphylium* species by a simple PCR-reaction. In addition to the qualitative analysis, the frequencies of these species were detected directly from asparagus field samples with the help of qPCR. In all German samples collected in 2010, 2011, 2013 and 2014 only *S. vesicarium* could be identified.

Keywords: *Stemphylium vesicarium*, *Stemphylium botryosum*, Purple spot disease, Asparagus, Species identification

2.2. Introduction

The purple spot disease or *Stemphylium* leaf spot of asparagus (*Asparagus officinalis*) has become a significant problem in all asparagus growing regions worldwide (Suzui 1973; Menzies 1980; Lacy 1982; Blancard et al. 1984; Falloon et al. 1984; Gindrat et al. 1984),

and become a serious problem in Germany in the late 80s (Menzinger and Weber 1990). Due to the premature defoliation of fern in autumn and the resulting reduced photosynthetic potential, up to 52 % yield loss can be caused (Bansal et al. 1992). *Stemphylium* Wallr. is a genus of filamentous ascomycetes with *S. botryosum* Wallr. (Teleomorph: *Pleospora tarda* E.G. Simmons) as the type species. The most important morphological characteristic to distinguish *Stemphylium* from the closely related genera *Ulocladium* and *Alternaria* is the pre-currently proliferating conidiophore (Simmons 1969). There are more than 30 recognizable species known for the genus *Stemphylium* (Câmara et al. 2002).

S. vesicarium (Wallr.) E.G. Simmons (Teleomorph: *Pleospora allii*), which is also known to cause the brown spot disease of pears, was identified also as causal agent of the purple spot disease of asparagus in the USA (Michigan (Hausbeck et al. 1997; Meyer et al. 2000), California (Falloon et al. 1987) and Washington (Johnson and Lunden 1984)), Australia (Cunnington and Irvine 2005), South Africa (Thompson and Uys 1992) and New Zealand (Bansal et al. 1992). The closely related species *S. botryosum* was detected in asparagus samples from Germany (Leuprecht 1988; Neubauer 1998), Japan (Suzui 1973) and Greece (Elena 1996). For many years, the identification of *Stemphylium* species was mainly based on morphological characteristics, such as conidial shape, size, length/width ratio, color, ornamentation and septation (Simmons 1967; 1969; 1985). Many of these characters overlap among related species, making determinations on species level difficult and in some cases incorrect (Cunnington and Irvine 2005; Shenoy et al. 2007; Wang et al. 2010). However, *S. botryosum* seems to be highly variable on plant material and in pure culture. *Stemphylium* species are also known to show high conidial variability at different temperatures and on different substrates (Leach and Aragaki 1970; Leuprecht 1990). With durations of 3 months to form fertile ascospores for *S. vesicarium* and 8 months for *S. botryosum* (Simmons 1985; Chaisrisook et al. 1995b), this morphological characteristic is not suitable for rapid species identification. As the two species, may differ in etiology, the identification of the causal agent is crucial for the development of a suitable pest management.

Sequences of the internal transcribed spacers (ITS) of the nuclear ribosomal DNA and protein coding genes, for example *gapdh*, are important molecular markers in phylogenetic analyses of fungi (White et al. 1990; Begerow et al. 2010; Schoch et al. 2012). Besides the monophyly of the genus *Stemphylium*, taxonomic relations could be verified

using ITS regions and *gapdh* gene sequences (Câmara et al. 2002; Inderbitzin et al. 2009; Köhl et al. 2009; Wang et al. 2010)

Furthermore, considerably large amounts of sequence data are available of the mitochondrial coded cytochrome b gene (*cyt b*), which was frequently analysed in regard to QoI resistance (Grasso et al. 2006; Sierotzki et al. 2007; Stammler et al. 2013). Due to this fact, the resolving power of this region as taxonomic marker could be verified for many agronomic important fungi. Besides the relatedness within the order Uredinales (Grasso et al. 2006), species identifications in the genera *Monilinia* and *Phyllosticta* (Miessner and Stammler 2010; Stammler et al. 2013) were done using *cyt b* sequences.

The aim of this study was: (i) to develop a molecular and genetic based differentiation method for *S. vesicarium* from *S. botryosum*, and (ii) to analyze asparagus samples from Germany with this method to identify the prevalent causal agent of the purple spot disease in Germany. The sequences of three molecular markers (ITS, *gapdh* and *cyt b*) were used to distinguish the two described causal agents (*S. vesicarium* and *S. botryosum*) of the purple spot disease of asparagus. In addition, we developed a method based on sequence aberrations in the *cyt b* gene, suitable for quantification of both pathogens in field samples.

2.3. Materials and methods

2.3.1. Origin of isolates

Four *S. vesicarium* and five *S. botryosum* isolates were obtained from international culture collections. Strain 224 is the type of *S. botryosum*, which was also used in the analyses of Köhl et al. (2009). Another eight *Stemphylium* isolates provided by Zapf et al. (2011) and two *Stemphylium* isolates provided by A. Wichura / R. Weber (Agricultural Chamber of Lower Saxony), which were all isolated from asparagus, were also analysed. Details of the used isolates are given in Table 2.1. Isolates of related *Stemphylium* species, like *S. herbarum*, *S. alfalfa*, *S. sedicola* and *S. tomatonis*, were not included as these species are from different hosts and assumed to be identical (synonymous) to *S. vesicarium* (Câmara et al. 2002; Inderbitzin et al. 2009; Köhl et al. 2009).

2.3.2. Analyses of the DNA marker regions

Fungal mycelium (~25 mg) from 14 days old cultures grown on potato dextrose agar (PDA) was used for DNA and RNA extraction using the Nucleospin® Plant II Kit and Nucleospin® RNA Kit (Machery and Nagel, Düren, Germany), respectively. According to the manufacturer's instructions, reverse transcription of the RNA for the cDNA synthesis was made with the Verso cDNA kit (Thermo, Ulm, Germany). PCR reactions were carried out for sequence analyses. Primers KES 1968 (5'-GCACCGACCACAAAATC-3') and KES 1969 (5'-GGGCCGTCAACGACCTTC-3') were used for amplification of *gapdh* according to Câmara et al. (2002). For the ITS region primer sequences of White et al. (1990) ITS1 (5'-TCCGTAGGTGAACCTGCGG-3') and modified ITS4 (5'-TCCTCCGCTTATTGATATGCTTAA-3'), were used. The following reaction conditions were used for both the *gapdh* and ITS regions. Phusion MasterMix 2 × (Thermo, Ulm, Germany) with an initial heating step for 30 s at 98 °C followed by 35 cycles of 5 s at 98 °C, 5 s at 64 °C, 10 s at 72 °C and 1 min at 72 °C for final elongation. With the help of the Sanger method, the PCR products were sequenced. Alignments of these DNA sequences and database sequences were done to identify the different *Stemphylium* spp. The partial *cyt b* gene was amplified using the primers KES 183 (5'-CGATAGCTGCAGGAGTTTGC-3') and KES 184 (5'-GCTTCAGCATTTTTCTTCATAGTT-3'). PCR was performed using 2 × HotStart-IT FidelityTaq Mastermix (USB, Staufien, Germany) with an initial heating step of 1 min at 95 °C, followed by 35 cycles of 15 s at 95 °C, 30 s at 52 °C, 10 min at 68 °C and the final elongation for 5 min at 68 °C. PCR products were sequenced by primer walking sequencing. Alignments of DNA and corresponding cDNA sequences were used for the identification of the exon/intron structure of the amplified *cyt b* gene.

2.3.3. Molecular genetic species identification

The pre-assigned species assignment was checked using sequences of the ITS region and the partial *gapdh* gene. Sequences were aligned by using the Lasergene Programms (DNASTAR, Madison, USA). ITS and *gapdh* sequences of strains identified as *S. vesicarium* (ITS: AF442803; AF229484; *gapdh*: AF443902, AY278821.1) and *S. botryosum* (ITS: AF442782, KC584238; *gapdh*: AF443879; AF443881), obtained from Genbank, were used in this analysis in addition to the 19 *Stemphylium* isolates sequenced in this study.

Table 2.1 *Stemphylium* Isolates investigated in this study

Isolate ID	Country	Host	Origin	<i>Stemphylium</i> spp		
				Primary	After sequencing	
143	BE	<i>Allium cepa</i>	MUCL 3822	<i>S. vesicarium</i>	<i>S. vesicarium</i>	
144	US	Seaweed	MUCL 41719	<i>S. botryosum</i>	<i>S. vesicarium</i>	
145	BE	Barley	MUCL 20440	<i>S. botryosum</i>	<i>S. vesicarium</i>	
146	DE	<i>Lupinus spp.</i>	DSM 62928	<i>S. botryosum</i>	<i>S. vesicarium</i>	
147	BE	<i>Beta spp.</i>	MUCL 51851	<i>S. botryosum</i>	<i>S. vesicarium</i>	
148	NL	<i>Allium cepa</i>	CBS 486.92	<i>S. vesicarium</i>	<i>S. vesicarium</i>	
149	NL	<i>Allium cepa</i>	CBS 311.92	<i>S. vesicarium</i>	<i>S. vesicarium</i>	
221	DE	<i>Asparagus</i>	Stem 12-21	<i>Stemphylium sp.</i>	<i>S. vesicarium</i>	
222	DE	<i>Asparagus</i>	Stem 12-29	<i>Stemphylium sp.</i>	<i>S. vesicarium</i>	
223	JP	<i>Asparagus</i>	NBRC 31381	<i>S. vesicarium</i>	<i>S. vesicarium</i>	Species identification
224 (T)	CA	<i>Medicago sativa</i>	MUCL 11717	<i>S. botryosum</i>	<i>S. botryosum</i>	
110	DE	<i>Asparagus</i>	Stembo 1	<i>S. botryosum</i>	<i>S. vesicarium</i>	
111	DE	<i>Asparagus</i>	Stembo 2	<i>S. botryosum</i>	<i>S. vesicarium</i>	
112	DE	<i>Asparagus</i>	Stembo 3	<i>S. botryosum</i>	<i>S. vesicarium</i>	
113	DE	<i>Asparagus</i>	Stembo 4	<i>S. botryosum</i>	<i>S. vesicarium</i>	
114	DE	<i>Asparagus</i>	Stembo 5	<i>S. botryosum</i>	<i>S. vesicarium</i>	
115	DE	<i>Asparagus</i>	Stembo 6	<i>S. botryosum</i>	<i>S. vesicarium</i>	
116	DE	<i>Asparagus</i>	Stembo 7	<i>S. botryosum</i>	<i>S. vesicarium</i>	
117	DE	<i>Asparagus</i>	Stembo 9	<i>S. botryosum</i>	<i>S. vesicarium</i>	
150	DE	Pear	St.sp.24.7.13.P4-K1	<i>S. vesicarium</i>	<i>S. vesicarium</i>	Validation of
152	DE	<i>Asparagus</i>	St.sp.25.9.13.D	<i>S. vesicarium</i>	<i>S. vesicarium</i>	differentiation methods
154	DE	<i>Asparagus</i>	St.sp.25.9.13.C	<i>S. vesicarium</i>	<i>S. vesicarium</i>	
155	DE	<i>Allium cepa</i>	St.sp.3.9.13.ZW	<i>S. vesicarium</i>	<i>S. vesicarium</i>	
156	DE	<i>Asparagus</i>	St.sp.25.9.13.F	<i>S. vesicarium</i>	<i>S. vesicarium</i>	
159	DE	<i>Asparagus</i>	St.sp.25.9.13.A	<i>S. vesicarium</i>	<i>S. vesicarium</i>	
160	IT	Pear	BASF SE	<i>S. vesicarium</i>	<i>S. vesicarium</i>	
161	IT	Pear	BASF SE	<i>S. vesicarium</i>	<i>S. vesicarium</i>	
162	IT	Pear	BASF SE	<i>S. vesicarium</i>	<i>S. vesicarium</i>	
163	IT	Pear	BASF SE	<i>S. vesicarium</i>	<i>S. vesicarium</i>	
164	IT	Pear	BASF SE	<i>S. vesicarium</i>	<i>S. vesicarium</i>	
165	IT	Pear	BASF SE	<i>S. vesicarium</i>	<i>S. vesicarium</i>	

Stembo 1-9 Isolate provided by Zapf et al. 2011; Stem12-21 and Stem 12-29 provided by A. Wichura / R. Weber

MUCL BCCM/MUCL fungi and yeasts catalogue, CBS Centraalbureau voor Schimmelcultures, DSM Deutsche Sammlung von Mikroorganismen und Zellkulturen, NBRC Nite Biological Resource Center

2.3.4. Species-specific identification of *Stemphylium* spp.

With the sequence information from the study above, a primer pair for the qualitative differentiation of *S. vesicarium* and *S. botryosum* KES 1999 (5'GAC-CGTCGGCCATATAAAGGGTTCG-3') and 2000 (5'-AACCGTCTCCGTC-TATCAATCCT GCT-3') was selected, which amplify the *cyt b* gene of the two species but generated products of different, species-specific length. Reaction conditions with an

initial heating step for 30 s at 98 °C followed by 35 cycles of 10 s at 98 °C, 5 s at 72 °C and 1 min at 72 °C with 2 × PhusionMastermix were used.

2.3.5. qPCR based differentiation of *S. vesicarium* and *S. botryosum*

Quantitative detection of *S. vesicarium* and *S. botryosum* was achieved by real-time PCR by coupling allele-specific primers with a 5'Nuclease Assay. A 214 bp fragment specific for *S. vesicarium* was amplified with the primers KES 1995 (5'AGGGTCGCTACAGACTGGGTCACT-3'), KES 1997 (5'-GCACTCATA AGGTTAGTAATAACTGTAGC-3') and the double-dye probe 5'FAM-CTGCTTAATGTACAGGCGAAAC-BHQ1-3'. For the amplification of *S. botryosum* (215 bp), the primers KES 1995 and KES 1998 (5'-CAGCTATTACTTCGCCTTTTAACTGTAGCA-3') and the previous mentioned double-dye probe were used. The reactions were performed on a Rotor-Gene Q (Qiagen, Hilden, Germany) with Takyon qPCR MasterMix Plus dTTP No Rox reagents (Eurogentec, Köln, Germany) under the following conditions: 3 min at 95 °C and 40 cycles at 95 °C for 10 s and 60 °C for 45 s. The received Ct-values of the *S. vesicarium* reaction and the *S. botryosum* reaction were used to calculate the relative allele frequencies based on the method described by Germer et al. (2000).

2.3.6. Validation of the developed differentiation methods

To validate the developed differentiation methods (qualitative PCR and quantitative qPCR) six *S. vesicarium* strains isolated from pears and six isolates provided by H. Bohlen-Janßen (Agricultural Chamber of Lower Saxony) were used. Details of these isolates are given in Table 2.1.

2.3.7. Monitoring of Asparagus fields

Samples of infested asparagus fields were taken all over Germany in the years 2010, 2011, 2013 and 2014 at different stages of epidemiological development.

2.4. Results

2.4.1. Species identification

PCR with primer pair KES 1968 and KES 1969 for the *gapdh* gene resulted in an amplification product of 850 bp. Amplification of the ITS region with primer pair KES 1806 and KES 1816 resulted in a product of 558 bp. For the identification at species level, the *gapdh* gene and the ITS region of the reference strains, ordered from different international culture collections or received from Zapf et al. (2011), were sequenced and compared to database sequences of *S. vesicarium* (ITS: AF442803 (T); AF229484; *gapdh*: AF443902 (T), AY278821.1) and *S. botryosum* (ITS: AF442782 (T), KC584238; *gapdh*: AF443879; AF443881 (T)). The sequences were compared with sequences from type material (T). All strains except strain 224 were found to be identical with the *S. vesicarium* sequences in both regions, even though four of them (Table 2.1) were preliminary classified as *S. botryosum*. Strain 224 and the published *S. botryosum* sequences were identical in their *gapdh* and ITS sequence. Comparing *S. vesicarium* and *S. botryosum*, six single substitutions in the ITS region and 24 in the amplified *gapdh* region were found. Identical sequences were found in strains of the same species originating from different hosts and different countries.

2.4.2. Cyt b of *S. vesicarium* and *S. botryosum*

With the primer pair KES 183 and KES 184, the *cyt b* region could be amplified with DNA and cDNA, respectively. The cDNA fragments showed identical sizes of 550 bp for both *Stemphylium* species. While the DNA fragments showed a length of 3 kb for *S. vesicarium* (KJ934233) and 6 kb for *S. botryosum* (KJ934234). The discrepancy between the DNA and cDNA fragments indicated intron regions which are removed during the splicing process. Alignments of the DNA and cDNA sequences revealed two introns (1323 bp and 1252 bp) for *S. vesicarium*. The same introns plus an additional intron of 2931 bp were found in *S. botryosum* (Fig. 2.1).

2.4.3. Differentiation of *S. vesicarium* from *S. botryosum*

Due to the large size differences in the *cyt b* gene it was possible to differentiate *S. vesicarium* and *S. botryosum* via fragment length comparisons.

A simple PCR-reaction with the primer pair KES 1999 and KES 2000 showed fragments of 420 bp for *S. vesicarium* and 3350 bp for *S. botryosum* (Fig. 2.2). When using a mixture (1:1) of the DNA of *S. vesicarium* and *S. botryosum* only the short fragment of *S. vesicarium* was amplified. Therefore, only pure cultures can be analysed with this method. Cross reactions could be excluded using DNA extracts from other fungal pathogens such as *Alternaria alternata* and *Botrytis cinerea* (for *A. solani*, *A. brassicae* data not shown). Additionally, DNA of *Puccinia triticina* was used as a related species of *P. asparagi* which is causing the rust disease on asparagus.

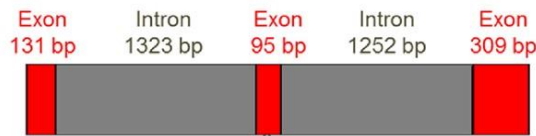
To quantify the two *Stemphylium* species directly from asparagus samples, a specific qPCR assay was developed using the *cyt b* gene as a suitable basis. The identical forward primer KES 1995 and probe in combination with the species specific reverse primers KES 1997 and KES 1998 were used to determine the abundances of *S. vesicarium* (KES 1997) and *S. botryosum* (KES 1998). The calculation of the frequency was done with the formula based on Germer et al. (2000). Each DNA was analysed in two separate PCR reactions, each with a primer pair specific to one or the other *Stemphylium* species. Theoretically, only the fragment of the matching species would be amplified. In practice, the mismatching fragment was amplified as well, but in a much less quantity. A delay of eight cycles could be observed between mismatched and correct amplification. To test the sensitivity of this assay, the following parameters were determined. With a serial dilution of the DNA of both organisms, the linearity (regression line which gives information about the proportionality of the Ct-value to the amount of DNA) and the PCR efficiency could be investigated. The efficiency of the PCR reactions was calculated and found to be very similar (*S. vesicarium*: 99 %, *S. botryosum*: 97 %), which makes the reactions comparable and suitable for the quantification of *S. vesicarium* and *S. botryosum*. The detection and the quantification limit (0.001 ng/ μ g) was also defined by determining the lowest amount of target DNA that the tested assay can detect and quantify, respectively. The latter was accomplished by using a serial dilution of a 1:1 mixture of *S. vesicarium* and *S. botryosum* DNA. To exclude cross reactions with other fungal pathogens, DNA of *A. alternata*, *A. solani*, *A. brassicae*, *B. cinerea* and *P. triticina* were analysed. None of these organisms could be detected with the developed qPCR assay.

2.4.4. Analysed asparagus samples

With the qPCR method above, 15 samples from 2014, 87 samples from 2013, 90 isolates from 2011 and 40 samples from 2010 were analysed. All tested samples and isolates were from asparagus growing regions in Germany (Fig. 2.3).

S. vesicarium could be identified with a frequency of 98-100 %. There was no evidence for *S. botryosum* to be the causal agent of the purple spot disease in Germany in the years of sampling.

S. vesicarium (3110 bp):



S. botryosum (6041 bp):



Figure 2.1 Intron-exon organization of the *cyt b* gene (partial) of *S. vesicarium* and *S. botryosum*

2.5. Discussion

In this study a cost-efficient alternative, with which large quantities of asparagus samples can be analysed, was used and the causal agent of the purple spot disease was developed based on differences in the intron-exon structure of the *cyt b* gene. Characteristic substitutions in the ITS region and the *gapdh* gene, which were preliminary defined by Câmara et al. (2002), could also be verified. Based on these two loci *S. vesicarium* and *S. botryosum* could be placed into two distinct clusters, in which *S. vesicarium* showed identical sequences with *S. herbarum* and *S. alfalfa*. Even a four locus phylogeny made by Inderbitzin et al. (2009), could not differentiate between these three *Stemphylium* species as well as *S. tomatonis* and *S. sedicola*. Therefore, the separating into single species could not be supported by phylogenetic analyses and should be regarded as synonymous (Câmara et al. 2002; Inderbitzin et al. 2009; Köhl et al. 2009). So far, *cyt b* was not sequenced for *S. herbarum*, *S. alfalfa*, *S. tomatonis* and *S. sedicola* and therefore it is not

known if there are differences in the sequence. Further analyses regarding cyt b sequences of these five closely related or even synonymous *Stemphylium* species could provide a further step on the clarification of the taxonomic relationship.

All used reference strains, except strain 224 were identified as *S. vesicarium* even though some of them were initially classified as *S. botryosum*.

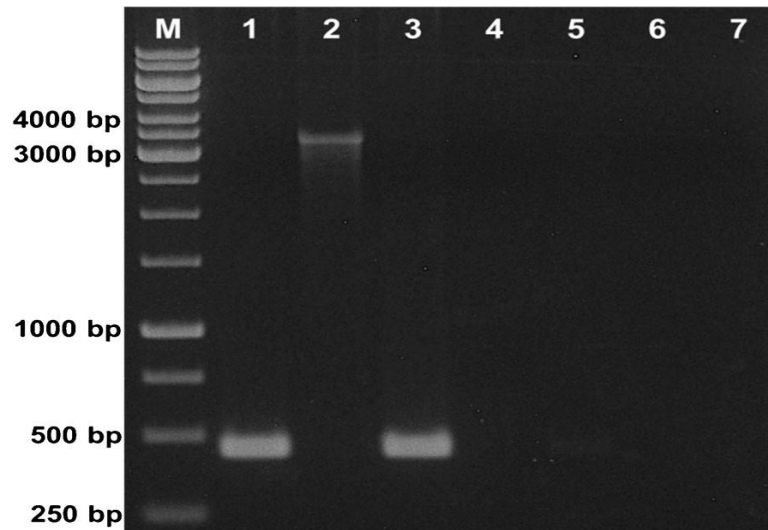


Figure 2.2 Principle of the qualitative differentiation of the *Stemphylium* spp.. 1: *S. vesicarium*, 2: *S. botryosum*, 3: 1:1 Mixture of *S. vesicarium* and *S. botryosum*, 4: *A. alternata*, 5: *B. cinerea*, 6: *P. triticina*, 7: NTC, M: 1 kb DNA

The location of this gene on mitochondrial DNA (mtDNA) and the resulting high copy number gives it an advantage and reduces the detection limit for the development of reliable PCR assays (Stammler et al. 2013). Based on the development of resistances against QoI fungicides, the cyt b sequences of many different plant pathogenic fungi have been analysed. The cyt b region is intraspecific very conserved but shows interspecific differences. These differences relate to the base sequence as well as the location of non-coding regions (Grasso et al. 2006; Sierotzki et al. 2007; Stammler et al. 2013). Referring to this, the species-specific presence or absence of intronregions could be shown for other fungal pathogens such as *Monillinia* spp. and *Phyllosticta* spp. (Miessner and Stammler 2010; Stammler et al. 2013).

The *Stemphylium* species could be qualitatively differentiated in a single PCR reaction with one primer pair. In addition to this qualitative differentiation it was possible to create a quantitative method with the help of qPCR to estimate the frequencies of the two *Stemphylium* species directly from asparagus material. With this Taqman based assay asparagus samples and *Stemphylium* isolates from Germany were analysed and the frequencies

were determined. Only *S. vesicarium* could be identified in every sample. There was no hint for *S. botryosum* as causal agent of the purple spot disease.

So far, only *S. botryosum* had been described as the causal agent in Germany, a description based on morphological characteristics (Leuprecht 1988; 1990; Neubauer 1997; 1998; Zapf et al. 2011). Although a misidentification of German isolates was supposed by Falloon et al. (1987), there was no clear proof for a high abundance of *S. vesicarium* in Germany until now. Due to the results of this study the prevalent pathogen of asparagus leaf spot in Germany could be identified as *S. vesicarium*.

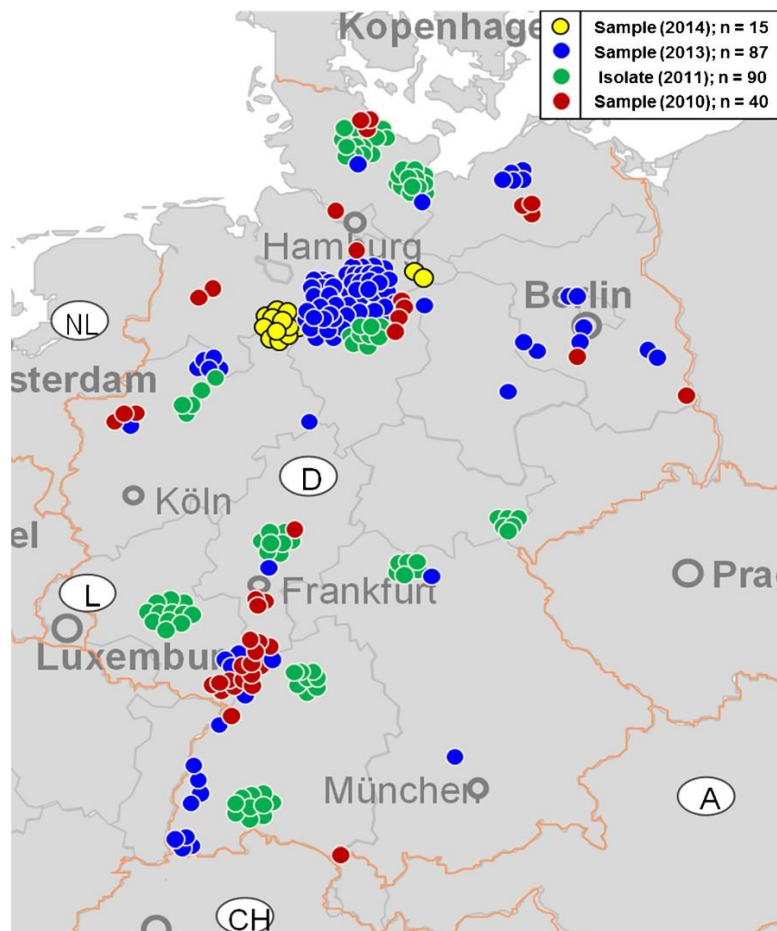


Figure 2.3 Distribution of analysed asparagus samples and *Stemphylium*-isolates

Acknowledgments

We would like to thank all colleagues of the plant protection services and consultants providing plant samples. This work was a support for the project (313-06.01-28-1-47.02511) funded by the German Ministry of Food and Agriculture (BMEL) and the Office for Agriculture and Food (BLE).

3. Modelling some aspects of the monocyclic phase of *Stemphylium vesicarium*, the pathogen causing purple spot on asparagus (*Asparagus officinalis* L.)

3.1. Abstract

The monocyclic phase of *Stemphylium vesicarium* is part of its life cycle and a possible factor for forecasting and the integrated control of purple spot on asparagus. The purpose of the study was to model the flight, germination and germ tube growth of ascospores as basis for the development of a forecasting system. During 2014-2016, the flight period was determined by spore traps. The ascospores flew between March and early July, but most were released in early May. The cumulative percentage of trapped ascospores depending on the daily summed temperature (base 5 °C) on rainy days starting from February 1st was described best by a Chapman Richards function. The germination and germ tube length of ascospores depending on leaf wetness duration and temperature were investigated in laboratory trials. Ascospores germinated rapidly in a wide temperature range. The fitted Chapman Richards function with a temperature-dependent capacity and rate described germination adequately with a calculated optimal temperature of 31.04 °C. The germ tube length was modelled by a combined generalised beta-linear function and it was optimal at 30.4 °C with a narrow temperature range of 25-35 °C for values close to the optimum length. Therefore, the infection process is restricted more severely by the germ tube length than by germination. The ascospore flight is often finished before the end of the harvest, so fungicide treatments during the monocyclic phase might be ineffective in many production sites in Germany. The situation could be different for shorter harvest periods and in non-harvested young plants.

Keywords: Asparagus, *Pleospora allii*, Purple spot, SIMSTEM, *Stemphylium vesicarium*

3.2. Introduction

Purple spot or *Stemphylium* leaf spot disease of asparagus (*Asparagus officinalis* L.) is caused by *Stemphylium vesicarium* (Wallr.) E.G. Simmons 1969 and is an important

disease that affects asparagus production in Germany (Menzinger and Weber 1990) and other countries worldwide (Suzui 1973; Menzies 1980; Lacy 1982; Blancard et al. 1984; Falloon et al. 1984; Gindrat et al. 1984; Thompson and Uys 1992; Cunnington and Irvine 2005). Based on morphological characteristics (Simmons 1967; 1969; 1985), the causal pathogen of asparagus purple spot was first identified in Germany as *Stemphylium botryosum* (Wallroth) (Leuprecht 1988; Neubauer 1997; Zapf et al. 2011), but the main pathogen was found to be *S. vesicarium* very recently using molecular methods (Graf et al. 2016).

In winter, the saprophytic fungus survives as pseudothecia on plant debris (Falloon et al. 1984). Depending on the weather conditions, ascospores are released and can cause primary infections, which usually occur at the base of young plants. Conidia develop on primary infections, which lead to secondary infections in late summer to autumn (Falloon and Tate 1986). Due to the premature defoliation of the ferns in the autumn, the photosynthetic potential may be reduced and severe yield losses can occur (Menzies et al. 1992).

Beside the weather conditions, the crop cultivation methods are influencing the ascospore flight. Removing ferns from the previous year (Falloon et al. 1984) and burying asparagus debris physically can reduce the ascospore flight but pseudothecia are not decomposed after burial for 10-14 weeks (Johnson 1990). This aspect for inhibiting the release of ascospores is not taken into consideration in this study.

The seasonal course of ascospores in asparagus is already known. In New Zealand, the ascospores fly mainly from September to January, with only a few from February to April (Menzies et al. 1992). This flight pattern corresponds to the spring to summer seasons in the southern hemisphere. Spring to early summer was also the time observed for ascospore release in Davis, California, USA (Falloon and Tate 1986). In Michigan, USA, the highest daily ascospore concentrations were detected in June during three years with the highest peak on 5th June (Granke and Hausbeck 2012). Detailed information about the release of *S. vesicarium* ascospores in Europe is known only in other horticultural crops. Thus, in Spain, ascospores flew in garlic fields from February to March (Prados-Ligero et al. 2003). Ascospore flight sourcing from pear leaf litter in Italy were found from December to April (Rossi et al. 2008). Thus, an important part of the monocyclic life cycle is already clear from previous studies, but other biological data required to model the disease's progression, such as germination data for asparagus strains, are missing.

The effects of temperature and the leaf wetness duration on the infection and growth of fungal plant diseases can be modelled to forecast infection periods (Lalancette et al. 1988; Carisse and Kushalappa 1990; Broome et al. 1996; Montesinos and Vilardell 1992; Montesinos et al. 1995b). For example, the FAST model is a system for forecasting *Alternaria solani* on tomato plants (Madden et al. 1978). Subsequently, BSPcast was derived from FAST by adapting it to the aetiology and epidemiology of *S. vesicarium* on pear plants (Montesinos and Vilardell 1992; Montesinos et al. 1995a; Montesinos et al. 1995b; Llorente et al. 2000; Llorente et al. 2011). The TOM-CAST model was also derived from FAST as a weather-timed fungicide spray forecasting system for tomato anthracnose, *Septoria* leaf spot and late blight (Pitblado 1992). TOM-CAST was later tested to reduce the application of sprays in the control of purple spot in asparagus (Meyer et al. 2000; Eichhorn et al. 2010).

A new forecast model for the integrated control of purple spot requires more detailed information of the pathogen's biology because the existing models, BSPcast and TOM-CAST, are not sufficiently adapted to the pathosystem *S. vesicarium* - asparagus. Therefore, the aim of this study was to determine and mathematically describe the period of ascospore flight in the field as well as how the biological processes comprising ascospore germination and ascospore germ tube growth depend on the temperature and leaf wetness duration, measured in a controlled environment.

3.3. Materials and methods

3.3.1. Effects of temperature and rain amount on ascospore flight

The ascospore flights of *S. vesicarium* were measured by spore traps at Hannover-Ahlem in 2014 and 2015, at Fuhrberg (25 km north of Hannover) in 2015 and at Schifferstadt in 2016 (17 km south-west of Mannheim). The reservoir of a trap-frame, which comprised a heavy water gutter and a wire grid, was filled with plant debris including pseudothecia up to two-thirds of the height. The debris was collected during the spring of each year for all the test locations in the same asparagus plantation in Fuhrberg. At least three microscope slides (traps) were coated with Vaseline and placed horizontally in the wire grid with the adhesive side down and above the plant debris. An area of 10 cm² (2.60 cm × 3.85 cm) was marked on each slide. Evaluations were performed weekly, or rarely after rain periods, by using a Leica DM2000 microscope at 200× magnification (Leica N Plan

20×/040 506096 lens × Leica HC Plan 10×/22 507807). Spores were counted on three tracks in the longitudinal direction on the slides and the average value for the three slides was then calculated. The number of spores per observation date was related to an area of 0.42 cm² according to the objective lens, the ocular and the length of the tracks. Spore catches were compared in each year and region with interpolated weather data obtained from meteorological stations and radar measurements from the German Meteorological Service (DWD), as described by Racca et al. (2010), which were provided by www.isip.de. Based on the methods used previously for similar diseases (Rossi et al. 2003; 2005; 2008), all of the data were used to model the cumulative percentage of trapped ascospores depending to the summed mean daily temperature T_{mean} (base 5 °C) starting from February 1st, together with the daily rain amount RA (either $RA > 0.0$ mm or $RA > 0.2$ mm). The summed temperature $SumT$ was then calculated as follows:

$$\begin{aligned} SumT(\text{day}) &= SumT(\text{day}-1) + (T_{mean} - 5) && \text{if } T_{mean} \geq 5^\circ \text{ C and } RA > 0.2 \text{ mm} \\ SumT(\text{day}) &= SumT(\text{day}-1) && \text{Otherwise} \end{aligned}$$

The cumulative percentage of trapped ascospores was modelled with a logistic, Gompertz (Gompertz 1828) and Chapman Richards function (von Bertalanffy 1957; Richards 1959):

$$\text{logistic:} \quad y(SumT) = 1 / (1 + \left(\frac{1-y_0}{y_0} \right) * \exp(-r_{LA} * SumT)) \quad [3.1]$$

$$\text{Gompertz:} \quad y(SumT) = \exp(\ln(y_0) * \exp(-r_{GA} * SumT)) \quad [3.2]$$

$$\text{Chapman:} \quad y(SumT) = (1 - \exp(-r_{CA} * SumT))^m, \quad [3.3]$$

where:

$y(SumT)$ = cumulative percentage of trapped ascospores depending on the summed temperature $SumT$

y_0 = $y(SumT = 0)$ = cumulative percentage of trapped ascospores at $SumT = 0$

r_{LA}, r_{GA}, r_{CA} = rate parameters for the logistic, Gompertz, and Chapman Richards function, respectively

$SumT$ = summed temperature (base 5 °C) and rainfall combination ($RA > 0.0$ or 0.2 mm)

m = shape parameter.

3.3.2. Effects of temperature and wetness duration on germination and germ tube length

The germination percentage (%) and the germ tube length (μm) were measured for ascospores at 5, 10, 15, 20, 25 and 30 °C after 1, 3, 6, 12 and 24 h with a Leica DM2000 microscope at 200 \times magnification and an ocular micrometre. The time steps represented the leaf wetness duration simulated on water agar. The ascospores were obtained from asparagus material with pseudothecia from the previous season, which were collected in the spring and frozen immediately at -22 °C. The asparagus material was defrosted under warm water, where the upper loose overlying epidermis was removed with tweezers and the pseudothecia were squeezed with a needle. The broken pseudothecia were then diluted in 25 ml of distilled water and 1000 μl of this suspension was transferred onto water agar plates (15 g agar per litre), before spreading with a disposable bacterial cell spreader (Roth®, AY19.1) with slight pressure on the surface. For each temperature, four replicates of 100 spores were prepared for germination and four replicates of 25 spores for determining the germ tube length.

At each of the six temperatures, the influence of leaf wetness duration (WD) on ascospore germination (GA) was modelled with a Chapman Richards function (von Bertalanffy 1957; Richards 1959):

$$GA(WD) = GA_{max} * [(1 - \exp(-r_{GA} * WD))]^m, \quad [3.4]$$

where:

$GA(WD)$ = percentage germinated ascospores (in %) depending on the leaf wetness duration WD (in h)

GA_{max} = maximum germination percentage (in %)

r_{GA} = rate parameter (in h^{-1})

m = shape parameter of the Chapman Richards function.

To model the combined influence of the leaf wetness duration (WD) and temperature (T) on ascospore germination (GA), the three parameters in the Chapman Richards function were treated as linear functions of the temperature: $GA_{max}(T) = a_k + b_k * T$, $r_{GA}(T) = a_r + b_r * T$ and $m(T) = a_m + b_m * T$. In a stepwise manner a_r and b_m were eliminated as they were

not significantly different from 0. Thus, the following function was fitted to the germination data:

$$GA(WD, T) = (a_k + b_k * T) * (1 - \exp(-(b_r * T) * WD))^{a_m}, \quad [3.5]$$

where:

$GA(WD, T)$ = percentage germinated ascospores (in %) depending on the leaf wetness duration WD (in h) and temperature T (in °C)

a_k = intercept of the linear temperature function $GA_{max}(T)$

b_k = slope of the linear temperature function $GA_{max}(T)$

b_r = proportionality factor for the temperature function $r_{GA}(T)$

a_m = shape parameter of the Chapman Richards function.

At each of the six temperatures, the effect of the leaf wetness duration WD on the germ tube length of ascospores LA (in μm) was modelled with a linear function that passed through the origin:

$$LA(WD) = b_{LA} * WD, \quad [3.6]$$

where:

$LA(WD)$ = germ tube length (in μm) depending on the leaf wetness duration WD (in h)

b_{LA} = slope (in $\mu\text{m h}^{-1}$).

In the second step, the resulting parameter values for b_{LA} were expressed as a temperature function, i.e. a generalised beta function (Hau 1988) as modified by Bassanezi et al. (1998):

$$b_{LA}(T) = b_{LAopt} \left(\frac{T - T_{min}}{T_{opt} - T_{min}} \right)^{n * \frac{T_{opt} - T_{min}}{T_{max} - T_{opt}}} * \left(\frac{T_{max} - T}{T_{max} - T_{opt}} \right)^n, \quad [3.7]$$

where:

$b_{LA}(T)$ = slope depending on temperature T (in °C)

b_{LAopt} = slope at T_{opt}

T_{max} = maximal temperature (in °C)
 T_{min} = minimal temperature (in °C)
 T_{opt} = optimal temperature (in °C)
 n = shape parameter of the beta function.

According to the results obtained by Montesinos et al. (1995b), the cardinal temperatures T_{min} and T_{max} were fixed at 0 °C and 35 °C, respectively.

In the final step, the two models were combined to describe the dependence of the germ tube length of ascospores LA on the leaf wetness duration WD and temperature T , as follows:

$$LA(WD, T) = b_{LA}(T) * WD \quad [3.8]$$

The three parameters in Eq. 3.8 (T_{opt} , n and b_{LAopt}) were estimated simultaneously.

3.3.3. Statistical software

Data preparation and statistical modelling were performed with Microsoft Excel 2016™, XLSTAT Version 2016.05.33324 (Copyright Addinsoft 1995-2016) and SigmaPlot for Windows Version 13.0 (Copyright Systat Software, Inc. 2014). The nonlinear functions were fitted to the data by nonlinear regression using the Levenberg-Marquardt algorithm.

3.4. Results

3.4.1. Effects of temperature and rain amount on ascospore flight

In the three years considered, ascospore flights occurred between March and early July, but most ascospores were released in early May (Fig. 3.1). There were large differences in the total amounts of ascospores trapped in Hannover-Ahlem (185.7 spores per 0.42 cm²) and Fuhrberg (104.1 spores per 0.42 cm²) during 2015. At both sites, there was a high release peak in the week before 1st May. The earliest flight and largest total amount of ascospores (537 spores per 0.42 cm²) occurred at Hannover-Ahlem in 2014.

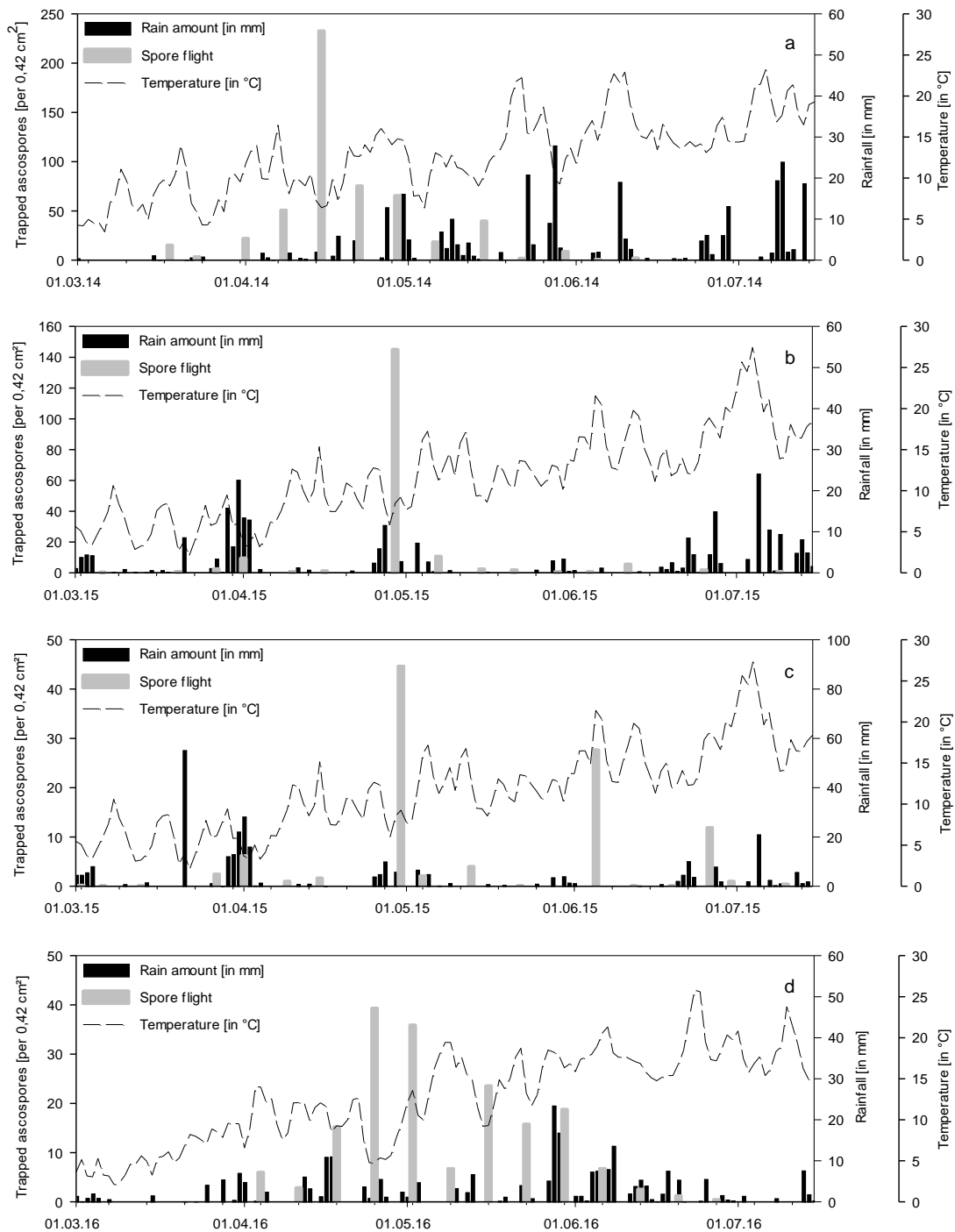


Figure 3.1 Weekly trapped ascospores [per 0.42 cm²] of *S. vesicarium* with daily mean temperature [in °C] and daily rainfall [in mm] from March 1st at (a) Hannover-Ahlem 2014, (b) Hannover-Ahlem 2015, (c) Fuhrberg 2015 and (d) Schifferstadt 2016

Different growth functions (Eqs. 3.1-3.3) were tested to model the cumulative number of trapped ascospores depending on the amount of rain and temperature. The best fit (Table 3.1) was obtained using the summed mean daily temperature (base 5 °C) as the

independent variable only on days when the amount of rain exceeded 0.0 mm starting from 1st February. All three tested functions showed a similar good fit, but the best result was achieved with a Chapman Richards function ($P < 0.0001$; $R^2 = 0.93$). At a $SumT$ value of 200 degree-days, about 50 % of all ascospores were trapped and 90 % of all ascospores were trapped at 400 degree-days (Fig. 3.2). Ascospore flights started at about 100 degree-days. The equivalent dates were 21st March for Hannover-Ahlem in 2014, 19th April for Hannover-Ahlem in 2015 and Fuhrberg in 2015 and 6th April for Schifferstadt in 2016. Due to the rapid increase of the model, the 95 % prediction band was broad, e.g. from 27 to 75 for 200 degree-days.

Table 3.1 Estimated parameter values for the logistic, Gompertz, and Chapman Richards functions (Eq. 3.1-3.3) for the cumulative percentage of trapped ascospores of *S. vesicarium* (r_{LA} , r_{GA} , and r_{CA} = rate parameters for the logistic, Gompertz, and Chapman Richards function, respectively; y_0 = y-intercept; m = shape parameter of the Chapman Richards function; $n = 81$).

	R ²	Parameter	Estimate	Standard error	P
logistic Base 5 °C; RA > 0.0	0.915	r_{LA}	0.017	0.002	<0.0001
		y_0	0.032	0.011	0.006
logistic Base 5 °C; RA > 0.2	0.864	r_{LA}	0.036	0.005	<0.0001
		y_0	0.044	0.017	0.013
Gompertz Base 5 °C; RA > 0.0	0.924	r_{GA}	0.011	0.001	<0.0001
		y_0	0.003	0.003	0.414
Gompertz Base 5 °C; RA > 0.2	0.868	r_{GA}	0.023	0.003	<0.0001
		y_0	0.012	0.011	0.306
Chapman Base 5 °C; RA > 0.0	0.925	r_{CA}	0.010	0.001	<0.0001
		m	4.290	1.102	<0.001
Chapman Base 5 °C; RA > 0.2	0.867	r_{CA}	0.019	0.003	<0.0001
		m	2.888	0.867	0.001

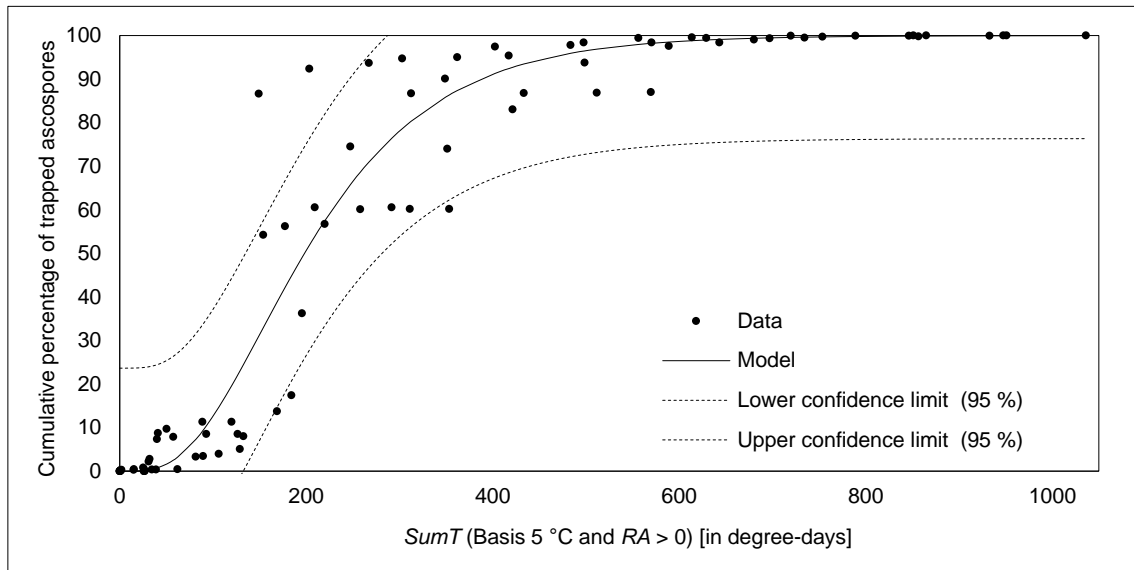


Figure 3.2 Cumulative percentage of trapped ascospores of *S. vesicarium* [in %] that is modelled by a Chapman Richards function (Eq. 3.3) depending on *SumT* (Base 5 °C and *RA* > 0.0) from February 1st (points = data, line = fitted Eq. 3.3 with parameter values from Table 3.1 and dotted line = lower and upper confidence limit (95 %))

3.4.2. Effects of temperature and wetness duration on germination

The dependence of germination on the temperature and leaf wetness was modelled using the data obtained from laboratory experiments. The shape of the germination curve changed with the temperature, where the curve at 5 °C looks S-shaped, but the curves at higher temperatures resemble monomolecular functions without points of inflection (Fig. 3.3). At each temperature level, the effect of the leaf wetness duration was described by a Chapman Richards function (Eq. 3.4) with $R^2 \geq 0.96$ (Table 3.2). The estimated values of r_{GA} and m at temperatures of 10 °C and 15 °C were not statistically significantly different from 0, because P -values were > 0.05 (Table 3.2). The high values of r_{GA} and m at 20 °C were influenced by the strong increase in germination observed between the first and third hour of the leaf wetness duration (Fig. 3.3). The G_{max} values roughly increased from 5 °C to 30 °C (Table 3.2). Excluding the extraordinary parameter values at 20 °C for a moment (Table 3.2), an increase in the temperature caused a weakly increasing trend in the values of r_{GA} and a decreasing trend in the values of m .

For simplicity, the three parameters in the Chapman Richards function were treated as linear functions of the temperature. As a_r and b_m were not significantly different from 0, they were eliminated in a stepwise manner. Therefore, the ascospore germination (GA) was modelled by function 5 ($R^2 = 0.90$; Table 3.3). The result was a Chapman Richards

function for WD where GA_{max} and r_{GA} were temperature dependent, while a_m was constant. This specific adaptation was made because various other models, like a generalized beta-Chapman Richards function, had led to worse results. The optimum temperature, calculated as the intersection point at 100 %, was 31.04 °C (not shown in Fig. 3.4). The surface of the three-dimensional graph described the data reasonably well, although the germination percentage after 24 h was underestimated at low temperatures.

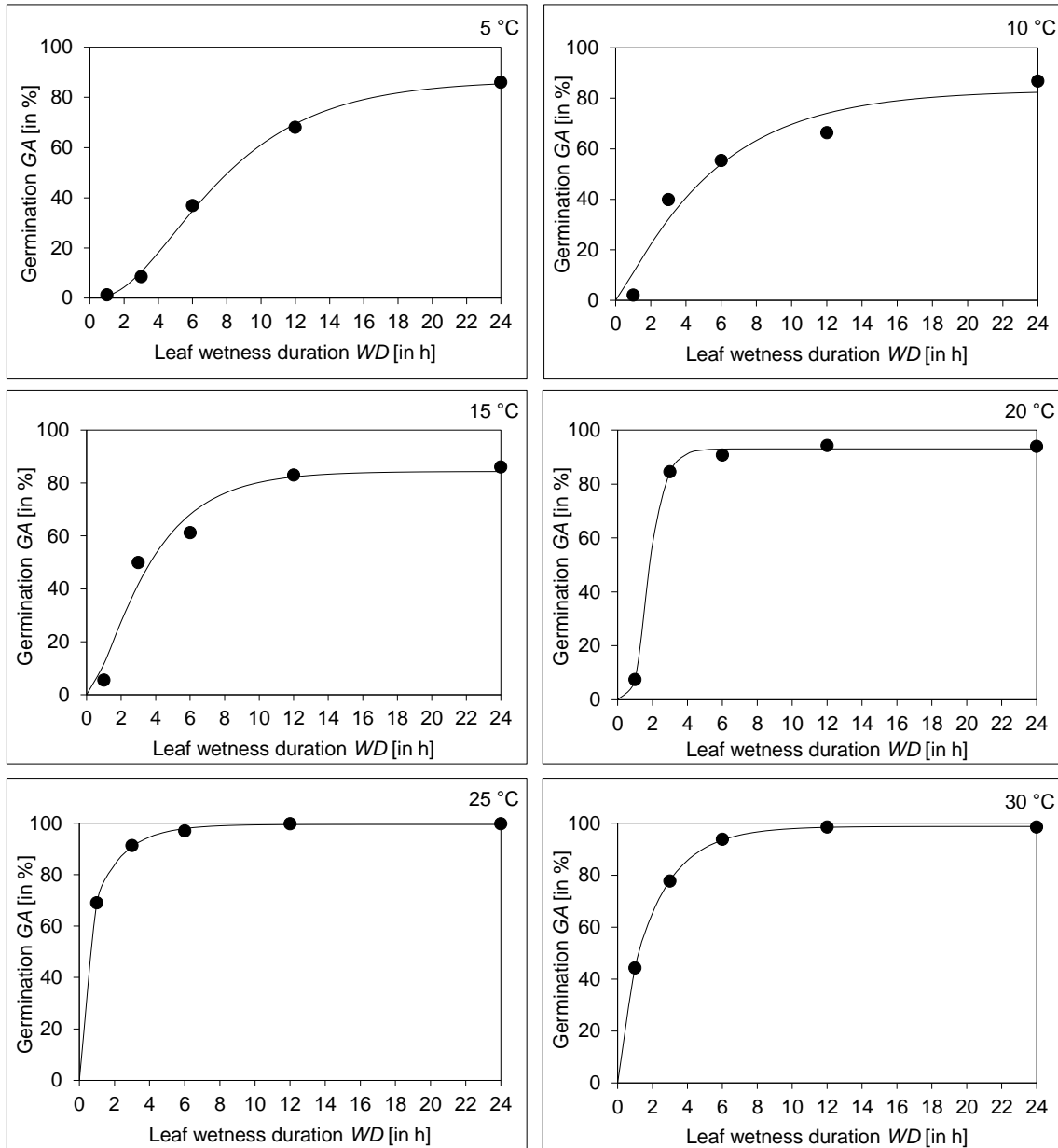


Figure 3.3 Germination of ascospores of *S. vesicarium* GA [in %] depending on the leaf wetness duration WD for different temperature levels (points = data, line = fitted Eq. 3.4 with parameter values from Table 3.2)

Table 3.2 Estimated parameter values for the Chapman Richards function (Eq. 3.4) for the germination of ascospores of *S. vesicarium* GA (in %) depending on leaf wetness duration WD for temperatures of 5, 10, 15, 20, 25, and 30 °C (GA_{max} = maximum germination of ascospores (in %); r_{GA} = rate parameter (h^{-1}); m = shape parameter).

Temperature	R ²	Parameter	Estimate	Std. Error	P
5 °C	0.99	GA_{max}	86.803	2.253	<0.0001
		r_{GA}	0.216	0.024	0.003
		m	2.852	0.439	0.007
10 °C	0.96	GA_{max}	83.252	9.582	0.003
		r_{GA}	0.196	0.121	0.204
		m	1.175	0.642	0.165
15 °C	0.97	GA_{max}	84.371	5.823	0.001
		r_{GA}	0.348	0.149	0.102
		m	1.620	0.818	0.142
20 °C	0.99	GA_{max}	93.044	0.906	<0.0001
		r_{GA}	1.573	0.122	0.001
		m	10.827	1.974	0.012
25 °C	0.99	GA_{max}	99.508	0.416	<0.0001
		r_{GA}	0.544	0.049	0.002
		m	0.420	0.034	0.001
30 °C	0.99	GA_{max}	98.730	0.168	<0.0001
		r_{GA}	0.453	0.008	<0.0001
		m	0.796	0.013	<0.0001

Table 3.3 Estimated parameter values for the modified function (Eq. 3.5) for the germination of ascospores of *S. vesicarium* GA (in %) depending on the temperature T and leaf wetness duration WD (a_k and b_k = parameters of the linear temperature function $GA_{max}(T)$; b_r = proportionality factor for the temperature function $r_{GA}(T)$; a_m = shape parameter of the Chapman Richards function).

R ²	Parameter	Estimate	Std. Error	P
0.90	a_k	71.906	7.091	<0.0001
	b_k	0.905	0.310	0.007
	b_r	0.039	0.011	0.001
	a_m	2.110	0.800	0.014

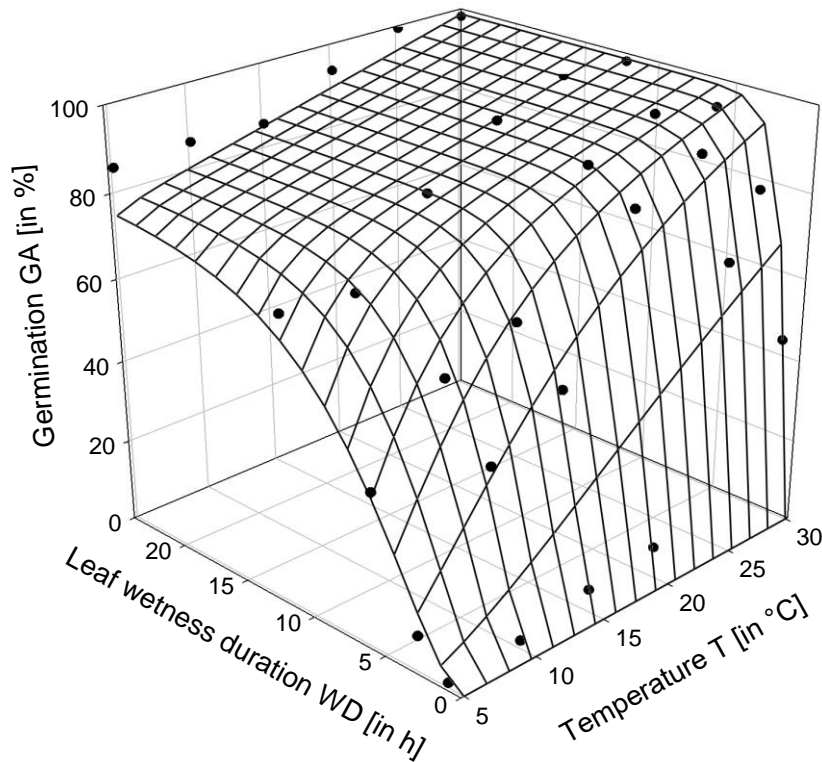


Figure 3.4 Modelled germination of ascospores of *S. vesicarium* GA [in %] depending on temperature T and the leaf wetness duration WD (points = data, surface = fitted Eq. 3.5 with parameter values of Table 3.3)

3.4.3. Effects of temperature and wetness duration on germ tube length

At each temperature level, the germ tubes grew in a linear manner depending on the WD (Fig. 3.5), and thus the length was modelled as a linear function of WD (Eq. 3.6). The highest slope ($27.07 \mu\text{m h}^{-1}$) for the germ tube length occurred at $25 \text{ }^\circ\text{C}$ and the lowest ($3.27 \mu\text{m h}^{-1}$) at $5 \text{ }^\circ\text{C}$ (Table 3.4). In addition to the linear function, an exponential adjustment was also tested, which led to a much worse fit.

The relationship between the slope values and temperature T could be described by a generalised beta function (Eq. 3.7) where $R^2 = 0.96$ (Fig. 3.6), with an estimated optimal temperature at $30.23 \text{ }^\circ\text{C}$ (Table 3.5). The combination of the generalised beta and linear function (Eq. 3.8) with the parameter values estimated for WD and T (Table 3.6) described the data very well (Fig. 3.7). The temperature range with high germ tube growth varied between $25\text{-}35 \text{ }^\circ\text{C}$, with an estimated optimal temperature of $30.42 \text{ }^\circ\text{C}$.

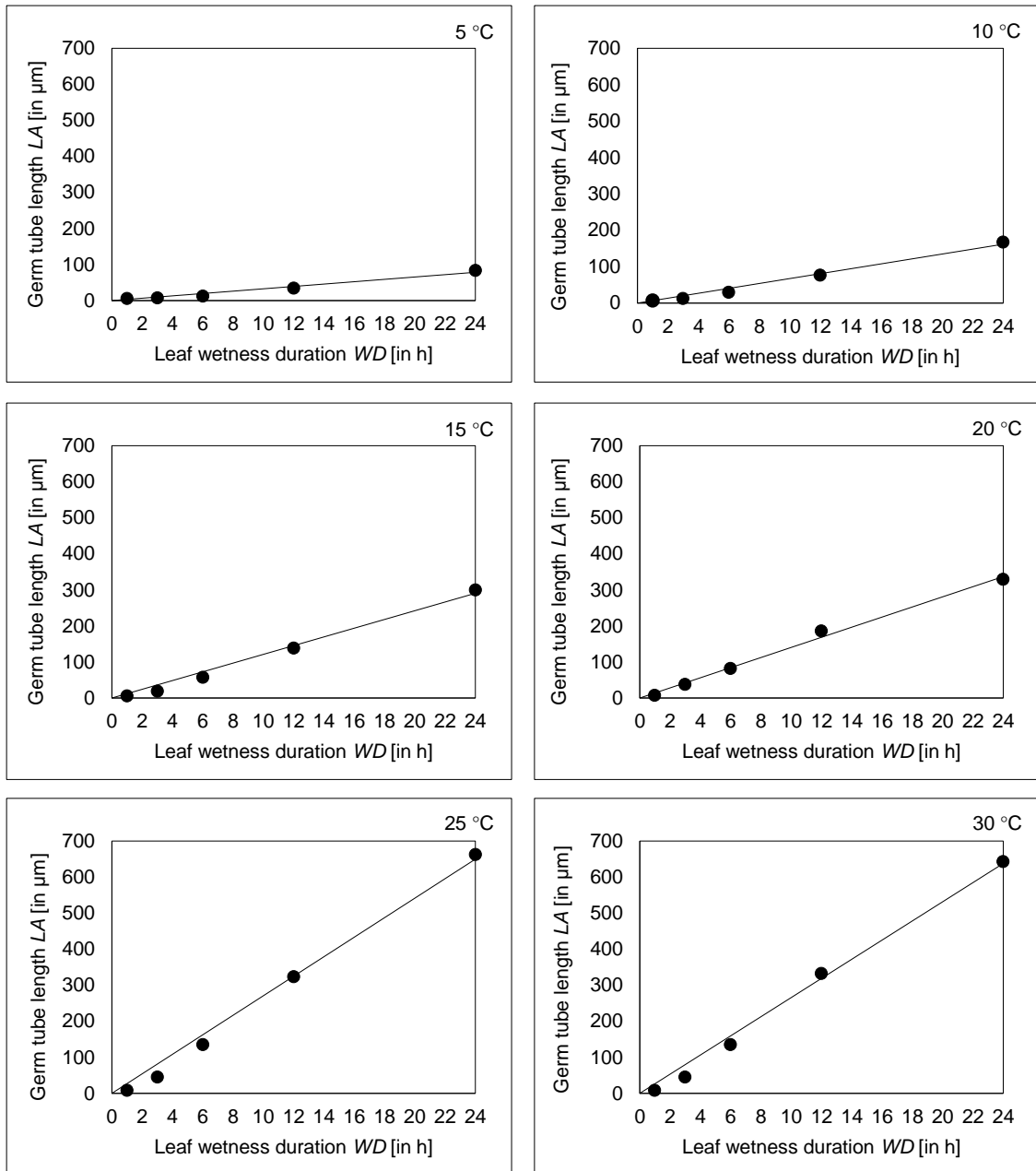


Figure 3.5 Germ tube length of ascospores of *S. vesicarium* LA [in μm] depending on the leaf wetness duration WD for temperature levels of 5, 10, 15, 20, 25 and 30 °C (points = data and line = fitted linear Eq. 3.6 with parameter values of Table 3.4)

Table 3.4 Estimated slope b_{LA} parameter values (in $\mu\text{m h}^{-1}$) for the linear function (Eq. 3.6) for the germ tube length of ascospores of *S. vesicarium* depending on the leaf wetness duration WD at temperatures 5 °C, 10 °C, 15 °C, 20 °C, 25 °C, and 30 °C

Temperature	R ²	b_{LA}	Std. Error	P
5 °C	0.97	3.272	0.191	<0.0001
10 °C	0.99	6.743	0.273	<0.0001
15 °C	0.99	12.107	0.482	<0.0001
20 °C	0.99	14.039	0.382	<0.0001
25 °C	0.99	27.070	0.930	<0.0001
30 °C	0.99	26.576	0.882	<0.0001

Table 3.5 Estimated parameter values for the generalized beta function (Eq. 3.7)* for the slope b_{LA} of the germ tube length (in $\mu\text{m h}^{-1}$) of ascospores of *S. vesicarium* depending on the temperature T (b_{LAopt} = slope of germ tube length at T_{opt} ; T_{opt} = optimal temperature (in °C); n = shape parameter).

R ²	Parameter	Estimate	Std. Error	P
0.96	b_{LAopt}	27.28	2.882	0.001
	T_{opt}	30.23	4.333	0.002
	n	0.284	0.513	0.610

* fixed values: $T_{min} = 0$ °C, $T_{max} = 35$ °C

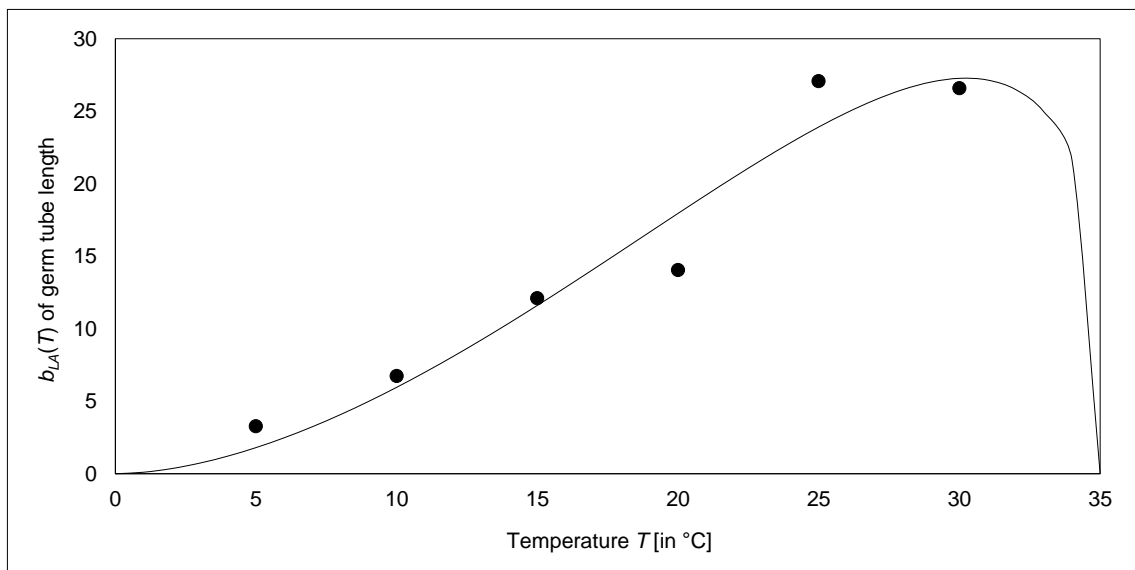


Figure 3.6 Modelled $b_{LA}(T)$ of the germ tube length of ascospores of *S. vesicarium* depending on temperature T (points = estimated data for b_{LA} from Table 3.4 and line = fitted Eq. 3.7 with parameter values from Table 3.5)

Table 3.6 Estimated parameter values for the generalized beta-linear function (Eq. 3.8)* for the germ tube length of ascospores of *S. vesicarium* LA (in $\mu\text{m h}^{-1}$) depending on the temperature T and leaf wetness WD (b_{LAopt} = slope of germ tube length (in μm) at T_{opt} ; T_{opt} = optimal temperature (in $^{\circ}\text{C}$); n = shape parameter)

R^2	Parameter	Estimate	Std. Error	P
0.97	b_{LAopt}	27.376	1.091	<0.0001
	T_{opt}	30.420	1.231	<0.0001
	n	0.266	0.113	0.024

* fixed values: $T_{min} = 0\text{ }^{\circ}\text{C}$, $T_{max} = 35\text{ }^{\circ}\text{C}$

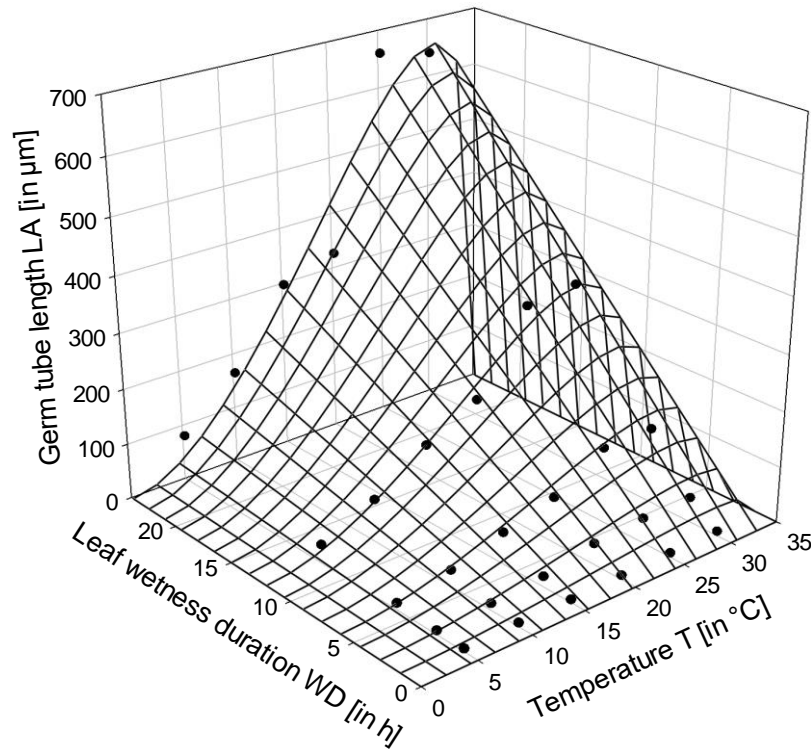


Figure 3.7 Modelled germ tube length of ascospores of *S. vesicarium* LA [in μm] depending on temperature T and the leaf wetness duration WD (points = data and surface = fitted Eq. 3.8 with parameter values from Table 3.6)

3.5. Discussion

Similar to other fungal pathogens, *S. vesicarium* must pass through several life phases until asparagus can be colonised and purple spot develops. The understanding of the seasonal course of ascospore flights is essential to avoid the occurrence and development of purple spot. In the three years of observations in this study, the ascospore flights occurred between March and June, and mostly after rain periods. The majority of the ascospores were released by early May. Despite climatic differences, the periods of

ascospore flights are roughly comparable with those reported previously (Falloon and Tate 1986; Menzies et al. 1992; Prados-Ligero et al. 2003; Rossi et al. 2008; Granke and Hausbeck 2012). In our trials, we stopped the measurements of ascospore release after several periods without spore catches and by carefully verifying that all of the pseudothecia were already empty. Thus, no later ascospore releases were possible from these pseudothecia.

In Hannover-Ahlem, a larger amount of ascospores was trapped during 2014 (Fig. 3.1a), which may have been a consequence of favourable conditions for the formation of sexual organs and the spreading of spores, particularly as the source and quantity of debris were equal to those in other years. Humidity is a decisive factor for the development of pseudothecia, as reported for *S. vesicarium* on pear (Llorente and Montesinos 2004) and garlic (Prados-Ligero et al. 1998), as well as for other related fungi (Gadoury et al. 1984; Trapero-Casas and Kaiser 1992). During winter, pseudothecia only developed at high relative humidity (> 96 %) and the optimum temperature for maturation was between 10 °C and 15 °C according to Llorente et al. (2006). In pear, the dynamics of pseudothecia maturation in the field were determined previously and the relationship between the proportion of mature pseudothecia and cumulative degree-days was modelled and validated (Llorente and Montesinos 2004). According to this model, ascospores mature from January to May, which agrees with our observations. The conditions for the maturation of pseudothecia (Llorente and Montesinos 2004; Llorente et al. 2006) were achieved in all years and regions for ascospore flight measurements. Similar to other fungi, the key factor that affects the release of mature ascospores is rain (Llorente and Montesinos 2006; Llorente et al. 2008). However, we found that it was dry from 1st March to 1st May during 2014 in Hannover-Ahlem, especially compared with the trials in 2015. The number of pseudothecia was not counted in the traps and thus the influence of the source material cannot be excluded, which is a reason why a relative view of the data is more meaningful, especially for modelling.

The accumulated ascospore flight was described best ($R^2 = 0.93$) by a Chapman Richards function (Eq. 3.3), depending on the sum of daily temperatures with a base of 5 °C summed on rainy days ($RA > 0.0$) only. This will allow us to calculate the daily ascospore flight potential in a future forecast model.

After release, ascospores must land on a suitable host to start the infection process. Infection by *S. vesicarium* depends on the temperature, leaf wetness, rainfall and vapour

pressure deficit (Montesinos and Vilardell 1992; Granke and Hausbeck 2010), while the relative humidity plays a role in the absence of rainfall (Prados-Ligero et al. 2003). As key components of the infection process, we modelled the dependence on the leaf wetness duration WD and temperature T for germination and the growth of the germ tube from ascospores. The fitted Chapman Richards function with a temperature-dependent germination capacity and rate (Eq. 3.5) exhibited a rapid increase in the first hours and a wide temperature range with a warm optimum above 30 °C (Fig. 3.4), which differs from the descriptions of these processes on other hosts in previous studies. The rapid germination of ascospores is known on pear plants, but with a significantly lower optimum temperature of 18.9 °C (Llorente et al. 2006). Rossi et al. (2006) found that strains isolated from pear plants exhibited maximum germination after incubation for 48 h in water at 21-23 °C. Few ascospores germinated below 15 °C and at 30-35 °C. At 100 % relative humidity, germination decreased by about one-third and no germination was observed below 80 % (Rossi et al. 2006).

Instead of using a linear temperature function (temperature range 5-30 °C) for the germination capacity in the Chapman Richards function, we also tested a generalised beta function with cardinal temperatures of 0 °C and 35 °C, where we estimated an optimum temperature close to 25 °C, but the shape parameter was not significantly different from 0 and the R^2 value was lower than for the linear function. Thus, the linear-Chapman Richards function could be used in the future forecast model in a temperature range from 5 °C to 30 °C. Above T_{opt} (31.04 °C), the model should decrease linearly to reach a value of 0 at 35 °C. Thus, the temperature dependence is described by a triangular function. This reflects the biological fact that an optimal temperature T_{opt} for germination exists and temperatures above T_{opt} have a damaging effect.

The germ tube length (Fig. 3.7) was modelled by a beta-linear function (Eq. 3.8) with a rather narrow optimum range around the optimal temperature of 30.4 °C. While germination has taken place in a very wide temperature range (Fig. 3.4), germ tube length was much more restricted, especially at low temperature levels (Fig. 3.7). Thus, germ tube length is a more limiting factor for infection and thus it could be more useful in a forecast model. There are no previous reports of ascospore germination on asparagus strains. To the best of our knowledge, no studies have investigated the influence of the leaf wetness duration and the temperature on the germ tube length of ascospores of *S. vesicarium*.

A maximum temperature of 35 °C was assumed for the germination (Fig. 3.4) and the germ tube growth (Fig. 3.6 and 3.7) based on disease severity data obtained for *S. vesicarium* on pear leaves and fruit (Montesinos et al. 1995b), and the mycelium growth of pear isolates (Montesinos and Vilardell 1992). Few germination between 30 °C and 35 °C is known for ascospores on pear (Rossi et al. 2006). Thus, it may be appropriate to examine additional high temperatures for both phases to determine the exact upper cardinal temperature. On the other hand, the high temperature optima (around 30 °C) that we found for both models play a subordinate role in Germany at the time of ascospore release. During the flights of ascospores until early July, the mean daytime temperatures were mostly below 20 °C (Fig. 3.1). In summary, the fixed maximum temperature of 35 °C is justifiable, even if the drop from 30 °C to 35 °C of the germination (Fig. 3.4) and the germ tube growth (Fig. 3.7) is drastic. Overall, the monocyclic phase can be roughly assigned into the mesophilic growth range, which is typically between 0 °C and 35 °C with an optimal temperature between 25 °C and 30 °C (Dix and Webster 1995).

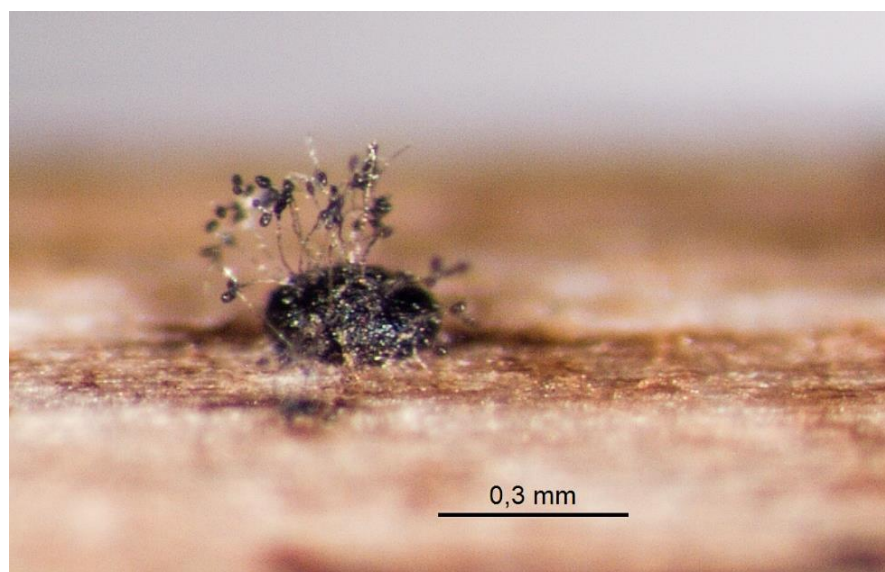


Figure 3.8 Conidia of *S. vesicarium* formed directly on pseudothecia on plant debris

During the experiments, we made observations related to further possible increases in the spread of the disease in asparagus. Similar to the results obtained for pear by Llorente et al. (2012), we observed that conidia formed directly on the asparagus debris, including directly on pseudothecia (Fig. 3.8). Johnson (1990) previously reported that conidial infections from overwintered asparagus debris produced typical primary infections on asparagus. During the monocycle phase, the extent of conidia formation directly on plant

residues and on pseudothecia as well as their effects on disease development have not been investigated.

Persistent moisture from dew seems to be an additional catalyst of the infection process, regardless of rainfall. The fine phylloclades form a very large surface for the attachment of moisture. Studies have shown that longer periods of dew or fog supported greater rates of infection by *Stemphylium* on *Trifolium* and *Medicago* (Bradley et al. 2003). A long duration of leaf wetness due to dew also occurs in the morning on asparagus, and the foliage also remains wet for several hours after overhead irrigation.

Understanding the monocyclic phase of *S. vesicarium* may explain parts of the early seasonal phase of purple spot. The flights of ascospores are often finished before the majority of asparagus fields have been harvested, so the control of the monocyclic phase of *S. vesicarium* with fungicides might be ineffective in Germany. Indeed, the influence of ascospore infection on epidemics in the field might be more severe when the harvest ends earlier or even in non-harvested young plantings. Finally, it is necessary to obtain data related to the more important polycyclic phase of *S. vesicarium* in asparagus to obtain comprehensive biological background data.

The modelled parts of the monocyclic phase of *S. vesicarium* have been integrated in the new forecast model SIMSTEM. Later versions of SIMSTEM will also include elements of the polycyclic phase. This model forecasts the beginning of the epidemics and the disease progression (proportional to the diseased leaf area). However, cultivation methods, like the choice of varieties, the plant's age, the end of harvest, and the selection of machines and fungicides, can have a major impact on the disease progression and thus on the accuracy of the model. As described in the introduction, the removal (Falloon et al. 1984) or burying of plant debris from the previous year is also influencing the occurrence of purple spot in the following season (Johnson 1990). Wounding of spears caused by sand can lead to more lesions and shorter wetting duration needed for the development of lesions (Lacy 1982; Johnson and Lunden 1986). Therefore, the SIMSTEM model cannot be seen as the only strategy to control purple spot, but it forms an essential computer-based tool for decision-support.

SIMSTEM uses area-specific weather data obtained from standard meteorological stations (provided by the German Meteorological Service or the Regional Plant Protection Offices) or simulated data (Racca et al. 2010). All of the modelled rates are calculated using hourly weather parameters for temperature (°C), relative humidity (%) and rainfall

(mm). The model's algorithm was developed by the Central Institute for Decision Support Systems in Crop Protection (ZEPP), and it will be available via the agricultural internet platform for integrated plant production (ISIP; www.isip.de), although it is currently in the test phase (2018). Strategies for the integrated management of purple spot on asparagus SIMSTEM model are currently in development.

Acknowledgements

This study was funded by the German Federal Ministry of Food and Agriculture (BMEL) and the Federal Office for Agriculture and Food (BLE) (grant number 2814702511).

4. Modelling the effects of temperature and wetness on the polycyclic phase of *Stemphylium vesicarium*, the pathogen causing purple spot on asparagus (*Asparagus officinalis* L.)

4.1. Abstract

The polycyclic phase of *Stemphylium vesicarium* is the key factor for the forecast and integrated control of purple spot on asparagus. The annual dynamics of airborne conidia were determined under field conditions by conidia traps. From 2013 to 2015, conidia became airborne at the earliest at mid-July, but the number trapped was considerably enhanced only after mid-August, early September. The cumulative percentage of trapped conidia was best described using a logistic function depending on the daily temperature sum (base 0 °C) accumulated only on days with > 0.2 mm of rainfall ($R^2 = 0.81$). The germination of conidia was modelled by a generalized beta-modified Chapman Richards function, and the germ tube length was modelled by a generalized beta-power function. Conidia germinated in a wide temperature range, with an optimum at 23.3 °C, whereas germ tube length had a narrow nearly optimum temperature range around 28.7 °C, which indicates that infection by conidia is more restricted by germ tube growth than by germination. The effect of temperature on the number of lesions produced by two strains on green asparagus spears had the narrowest optimum range (optimum at 21.9 °C) of all parts of the polycyclic phase. In plant tissue, the spread of the fungus depends on the mycelium growth. The mycelium growth of the four strains, which was modelled with data from a petri dish experiment, had an optimum temperature at 24.7 °C.

Keywords: Asparagus, Forecast, Purple spot, SIMSTEM, *Stemphylium vesicarium*

4.2. Introduction

Purple spot is an important fungal disease of asparagus caused by *Stemphylium vesicarium* (Wallr.) E.G. Simmons 1969, which affects asparagus-growing areas worldwide (Suzui 1973; Menzies 1980; Lacy 1982; Blancard et al. 1984; Falloon et al. 1984; Gindrat et

al. 1984; Thompson and Uys 1992; Cunnington and Irvine 2005), including Germany (Menzinger and Weber 1990). Over the winter, *S. vesicarium* produces ascospores in pseudothecia on plant debris, which are released from spring to early summer and present the primary inoculum source. The secondary inoculum (conidia) of *S. vesicarium* lead to infections in asparagus plantings during the summer to autumn (Falloon et al. 1984; Falloon and Tate 1986) and may induce premature defoliation of fern, which can cause yield losses up to 52 % during the next harvest season (Menzies et al. 1992).

The annual dynamics of airborne conidia of *S. vesicarium* has already been described in the literature. In asparagus fields in Michigan, only small amounts of conidia became airborne before July, slowly started rising in July, but significant amounts were measured in mid-August and September (Hausbeck et al. 1997; Granke and Hausbeck 2010). In pear cultivation, *S. vesicarium* is also of great economic importance and various biological processes of the fungus have already been described (Llorente et al. 2012). The annual conidia flight in pear happened from April to November, but 90 % of the conidia became airborne between July and September (Rossi et al. 2005; Llorente and Montesinos 2006; Llorente et al. 2008). This aspect of the polycyclic phase of *S. vesicarium* is known, but information about other biological processes of the conidia life cycle in asparagus is lacking.

Decision support systems can be useful for forecasting the date of exceeding control thresholds and of fungicide application. Using mathematical models, the time requirement for field evaluations can be minimized (Racca et al. 2002). The model FAST, for instance, is a forecast system for *Alternaria solani* on tomato (Madden et al. 1978). Later, BSPcast was derived from FAST by adapting it to the aetiology and epidemiology of *S. vesicarium* on pear (Montesinos and Vilardell 1992; Montesinos et al. 1995a; Montesinos et al. 1995b; Llorente et al. 2000; Llorente et al. 2011). The model TOM-CAST was also derived from FAST as a weather-timed fungicide spray forecast for tomato anthracnose, *Septoria* leaf spot and late blight (Pitblado 1992), and its potential to reduce spray applications for the control of purple spot of asparagus was also tested (Meyer et al. 2000; Eichhorn et al. 2010).

The integrated control of purple spot by a new forecast model requires more detailed information of the pathogen's biology because the existing models, BSPcast and TOM-CAST, are not sufficiently adapted to either the pathogen *S. vesicarium* or to the host asparagus. Important aspects of the monocyclic phase have been already modelled, and

the secondary polycyclic phase of purple spot seems to be more important for the modeling of the disease than the monocyclic phase (Bohlen-Janssen et al. 2018a). The aim of this study was to determine and mathematically describe the effect of temperature on five aspects of the polycyclic phase of *S. vesicarium* on asparagus as a base of a future forecast model. These aspects are the annual dynamics of airborne conidia, conidia germination, conidia germ tube growth, number of lesions as a measure of the disease efficiency, and mycelium growth.

4.3. Materials and methods

4.3.1. Spore traps and cumulative percentage of trapped conidia

The annual dynamics of airborne conidia of *S. vesicarium* was measured by spore traps in 12 m long double-rowed untreated (no fungicide treatments) experimental plots, with up to 2.20 m high fully developed plants, at Fuhrberg (25 km north of Hannover) in 2013, 2014 and 2015 and at Hannover-Ahlem in 2014 and 2015. Hannover is located in Lower Saxony in the Northern part of Germany. At Fuhrberg in 2013, a field with variety 'Backlim', planted in 2012, was used as a location for conidia catches. At Fuhrberg in 2014, the experiment was carried out in a plot with the variety 'Gijnlim', planted in 2009, and in 2015, with the variety 'Cumulus', planted in 2014. 'Gijnlim' was the variety of the fields at Hannover in both years, and in each case, asparagus was planted in the previous year. From early July to mid-October, two spore traps, microscopic slides with a marked area of 10 cm² (2.60 × 3.85 cm) coated with vaseline, were regularly checked at each of the five location-years. Traps were horizontally plugged in a self-built stand with the adhesive side up, 10 cm above the ground, directly under the asparagus plants in the middle of one row of the untreated plots. Evaluation was done weekly or sometimes after rain periods, with a Leica DM2000 microscope at 200× magnification (Leica N Plan 20×/040 506096 lens × Leica HC Plan 10×/22 507807). The species differentiation based on conidial morphology (Wiltshire 1938; Simmons 1967; 1969; 1985) is difficult and in some cases incorrect (Cunnington and Irvine 2005; Shenoy et al. 2007; Wang et al. 2010). However, based on clear results from Graf et al. (2016), we assumed that only *S. vesicarium* occurs in German asparagus plantings. Spores were counted on three tracks in the longitudinal direction of the slide, and then the average value was calculated. The indicated number of spores per trap corresponds to 0.42 cm². Spore catches were matched

with weather data for each year and region. Interpolated weather data from meteorological stations and radar measurements of the German Meteorological Service (DWD) were provided by www.isip.de as described by Racca et al. (2010).

To forecast the airborne conidia, correlations between the spore catch (transformed in % of the total number of conidia) and weather parameters were made following the methods used by other authors for similar diseases (Rossi et al. 2003; 2005; 2008). For the analyses of trapped conidia, the spore data were accumulated over time and expressed relative to the maximum. The data were modelled depending on the sum of daily mean temperatures T_{mean} (either T_{base} 0 °C or 5 °C) combined with the daily rain amount RA (either $RA > 0$ mm or $RA > 0.2$ mm) starting from the 1st of May. Then the temperature sum $SumT$ was calculated as follows:

$$SumT(\text{day}) = SumT(\text{day} - 1) + (T_{mean} - T_{base}) \quad \text{if } T_{mean} \geq T_{base} \text{ °C and } RA > 0 \text{ or } 0.2 \text{ mm}$$

$$SumT(\text{day}) = SumT(\text{day} - 1) + 0 \quad \text{Otherwise}$$

The cumulative percentage of trapped conidia was modelled with logistic, Gompertz (Gompertz 1828) and Chapman Richards functions (von Bertalanffy 1957; Richards 1959):

$$\text{Logistic:} \quad y(SumT) = 1 / (1 + \left(\frac{1-y_0}{y_0} \right) * \exp(-r_{LC} * SumT)) \quad [4.1]$$

$$\text{Gompertz:} \quad y(SumT) = \exp(\ln(y_0) * \exp(-r_{GC} * SumT)) \quad [4.2]$$

$$\text{Chapman:} \quad y(SumT) = (1 - \exp(-r_{CC} * SumT))^m, \quad [4.3]$$

where:

$y(SumT)$ = cumulative percentage of trapped conidia depending on $SumT$

y_0 = $y(SumT = 0)$ = cumulative percentage of trapped conidia at $SumT = 0$

r_{LC}, r_{GC}, r_{CC} = rate parameters for the logistic, Gompertz and Chapman Richards function, respectively

$SumT$ = Temperature sum (Base 0 °C or 5 °C) and rainfall combination ($RA > 0$ or 0.2 mm)

m = shape parameter.

4.3.2. Germination and germ tube length

The germination (in %) at 5 °C, 10 °C, 15 °C, 20 °C, 25 °C and 30 °C and germ tube length (in µm) at 15 °C, 20 °C, 25 °C and 30 °C of pure cultures St.sp.25.09.13.A and F were measured after 1, 3, 6, 12 and 24 h of leaf wetness with Leica DM2000 microscope at 200× magnifications and an ocular micrometre. Both strains had been identified as *S. vesicarium* by Graf et al. (2016). The strains were cultured on V8-medium (100 ml of V-8 juice, 2 g of CaCO₃, 16 g of agar per L) for 5 d in the dark and at 21 °C. To stimulate sporulation, the strains were exposed to UV-light for 30 min daily for another 9-15 d (Leach 1962; 1967). To create a spore suspension, the cultures were washed off with at least 25 ml of sterile deionized water. A volume of 1000 µl of this suspension was placed on water agar plates (15 g agar per L) and spread with disposable bacterial cell spreaders (Roth®, AY19.1) under slight pressure on the surface. For each temperature, four replications of 100 spores for germination and four replications of 25 spores of the germ tube length were considered. The dependence of the germination of the conidia (*GC*) on leaf wetness duration (*WD*) was modelled by the Chapman Richards function (von Bertalanffy 1957; Richards 1959):

$$GC(WD) = GC_{max} * (1 - \exp(-r_{GC} * WD))^m \quad [4.4]$$

where:

$GC(WD)$ = germinated conidia (in %) depending on leaf wetness duration WD (in h)

GC_{max} = maximum germination (in %)

r_{GC} = rate parameter (in h⁻¹)

m = shape parameter.

The maximal germination GC_{max} depending on temperature T was modelled with a generalised beta function (Hau 1988), as modified by Bassanezi et al. (1998).

$$GC_{max}(T) = GC_{opt} \left(\frac{T - T_{min}}{T_{opt} - T_{min}} \right)^{n*} \frac{T_{opt} - T_{min}}{T_{max} - T_{opt}} * \left(\frac{T_{max} - T}{T_{max} - T_{opt}} \right)^n \quad [4.5]$$

$GC_{max}(T)$ = maximal germination depending on temperature T (in °C)

GC_{opt} = germination at T_{opt}

T_{max} = maximal temperature (in °C)

T_{min} = minimal temperature (in °C)

T_{opt} = optimal temperature (in °C)

n = shape parameter

As cardinal temperatures 0 °C for T_{min} and 35 °C for T_{max} were chosen based on the results obtained by Montesinos et al. (1995b). GC_{opt} was fixed at 100 as the maximal germination was nearly 100 %.

In the final step, the two models (Eq. 4.4 and 4.5) were combined to describe germination in dependence on leaf wetness duration WD and temperature T . The rate parameter r_{GC} of the Chapman Richards function (Eq. 4.4) was assumed to be a linear function of temperature ($r_{GC}(T) = a_r + b_r T$) to describe the interactions between temperature and leaf wetness duration:

$$GC(WD, T) = GC_{max}(T) * (1 - \exp(-(a_r + b_r * T) * WD))^m \quad [4.6]$$

where:

$GC(WD, T)$ = germinated conidia (in %) depending on leaf wetness duration WD (in h) and Temperature T (in °C)

$GC_{max}(T)$ = maximal germination depending on temperature T (in °C)

a_r = intercept of the linear temperature function of $r_{GC}(T)$

b_r = slope parameter of the linear temperature function of $r_{GC}(T)$

m = shape parameter.

The effect of leaf wetness duration WD on the germ tube length of conidia LC (in μm) was modelled with a power function:

$$LC(WD) = a * WD^d \quad [4.7]$$

where:

$LC(WD)$ = germ tube length (in μm) depending on leaf wetness duration WD (in h)

a = scaling factor of the power function

d = exponent of the power function.

The effect of temperature T on the scaling factor a was modelled again with a generalised beta function (Hau 1988; Bassanezi et al. 1998) as in Eq. 4.5. For the germ tube length, $GC_{max}(T)$ is replaced by $a(T)$ and GC_{opt} by a_{opt} . Again, the cardinal temperatures $T_{min} = 0$ °C and $T_{max} = 35$ °C were chosen (Montesinos et al. 1995b). In the final step, the two models were combined to reach the dependence on leaf wetness duration WD and temperature T .

$$LC(WD, T) = a(T) * WD^d \quad [4.8]$$

4.3.3. Number of lesions as a measure for disease efficiency

The number of lesions appearing after artificial inoculation with the two strains St.sp.25.09.13.A and F were counted at temperature levels 10 °C, 15 °C, 20 °C, 25 °C and 30 °C. For each strain and temperature level, 7-8 green asparagus spears (approximate 1-1.5 cm in spear diameter; 18-19 cm in length) were placed close together (touching) on a 1 cm high wire frame in a plastic humidity chamber until the entire area (19 × 9 cm) was filled out. Below the wire frame, a 0.5 cm high water reservoir was filled in to guarantee high air humidity. A volume of 2 ml of a spore suspension with 5×10^4 spores per mL was sprayed on top of the spears, and after 5 d, the lesions per total area were counted. This trial was performed without light. For each strain, the number of lesions of the different temperature levels was expressed in percentage of the highest number at 20 °C. The number of lesions L (in %), depending on temperature T , was modelled again with a generalized beta function (Hau 1988; Bassanezi et al. 1998) as described in Eq. 4.5. In this case, $GC_{max}(T)$ is replaced by L and GC_{opt} by L_{opt} . Again, the cardinal temperatures $T_{min} = 0$ °C and $T_{max} = 35$ °C were chosen (Montesinos et al. 1995b), and L_{opt} was fixed at 100 %.

4.3.4. Mycelium growth

The optimum temperature curves for mycelium growth of the four strains St.sp.25.09.13.A, C, D and F were obtained. They all had been identified as *S. vesicarium* by Graf et al. (2016). 8-mm pieces from pure cultures were gouged by hand cork borers, (Roth® 0581.1) and transferred centrally with a needle on water agar. The radial growth of 2 × 15 plates of each fungal strain at temperature levels of 10 °C, 15 °C, 21 °C, 25 °C,

and 30 °C was measured after 9 d. For each strain, the radial growth of the different temperature levels was expressed in percentage of the highest growth (at 25 °C). The radial mycelium growth MG , depending on temperature T , was modelled again with a generalized beta function (Hau 1988; Bassanezi et al. 1998) as in Eq. 4.5. For the mycelium growth, $GC_{max}(T)$ is replaced by MG , and GC_{opt} by MG_{opt} . MG_{opt} was fixed at 100; again, the cardinal temperatures $T_{min} = 0$ °C and $T_{max} = 35$ °C were chosen (Montesinos et al. 1995b).

4.3.5. Statistical software

Data preparation and statistical modelling was done with software Microsoft Excel 2016™, XLSTAT Version 2016.05.33324 (Copyright Addinsoft 1995-2016) and SigmaPlot for Windows Version 13.0 (Copyright Systat Software, Inc. 2014). The nonlinear functions were fitted to the data by nonlinear regression using the Levenberg-Marquardt algorithm.

4.4. Results

4.4.1. Spore traps and cumulative percentage of trapped conidia

From 2013 to 2015, the dynamics of airborne conidia began at mid-July at the earliest, but only after mid-August, early September, the number of conidia trapped was considerably enhanced (Fig. 4.1). At Fuhrberg, the amount of trapped conidia was extremely low until September in all 3 years (Fig. 4.1a, b, d). In Hannover-Ahlem 2015 (Fig. 4.1e), there was only one week before September with more than 100 spores per 0.42 cm². The spore flight in Hannover-Ahlem 2014 (Fig. 4c), however, was much earlier and more pronounced than in all other cases. Here 102 spores per 0.42 cm² were already counted until the end of July, and spores were caught at all four sampling dates in August. In the first and second sampling period of August, over 500 spores per 0.42 cm² were trapped.

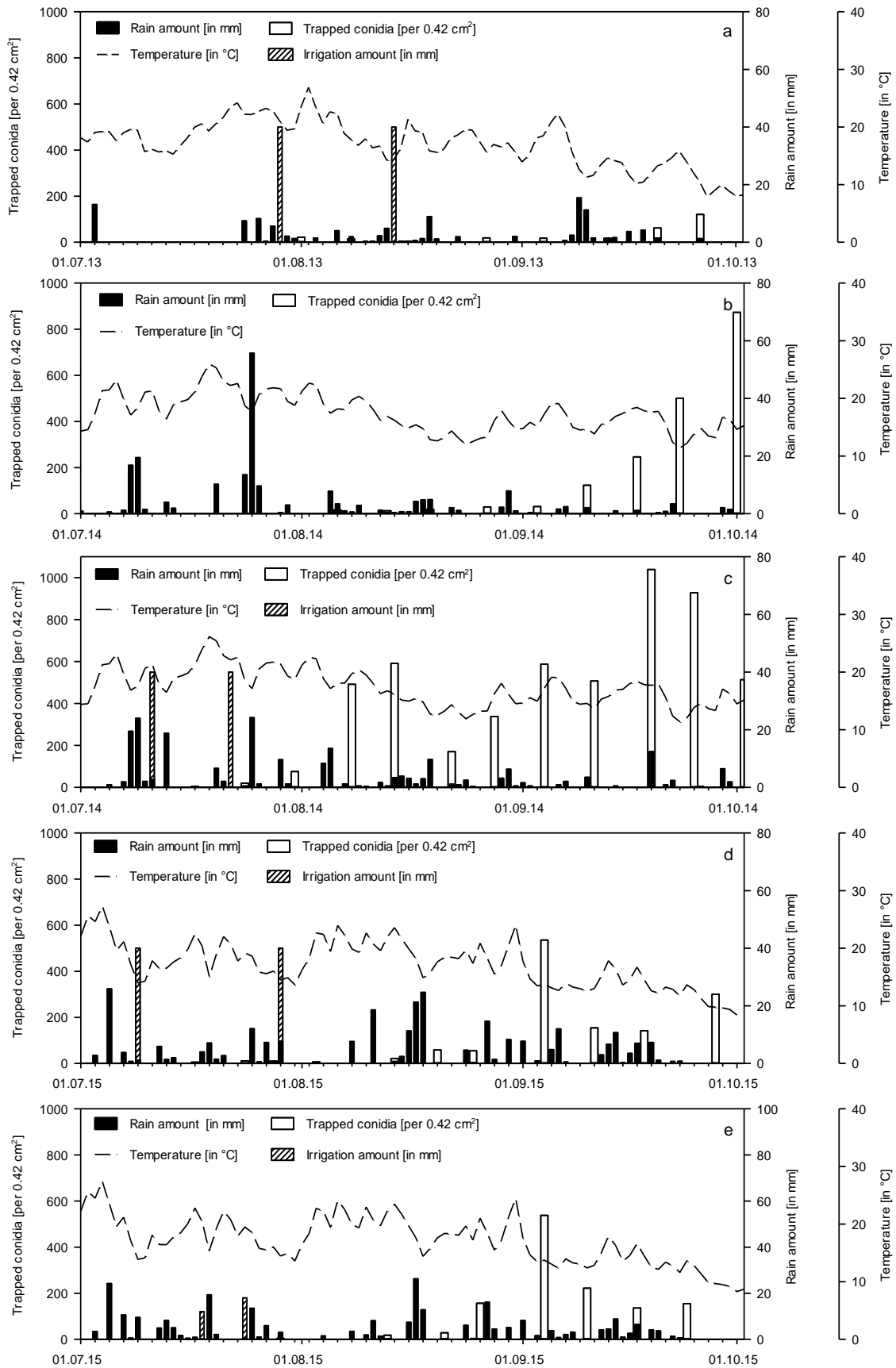


Figure 4.1 Weekly trapped *S. vesicarium* conidia [per 0.42 cm²] illustrated with daily temperature [in °C], daily rainfall [in mm], and irrigation amount [in mm] at Fuhrberg 2013 (a), Fuhrberg 2014 (b), Hannover-Ahlem 2014 (c), Fuhrberg 2015 (d) and Hannover-Ahlem 2015 (e)

For the mathematical description of the airborne conidia, the best fit was obtained using a logistic function (Eq. 4.1) and as an independent variable the sum of the mean daily temperature base 0 °C only on days with *RA* above 0.2 mm starting from the 1st of May. The variation of the base temperature and *RA* values in calculating *SumT* did not make any significant difference (Table 4.1). We have tested further combinations between 0 °C and 5 °C, each at *RA* over 0 mm and 0.2 mm, however, all attempts did not lead to a better fit of the model. The results of the Gompertz (Eq. 4.2) and the Chapman Richards functions (Eq. 4.3) were not listed separately for each temperature and rain combinations because the *AIC* values were higher (Spiess and Neumeyer 2010) and the R^2 values were lower (not significant) or equal, compared to the results of the logistic function. For all three functions, the *SumT* combination of 0.0 °C and 0.2 mm resulted in the best R^2 and *AIC* values.

The cumulative percentage of trapped conidia visibly starts at *SumT* of 600 degree-days (Fig. 4.2) which corresponds to the 1st of August for Fuhrberg 2013; the 20th of July for Fuhrberg 2014; the 24th of July for Hannover-Ahlem 2014; the 4th of August for Fuhrberg 2015; and the 24th of July for Hannover-Ahlem. Thus, it can be expected that conidia became airborne between July 20th and August 4th in the experimental years. A *SumT* value of 800 degree-days corresponds to approximately 10 % and of 1000 degree-days to approximately 50 % of the total number of conidia trapped.

Table 4.1 Estimated parameter values of the logistic function (Eq. 4.1) for the cumulative percentage of trapped *S. vesicarium* conidia (in %) (y_0 = y-intercept; r_{LC} = rate parameter of the logistic function, $n = 82$)

	R^2	<i>AIC</i>	Parameter	Estimate	Standard error	<i>P</i>
<i>SumT</i> (Basis 0 °C and <i>RA</i> > 0.0 mm)	0.79	-305.29	y_0	<0.001	<0.001	0.557
			r_{LC}	0.010	0.001	<0.001
<i>SumT</i> (Basis 0 °C and <i>RA</i> > 0.2 mm)	0.81	-312.23	y_0	<0.001	<0.001	0.5322
			r_{LC}	0.012	0.002	<0.0001
<i>SumT</i> (Basis 5 °C and <i>RA</i> > 0.0 mm)	0.79	-303.49	y_0	<0.001	<0.001	0.555
			r_{LC}	0.015	0.002	<0.0001
<i>SumT</i> (Basis 5 °C and <i>RA</i> > 0.2 mm)	0.80	-309.27	y_0	<0.001	<0.000	0.525
			r_{LC}	0.017	0.002	<0.001

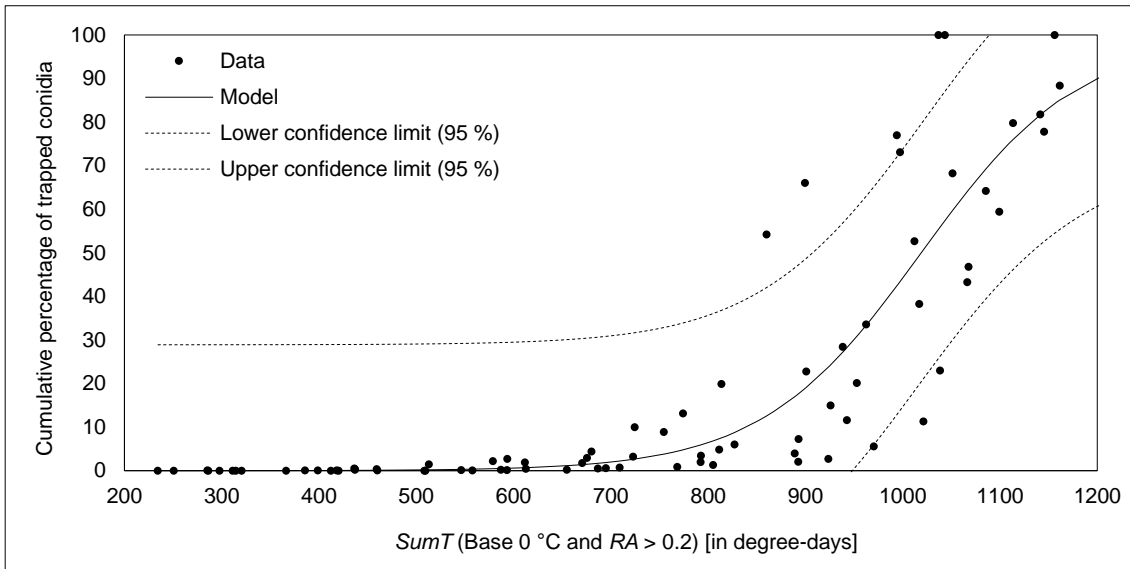


Figure 4.2 Cumulative percentage of trapped *S. vesicarium* conidia [in %] depending on *SumT* (base 0 °C and *RA* > 0.2 mm) starting on 1st May (points = data; line = fitted Eq. 4.1 with parameter values from Table 4.1; dotted line = lower and upper confidence limits (95 %))

4.4.2. Germination

The shape of the germination curves changed with temperature. At 5 °C, for instance, the curve was S-shaped, whereas at higher temperatures, the curves resembled graphs of monomolecular functions without a point of inflection (Fig. 4.3). At 10 °C, 80 % of the conidia germinated after 6 h, whereas at 20 °C, 25 °C and 30 °C over 90 % of the conidia germinated after only 3 h of leaf wetness. For each temperature level (Fig. 4.3), the effect of the leaf wetness duration was described by the Chapman Richards function (Eq. 4.4) with R^2 values ≥ 0.99 . At 20 °C, the value of parameter m was especially high (Table 4.2), which can be explained by the large increase in the germination between 1 and 3 h (Fig. 4.3). Based on the obtained model curves (Fig. 4.3) and values of the parameter r_{GA} and m (Table 4.2), we can conclude that there are interactions between temperature and leaf wetness duration.

Table 4.2 Estimated parameter values of the Chapman Richards function (Eq. 4.4) of the mean germination value of conidia of two *S. vesicarium* strains GC (in %) depending on leaf wetness duration WD at temperature levels of 5 °C, 10 °C, 15 °C, 20 °C, 25 °C and 30 °C (GC_{max} = maximum germination (in %); r_{GC} = rate parameter; m = shape parameter)

Temperature	R ²	Parameter	Estimate	Std. Error	P
5 °C	0.99	GC_{max}	79.750	2.863	0.000
		r_{GC}	0.227	0.030	0.005
		m	6.228	1.656	0.033
10 °C	0.99	GC_{max}	90.963	1.092	<0.0001
		r_{GC}	0.573	0.049	0.001
		m	3.740	0.594	0.008
15 °C	0.99	GC_{max}	95.753	1.241	<0.0001
		r_{GC}	0.962	0.086	0.002
		m	5.716	1.237	0.019
20 °C	0.99	GC_{max}	98.588	0.205	<0.0001
		r_{GC}	1.978	0.060	<0.0001
		m	14.012	0.944	0.001
25 °C	0.99	GC_{max}	96.946	0.672	<0.0001
		r_{GC}	1.537	0.141	0.002
		m	5.414	0.895	0.009
30 °C	0.99	GC_{max}	97.919	0.148	<0.0001
		r_{GC}	1.964	0.099	0.000
		m	5.761	0.616	0.003

The parameter values of G_{max} estimated for the six temperatures follow an optimum temperature curve. Therefore, a generalized beta function (Eq. 4.5) was used to describe the effect of temperature on G_{max} . As the estimated values of the rate parameter r_{GC} had an increasing trend with temperature (Table 4.2), we assumed that the rate parameter is a linear function of temperature, $r_{GC}(T) = a_r + b_r T$. The shape parameter m , however, was treated as a constant due to the absence of a clear trend of the estimated m values with temperature alterations (Table 4.2). Thus, the Chapman Richards function (Eq. 4.6) with temperature-dependent capacity and rate was fitted simultaneously to all six germination curves. This function describes the influence of temperature and leaf wetness duration on conidia germination very well ($R^2 = 0.99$). The optimal temperature of germination is 23.3 °C (Table 4.3). The temperature range with high germination rate is rather broad (Fig. 4.4) which is reflected in the low value estimated for parameter n (Bassanezi et al. 1998).

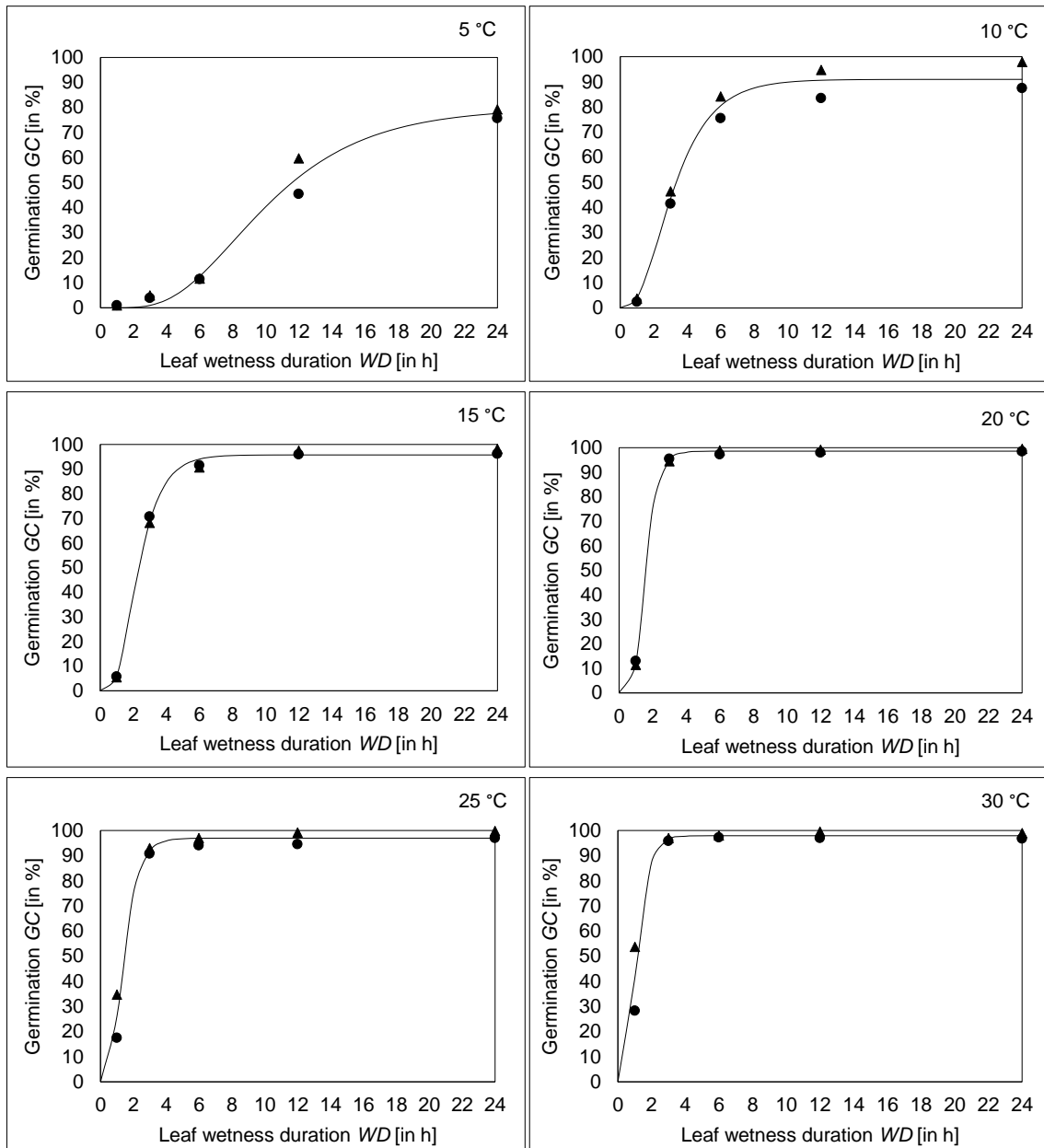


Figure 4.3 Germination of conidia of *S. vesicarium* GC [in %] depending on leaf wetness duration WD at temperature levels of 5 °C, 10 °C, 15 °C, 20 °C, 25 °C, and 30 °C (triangles = data of St.sp.25.9.13.A; points = data of St.sp.25.9.13.F; line = fitted Eq. 4.4 with parameter values from Table 4.2)

Table 4.3 Estimated parameter values of the modified generalized beta-Chapman Richards function (Eq. 4.6)* for the mean germination value of conidia of two *S. vesicarium* strains GC (in %) depending on temperature T and leaf wetness duration WD (T_{opt} = optimal temperature (in °C); n = shape parameter of the beta function; a_r = intercept of the linear temperature function of $r_{GC}(T)$; b_r = slope parameter of the linear temperature function of $r_{GC}(T)$; m = shape parameter of the Chapman Richards function)

R^2	Parameter	Estimate	Std. Error	P
0.99	T_{opt}	23.344	1.264	<0.0001
	n	0.105	0.029	0.001
	a_r	-0.144	0.024	<0.0001
	b_r	0.078	0.007	<0.0001
	m	6.554	1.220	<0.0001

* fixed values: $T_{min} = 0$ °C, $T_{max} = 35$ °C

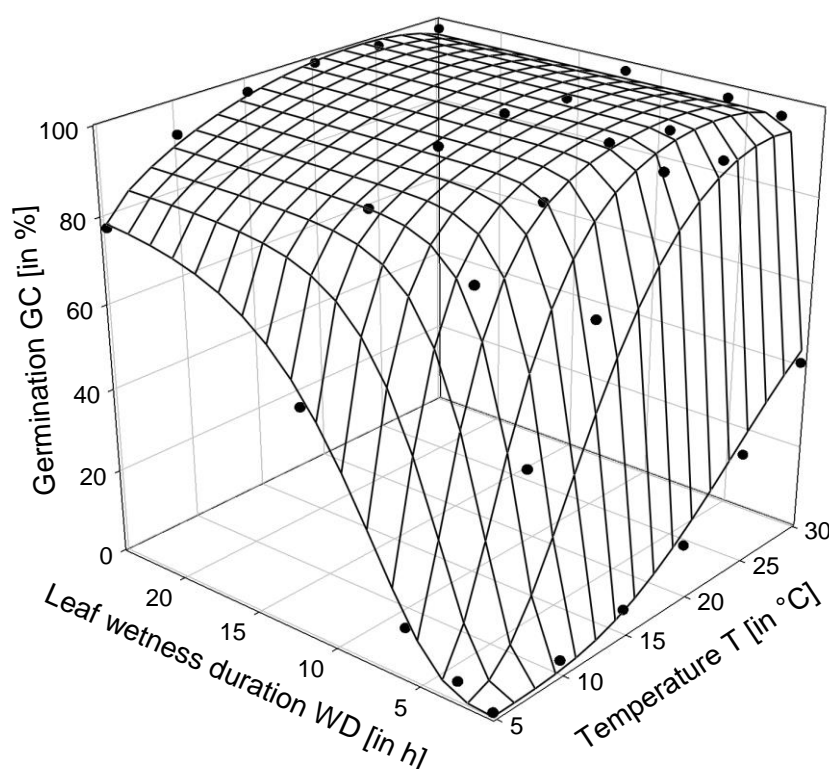


Figure 4.4 Modelled germination of conidia of *S. vesicarium* GC [in %] depending on temperature T and leaf wetness duration WD (points = mean value of two strains; surface = fitted Eq. 4.6 with parameter values from Table 4.3)

4.4.3. Germ tube length

For each of the four temperature levels, the germ tube of the conidia did not grow linearly, but with an increasing rate over time (Fig. 4.5). Accordingly, the power function (Eq. 4.7) resulted in a high goodness of fit with R^2 values ≥ 0.99 (Table 4.4). The highest germ tube length was observed at 25 °C and 30 °C (Fig. 4.5). From 15 °C to 30 °C the estimated

values of parameter d remained almost constant (Table 4.4). For parameter a , we assumed that the effect of temperature can be described by a generalized beta function (Eq. 4.5). Thus, the combined generalized beta-power function (Eq. 4.8) was simultaneously fitted to the germ tube data at the four temperature levels, resulting in the estimated parameter values presented in Table 4.5. The combined effect of WD and T is well described ($R^2 = 0.99$) as shown in the 3D-graph (Fig. 4.6). The estimated optimal temperature of the germ tube length is 28.7 °C and the shape parameter n is 0.56, i.e. considerably higher than that for the germination (Table 4.3).

Table 4.4 Estimated parameter values of a power function (Eq. 4.7) of the mean germ tube length value of conidia of two *S. vesicarium* strains *LC* (in μm) depending on leaf wetness duration WD for temperature levels of 15 °C, 20 °C, 25 °C and 30 °C (a = scaling factor of the power function, d = exponent)

Temperature	R^2	Parameter	Estimate	Std. Error	P
15 °C	0.99	a	5.003	1.476	0.043
		d	1.381	0.096	0.001
20 °C	0.99	a	13.807	3.365	0.026
		d	1.261	0.080	0.001
25 °C	0.99	a	11.169	0.899	0.001
		d	1.425	0.026	<0.0001
30 °C	0.99	a	14.313	2.666	0.013
		d	1.375	0.061	0.000

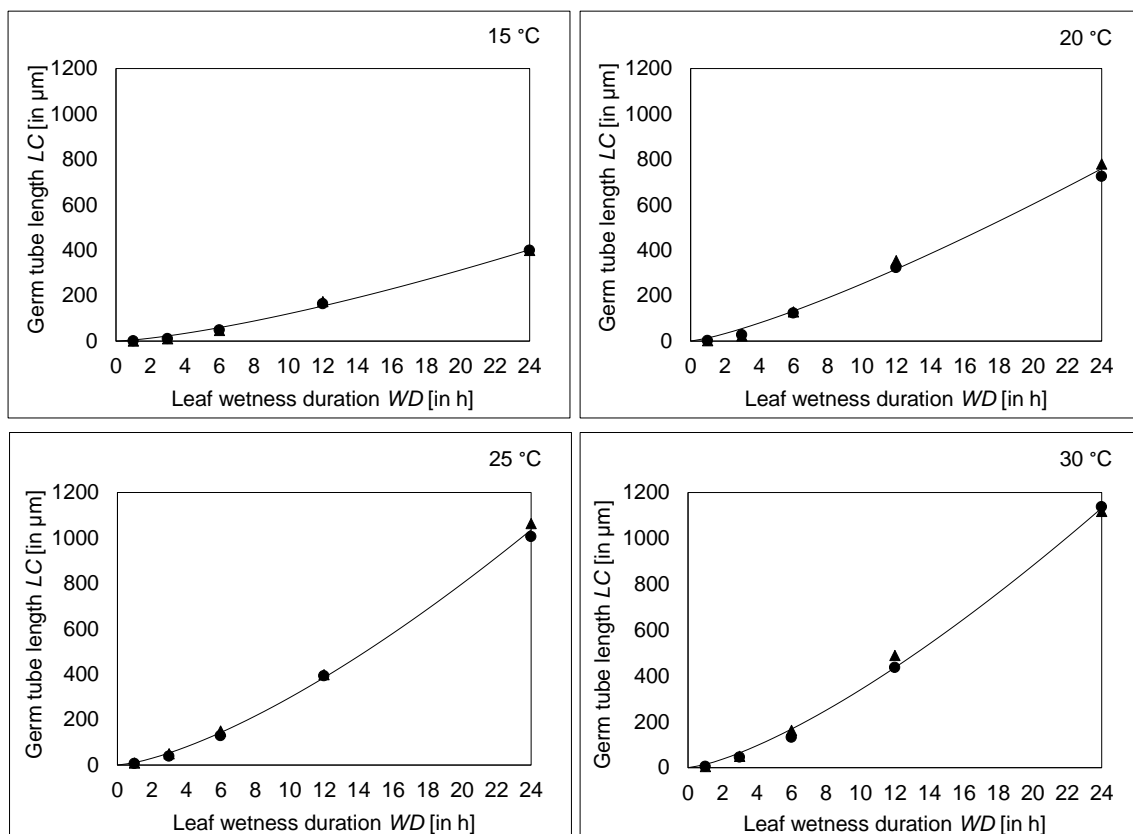


Figure 4.5 Germ tube length of conidia of *S. vesicarium* LC [in μm] depending on leaf wetness duration WD for temperature levels of 15 °C, 20 °C, 25 °C, and 30 °C (triangles = data of St.sp.25.9.13.A; points = data of St.sp.25.9.13.F; line = fitted Eq. 4.7 with parameter values from Table 4.4)

Table 4.5 Estimated parameter values of the generalized beta-power function (Eq. 4.8)* for the mean germ tube length value of conidia of two *S. vesicarium* strains LC (in μm) depending on temperature T and leaf wetness duration WD (a_{opt} = scaling factor of the power function at T_{opt} ; T_{opt} = optimal temperature (in °C); n = shape parameter of the generalized beta function; d = exponent of the power function)

R^2	Parameter	Estimate	Std. Error	P
0.99	a_{opt}	14.777	1.574	<0.0001
	T_{opt}	28.677	0.353	<0.0001
	n	0.564	0.075	<0.0001
	d	1.369	0.035	<0.0001

* fixed values: $T_{min} = 0$ °C and $T_{max} = 35$ °C

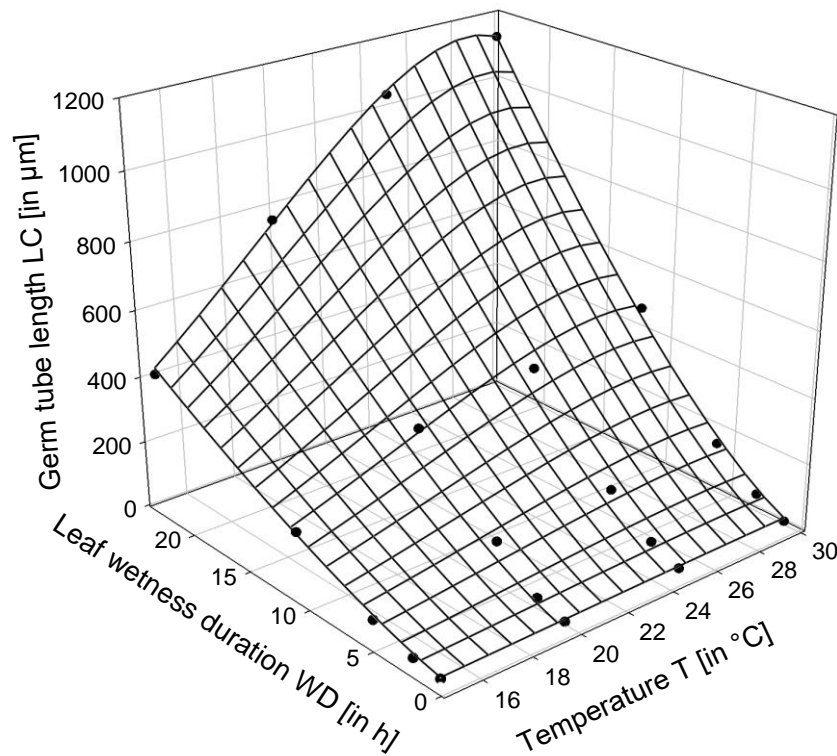


Figure 4.6 Modelled germ tube length of conidia of *S. vesicarium* LC [in μm] depending on temperature T and leaf wetness duration WD (points = mean value of two strains; surface = fitted Eq. 4.8 with parameter values from Table 4.5)

4.4.4. Number of lesions as a measure for disease efficiency

For both strains, the highest absolute number of lesions was observed at 20 °C, but the number of lesions of strain St.sp.25.09.13.F reached only 75.24 % of the number of lesions of St.sp.25.9.13.A. The generalized beta function (Eq. 4.5) was fitted to the relative lesion number (in % of the maximum values at 20 °C) resulting in an optimum temperature of 21.89 °C for the mean values of both strains (Table 4.6). The highest formation of lesions was in the range from 20 °C to 25 °C (Fig. 4.7). The mean value of parameter n was rather high (4.5), which led to an extremely narrow optimum range for temperature (Bassanezi et al. 1998). The duration of the incubation period was 4 d at 20 °C.

Table 4.6 Estimated parameter values of the generalized beta function (Eq. 4.5)* for number of lesions L (in %) of 2 different *S. vesicarium* strains depending on temperature T (T_{opt} = optimal temperature (in °C); n = shape parameter)

	R ²	Parameter	Estimate	Std. Error	P
St.sp.25.9.13.A	0.97	T_{opt}	22.296	0.399	<0.0001
		n	5.316	0.894	0.002
St.sp.25.9.13.F	0.95	T_{opt}	21.478	0.523	<0.0001
		n	3.485	0.577	0.002
MV (2 strains)	0.94	T_{opt}	21.89	0.374	<0.0001
		n	4.537	0.630	<0.0001

* fixed values: $T_{min} = 0$ °C, $T_{max} = 35$ °C, $L_{opt} = 100$ %

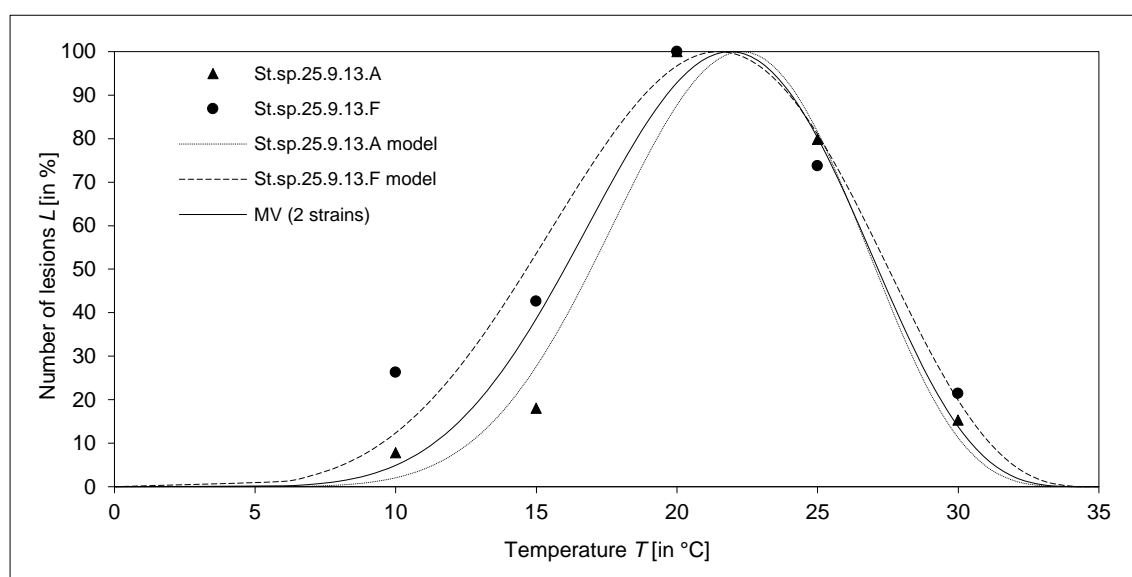


Figure 4.7 Effect of temperature T on the number of lesions L [in % of the maximum number at 20 °C] counted 5 d after the inoculation of conidia of two different *S. vesicarium* strains on green asparagus spears (points = data; line = fitted Eq. 4.5 with parameter values from Table 4.6; MV = mean value)

4.4.5. Mycelium growth

The highest radial growth for all four strains was observed at 25 °C, although the absolute mycelium growth differed among the strains. The growth of St.sp.25.09.13.F was most vigorous (2.98 cm) after 9 d at 25 °C. The strains St.sp.25.09.13.A and D reached only 83.9 % and 85.9 % of the growth of St.sp.25.09.13.F, whereas strain St.sp.25.09.13.C had a significantly lower growth with a relative value of only 71.5 %. The estimated optimum temperature of the generalized beta function (Eq. 4.5) for the mycelium growth of the four strains is 24.7 °C (Table 4.7). Strain St.sp.25.9.13.A has a clearly higher optimal temperature (26.0 °C) than those of the other three strains tested (Table 4.7, Fig. 4.8). The

value of parameter n for the mean values of all strains was 2.0, resulting in a wider optimal range than that for the number of lesions, but narrower than that for germination and germ tube length.

Table 4.7 Estimated parameter values of the generalized beta function (Eq. 4.5)* for the mycelium growth MG of 4 different *S. vesicarium* strains relative to the maximum (in %) depending on temperature T (T_{opt} = optimal temperature (in °C); n = shape parameter)

	R ²	Parameter	Estimate	Std. Error	P
St.sp.25.9.13.A	0.93	T_{opt}	25.965	0.524	<0.0001
		n	2.920	0.619	0.005
St.sp.25.9.13.C	0.94	T_{opt}	24.031	0.619	<0.0001
		n	1.985	0.374	0.003
St.sp.25.9.13.D	0.93	T_{opt}	23.990	0.666	<0.0001
		n	2.093	0.428	0.005
St.sp.25.9.13.F	0.98	T_{opt}	24.352	0.395	<0.0001
		n	1.964	0.243	0.001
MV (4 strains)	0.90	T_{opt}	24.726	0.349	<0.0001
		n	2.028	0.231	<0.0001

* fixed values: $T_{min} = 0$ °C, $T_{max} = 35$ °C, $MG_{opt} = 100$ %

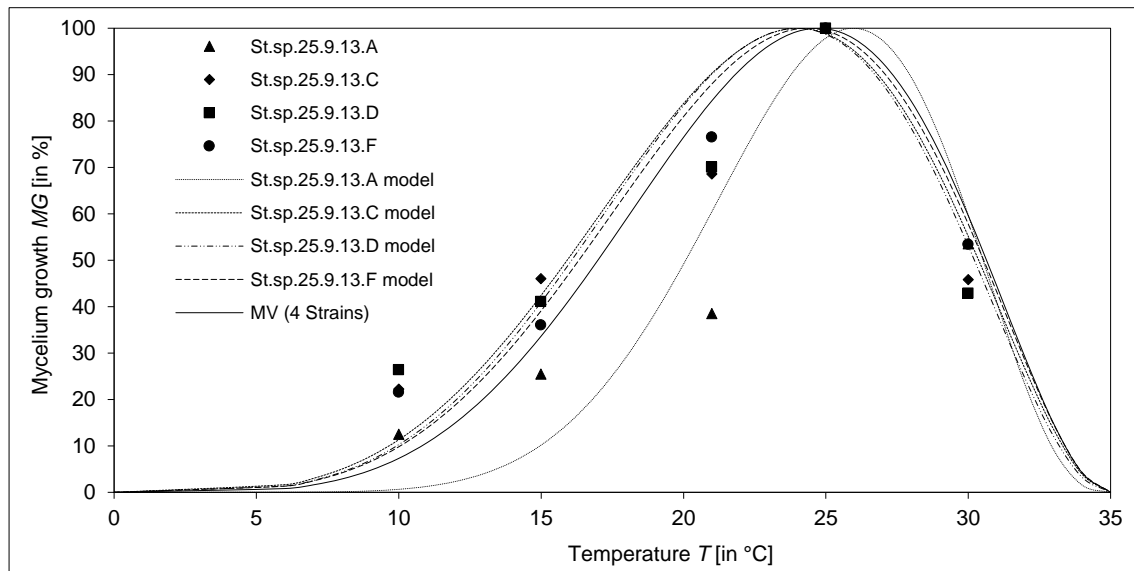


Figure 4.8 Modelled mycelium growth MG of four different *S. vesicarium* strains [in %] depending on temperature T (points = data; line = fitted Eq. 4.5 with parameter values from Table 4.7; MV = mean value)

4.5. Discussion and conclusions

Our data of seasonal dynamics of airborne conidia from 2013 to 2015 are in accordance with previous findings (Hausbeck et al. 1997; Rossi et al. 2005; Llorente and Montesinos 2006; Llorente et al. 2008; Granke and Hausbeck 2010). In this study, the daily rain amount was an important factor for inducing conidia becoming airborne. A logistic function (Eq. 4.1) was most suitable to model the cumulative percentage of trapped conidia. The *SumT* value of 600 degree-days can be seen as the point when the number of airborne conidia clearly increases. Over the five locations, the value of 600 degree-days was reached within a range of 16 calendar days, with a mean value on the 27th of July. In Germany, this date is approximately 1 month after the so called Johannis-sprout, which is often used as the date of harvest end. The term derives from the fact that this sprout usually starts after the 24th of June (Otto 2009). The 27th of July could, for example, be set in a forecast model as an important initial point for conidia flight.

As known from pear orchards, several species of *Stemphylium* coexist with *S. vesicarium*, where only *S. vesicarium* isolates were pathogenic on pear. By morphological methods, it is not possible to distinguish pathogenic spores from saprophytic strains or pathogenic strains from other hosts (Puig et al. 2015). Therefore, it cannot be said whether all our conidia counted direct under the microscope are from the pathogenic population or whether these conidia are from saprophyte isolates or other hosts. The determination of the prevalent species in German asparagus plantings has already been carried out, but the coexistence of different *Stemphylium* species could not be confirmed with the method used by Graf et al. (2016). On the other hand, it is known that isolates of the species *S. vesicarium*, *S. herbarum*, *S. alfalfa*, *S. tomatonis* and *S. sedicola* cannot be separated into single species by phylogenetic analyses and they should be regarded as synonymous (Câmara et al. 2002; Inderbitzin et al. 2009; Köhl et al. 2009). So far, *cyt b* was not sequenced for *S. herbarum*, *S. alfalfa*, *S. tomatonis* and *S. sedicola* and therefore it is not known if there are differences in the sequence (Graf et al. 2016).

On plant surface, conidia germinate under favourable conditions, specifically dependent on temperature and leaf wetness duration. The germination of conidia from pear occurred only when the relative humidity was within the range 98-100 % but was exceedingly rapid, reaching 50 % after only 1 h of exposure to temperatures between 20 °C and 30 °C, with an optimal temperature of 23 °C (Montesinos and Vilardell 1992). Our tested asparagus strains behaved similarly on water agar, which imitates permanent leaf wetness, with

a fast germination of 40 % after 1 h of exposure (Fig. 4.4) and an estimated optimum at 23.34 °C (Table 4.3). The Chapman Richards function with two parameters (Eq. 4.4) was sufficiently flexible to describe the germination in dependence of leaf wetness duration, although the temperature affected the shape of the germination curves (Fig. 4.3). The generalized beta-Chapman Richards function (Eq. 4.6) with temperature-dependent rate, $r_{GC}(T) = a_r + b_r T$, fits well (Table 4.3) and reflects the interaction between temperature and leaf wetness duration.

As germination was extremely fast, the growth of the germ tube was considered to be an additional factor for infection. According to Bassanezi et al. (1998), a lower shape parameter results in a broader temperature range for high values. Thus, the germ tube length has a narrower nearly optimum temperature range than the germination and can be considered the limiting factor for the infection process. The estimated optimum temperature for germ tube length was 28.7 °C, which was considerably higher than the one required for germination (23.3 °C). Comparable data for the germ tube length of conidia of *S. vesicarium* strains are not available in the literature. Germ tube length data from *S. botryosum* strains sourcing from lentil are similar, modelled by a Gompertz function with an optimum at 27.5 °C (Ahmad 2014). This value is only 1.18 °C (4.11 %) lower than our estimated optimal temperature and is therefore comparable.

The chosen maximum temperature of 35 °C is probably not always appropriate, because the decline from 30 °C to 35 °C in the model parts germination and germ tube length is very rapid (Fig. 4.9). We had also estimated the cardinal temperatures in the nonlinear regression analyses, but the results were unrealistically high for T_{max} . The maximum temperature of 35 °C was chosen based on the disease severity data of *S. vesicarium* on pear leaves and fruits (Montesinos et al. 1995b) and mycelium growth of pear isolates (Montesinos and Vilardell 1992). On the other hand, low germination at 35 °C had already been described for *S. vesicarium* (Montesinos and Vilardell 1992). For these reasons, it may be useful to examine additionally data at temperatures above 35 °C for all leaf wetness durations to estimate more exactly the upper cardinal temperature. On the other hand, in the regions of German asparagus cultivation, such high temperatures (above 35 °C) are only achieved in exceptional cases and therefore are not relevant for a future forecast model. The exact identification of T_{min} is also not important for the polycyclic phase and the forecast model, since such low temperatures do not occur in summer.

Similar to the estimated temperature optimum (21.9 °C) for the relative number of lesions in this study (Table 4.6), Montesinos et al. (1995b) reported temperature optima of 22.6 °C and 21.1 °C for infections on pear fruits and leaves. Menzies et al. (1991) found that the optimum temperature range for infections on leaves by an asparagus isolate from France was between 25 °C and 30 °C.

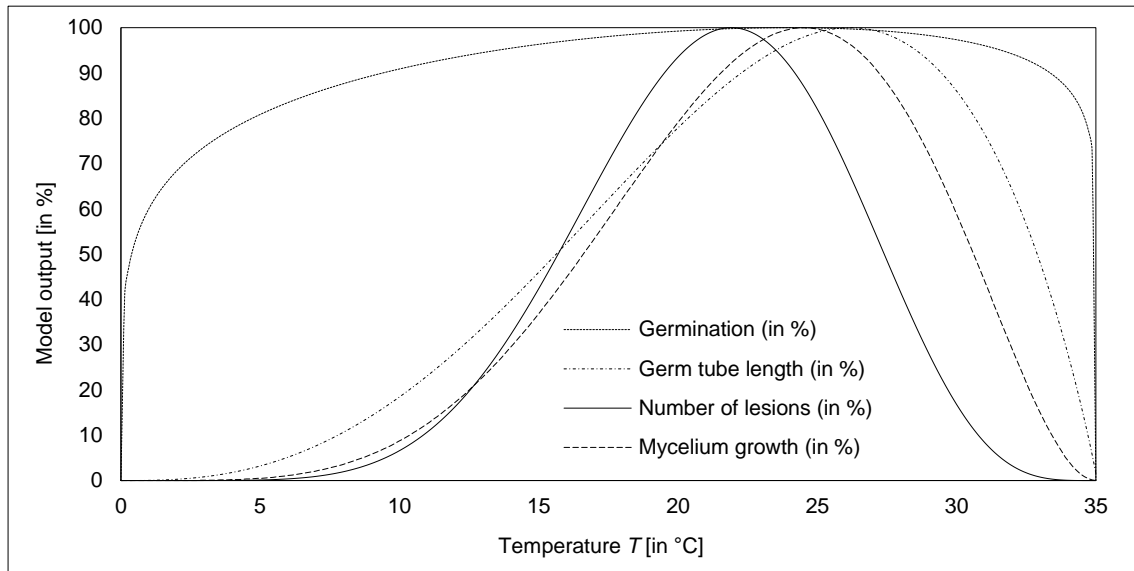


Figure 4.9 Comparison of the effect of temperature T on the four observed parts of the polycyclic phase of *S. vesicarium*

The number of lesions has the narrowest nearly optimal temperature range of all model parts (Fig. 4.9) and the lowest optimal temperature and can therefore be regarded as the most limiting factor in this study. However, one should have in mind that the incubation period is four days at 20 °C and therefore after five days at 10 °C the incubation period was not yet completely finished and the number of possible lesions was certainly underestimated (Fig. 4.7). Thus, for very low and high temperatures, the numbers counted after five days are lower than those expected after the real end of the incubation period. The assumption of the narrowest optimal temperature range must therefore be considered with caution.

After the infection is established, the development of lesions in the plant tissue depends on the mycelium growth. Basic research of biological parameters from isolates of pear showed maximum rates of radial mycelium growth within the range of 5-35 °C and an optimum at 21 °C (Montesinos and Vilardell 1992). Our estimated temperature optimum for *MG* was higher by 3.7 °C (Table 4.7), and this difference is one of the reasons de-

manding a more specific description of the disease on asparagus. One of the four investigated strains had even a higher temperature optimum, indicating the wide variability in the growth of the various strains.

A comparison of all temperature curves (Fig. 4.9) shows that the curve peaks are close together (> 20 °C) with a mean optimal temperature of 24.3 °C. All model parts of the polycyclic phase indicate that *S. vesicarium* can most likely be categorized into the group of mesophiles, as most other fungi. The mesophilic growth range is typically between 0 °C and 35 °C with an optimal temperature between 25 °C and 30 °C (Dix and Webster 1995). The optimum temperature of the number of lesions is clearly lower than this optimum range but fits well into the described growth range.

There are other factors that may favour the progress of disease in asparagus. In 2013, lesions were sometimes found on only one side of the asparagus base. It seems that sand was blasted on the spears by strong wind 10-14 days earlier. Wounding of spears caused by sand has already been reported in the literature to lead to more lesions and shorter wetting duration needed for the development of lesions (Lacy 1982; Johnson and Lunden 1986). The persistent moisture by dew seems to be another catalyst for infections, regardless of rainfall. The fine phylloclades form a huge surface that is utilized for the attachment of moisture. An earlier study showed that longer periods of dew or fog contributed to greater rates of infection by *Stemphylium* on trifolium and medicago (Bradley et al. 2003). In asparagus, long leaf wetness duration by dew happens in the morning.

All model parts of the polycyclic phase were connected with the existing model parts from the monocyclic phase (Bohlen-Janssen et al. 2018a) in the algorithm of the new forecast model SIMSTEM. The model forecasts the beginning of the epidemic and the disease progression (as a proportion of the diseased leaf area). SIMSTEM uses area-specific weather data either from standard meteorological stations (provided by the German Meteorological Service or by the Regional Plant Protection Offices) or simulated data (Racca et al. 2010). All model rates are calculated using hourly weather parameters: temperature (in °C), relative humidity (in %), and rainfall (in mm). The model algorithm is developed by the Central Institute for Decision Support Systems in Crop Protection (ZEPP) and will be available on the agricultural internet platform for integrated plant production ISIP (www.isip.de), which is currently in the test phase (2018). The strategy for the integrated disease management of purple spot on asparagus using the SIMSTEM model is currently in development.

Acknowledgements

This study was funded by the German Federal Ministry of Food and Agriculture (BMEL) and the Federal Office for Agriculture and Food (BLE) (grant number 2814702511).

5. SIMSTEM - a model to forecast the epidemic of purple spot (*Stemphylium vesicarium*) on asparagus (*Asparagus officinalis* L.).

5.1. Abstract

SIMSTEM is a new computer based forecast model for epidemics of purple spot in asparagus, caused by *Stemphylium vesicarium*. Aspects of the monocyclic and polycyclic phases of *S. vesicarium* were implemented in one algorithm. Using disease data of several years, a first validation was carried out. The model can be used flexibly because it can forecast the beginning of the epidemic, the first treatment, the disease progression (as a proportion of the diseased leaf area), and signal periods with high risk disease pressure indicating the need for fungicide treatments via a traffic light system. SIMSTEM will be available for consultation and interested producers after a test phase under www.ISIP.de with a user-friendly in- and output.

Keywords: Asparagus, Forecast, Purple spot, SIMSTEM, *Stemphylium vesicarium*

5.2. Introduction

Purple spot or *Stemphylium* leaf spot disease of asparagus (*Asparagus officinalis* L.), caused by *Stemphylium vesicarium* (Wallr.) E.G. Simmons 1969, is an important fungal disease in the asparagus production of Germany (Menzinger and Weber 1990) and of several other regions worldwide (Suzui 1973; Menzies 1980; Lacy 1982; Blancard et al. 1984; Falloon et al. 1984; Gindrat et al. 1984; Thompson and Uys 1992; Cunnington and Irvine 2005). Managing epidemics of *S. vesicarium* in asparagus, including the proper time and frequency of fungicide application, is of significant interest for growers, phytosanitary services and consultants.

The Integrated Pest Management (IPM) concept is based on the economical use of plant protection products, the benefit of natural enemies and their threat by plant protection measures, and includes a wide range of alternative pest control measures (Dent and Elliott

1995; Burth and Freier 1996). Beneficial experiences were achieved with computer-assisted decision support systems (Kleinhenz and Jörg 1998; Jörg et al. 1999). These systems can be useful for forecasting the date of exceeding a control threshold and, thus, the date of fungicide application. With mathematical models, the time requirement for field evaluations can be minimised (Racca et al. 2002). The effects of temperature and leaf wetness duration on the infection and growth of fungal plant diseases can be modelled to forecast infection periods (Lalancette et al. 1988; Carisse and Kushalappa 1990; Broome et al. 1996; Montesinos and Vilardell 1992; Montesinos et al. 1995b). The model FAST, for instance, is a forecast system for *Alternaria solani* on tomato (Madden et al. 1978). Later BSPcast was derived from FAST by adapting it to the aetiology and epidemiology of *S. vesicarium* on pear (Montesinos and Vilardell 1992; Montesinos et al. 1995a; Montesinos et al. 1995b; Llorente et al. 2000; Llorente et al. 2011). From FAST also the model TOM-CAST was derived as a weather timed fungicide spray forecast for tomato anthracnose, *Septoria* leaf spots and late blight (Pitblado 1992).

FAST uses hours of leaf wetness and the average temperature during wet periods, the mean air temperature, hours of relative humidity over 90 % and the total rainfall (Madden et al. 1978). The success of control measures of *S. vesicarium* on pear with the model FAST is similar to a 7-day application, with a reduction of fungicide applications of 28 % (Montesinos and Vilardell 1992). The model BSPcast is based on an empirical model (Montesinos and Vilardell 1992) and quantifies the effect of daily wetness duration and mean temperature during wetness periods on brown spot disease severity on leaves and fruits (Montesinos et al. 1995b). The efficiency of BSPcast in pear was similar to a fixed spray schedule (7 and 15-day protection period) and reduced fungicide use on average by 30 % (Llorente et al. 2000). BSPcast was later modified by including a daily infection risk, instead of a 3-day cumulative risk, and by considering the effect of relative humidity during interrupted wetness periods (Llorente et al. 2011).

TOM-CAST does not include the rain model of FAST but uses the duration of leaf wetness and the average air temperature during wet periods to calculate a daily severity value (DSV) for the disease (Pitblado 1992). TOM-CAST was later also tested to reduce the spray applications in the control of purple spot of asparagus (Meyer et al. 2000; Eichhorn et al. 2010). A 60 % reduction in the number of fungicide applications was achieved when compared with a standard variant with weekly treatments (up to ten) (Meyer et al. 2000).

But tested under practical conditions in Northern Germany, where only four or five fungicidal treatments are common, the use of TOM-CAST was not beneficial anymore (Wichura, unpublished data).

Our theoretical comparison of TOM-CAST and BSPcast showed a significantly more sensitive reaction and a better agreement with own empirical experiences of the model BSPcast at low temperatures. Nevertheless, the number of fungicide applications is today already lower than recommended by these two models and the new development of a forecast model is more efficient than the adaptation of an existing model, because BSPcast and TOM-CAST are not sufficiently adapted to the pathosystem *S. vesicarium*-Asparagus. In our previous papers, the biology of purple spot on asparagus was investigated and important components of the primary and the secondary life cycle were modelled using field observations and laboratory trials (Bohlen-Janssen et al. 2018a; Bohlen-Janssen et al. 2018b). Based on this information, an epidemiological simulation model for *Stemphylium vesicarium*, called SIMSTEM, is created to forecast the epidemiological development of this important disease. So, the aim of this study is to connect the monocyclic and polycyclic phases in the forecast model SIMSTEM and to implement it on the agricultural internet platform for integrated plant production ISIP (www.isip.de).

5.3. Materials and methods

5.3.1. Model description

The modelling approach to simulate the daily disease progression is an H-L-I-R epidemic model consisting of the four state variables *H*(ealthy) - *L*(atent) - *I*(nfectious) - *R*(emoved) and three rate parameters (β , ω and μ) (Madden et al. 2007). In this version of the SIMSTEM model, the crop growth is not considered. Thus, the four daily difference equations for the simulation, starting with $k = 0$ on June 1, are:

$$\begin{aligned} H_k &= H_{k-1} - \beta_{k-1} * H_{k-1} * I_{k-1} \\ L_k &= L_{k-1} + \beta_{k-1} * H_{k-1} * I_{k-1} - \omega * L_{k-1} \\ I_k &= I_{k-1} + \omega * L_{k-1} - \mu * I_{k-1} \\ R_k &= R_{k-1} + \mu * I_{k-1} \end{aligned}$$

Two of the rate parameters, ω and μ , are assumed to be fixed while the third one, β , is changing from day to day. The parameter ω ($= 0.25$) is the inverse of the mean latent period which was fixed at four days independent from the temperature variation during the season (Bohlen-Janssen et al. 2018b). The parameter μ is the inverse of the mean infectious period, but no information on its duration is available. As the fungus can survive as saprophyte also on dead plant residuals (Simmons 1969; Ellis 1971) and can sporulate for long time (Bohlen-Janssen et al. 2018b), the infectious period was taken as 120 days, the mean of the duration of a yearly epidemic from June/July till September/October). Thus, a value of $1/120$ was assumed for μ . The time-varying rate β_k is the daily infection probability which is calculated using various partial models from Bohlen-Janssen et al. (2018a; 2018b) as explained below.

From the four state variables, two additional states can be calculated: the daily total disease $Y_k = L_k + I_k + R_k$ and the visible disease $V_k = I_k + R_k$.

For simplicity, the value for H at day 0 was taken as $1-0.001$. The simulation is started with an initial value of $L_0 = 0.0$, $I_0 = 0.001$ and $R_0 = 0.0$.

Modelling the daily infection probability β_k

For the calculation of the infection probability β , the ascospores and the conidia are considered separately:

- in the monocyclic phase with ascospores:

$$\beta_A = ASC_{AV_k} * \min(ASC_{GER_k}; ASC_{GTL_k}) * MG_k$$

- in the polycyclic phase with conidia:

$$\beta_C = CON_{AV_k} * \min(CON_{GER_k}; CON_{GTL_k}) * MG_k$$

Both are calculated parallel and in the normal case, there is no overlap (Bohlen-Janssen et al. 2018a; Bohlen-Janssen et al. 2018b). When the ascospore discharge is over and β_A ends, only β_C is calculated. In the case of an overlap, the maximum value counts. The

infection probabilities, β_A or β_C , depend on the availability of spores, ASC_{AV_k} or CON_{AV_k} , the germination rate of spores, ASC_{GER_k} or CON_{GER_k} , the germ tube length of spores, ASC_{GTL_k} or CON_{GTL_k} , and on the mycelium growth, MG_k ; which is the same for both spores. The daily value is obtained at the end of the infection period (*AIP* and *CIP*) on the corresponding day. In case of two or more infection periods on the same day, the maximum value is chosen for the daily value (Schmitt et al. 2016).

Available ascospore ASC_{AV_k}

Since the pseudothecia remain close in dry periods and the ascospores are ejected only after rainfall (Prados-Ligero et al. 1998; Trail 2007), the available flying ascospores on a day of infection were calculated as the difference of ASC_{FLY_k} interrupted by dry periods.

$$ASC_{AV_k} = ASC_{FLY_k} - ASC_{FLY_{k-dp}}$$

Where:

ASC_{AV_k} = daily amount of flying ascospores available for the infection

ASC_{FLY_k} = ascospore fly rate on the actual day (k)

$ASC_{FLY_{k-dp}}$ = ascospore fly rate after the previous infection day

dp = dry period (in days)

The daily amount of flying ascospores available for infection was calculated using a Chapman Richards function (Richards 1959) with parameter values derived by Bohlen-Janssen et al. (2018a) as follows:

$$ASC_{FLY_k} = [1 - \exp(-0.01 * SumT_k)]^{4.25}$$

Where:

$SumT_k$ = sum of daily mean values of temperature (base $T = 5$ °C, only on day with $RA > 0$ mm), reached on day k starting from the 1st of February

Ascospore infection period (AIP)

The period in hours (h), in which ejected and flying ascospores can successfully infect begins with an hour of rainfall (RA) > 0.0 mm (ascospore ejection from the pseudothecia) and ends with the ending of a dew period (in h) after the rainfall. Dew periods beginning without rainfall are not considered for a successful infection as no spores are ejected. The hours are accumulated as long as there is a continuous leaf wetness. So, more than 24 hours of leaf wetness are possible.

Ascospore germination ASC_{GER_k}

The combined effect of temperature (T_{WD}) and leaf wetness duration (WD) on ASC_{GER_k} was calculated using a Chapman Richards function with temperature depending capacity and rate, and parameter values were derived by Bohlen-Janssen et al. (2018a) as follows:

$$ASC_{GER_k} = (71.906 + 0.905 * T_{WD}) * [1 - \exp(-(0.039 * T_{WD}) * WD)]^{2.11}$$

Where:

T_{WD} = mean temperature during the leaf wetness period (in °C)

WD = leaf wetness duration (in h)

Ascospore germ tube length ASC_{GTL_k}

The effect of the temperature (T_{WD}) and the leaf wetness duration (WD) on ASC_{GTL_k} was modelled with a combined beta-linear function and parameter values were derived by Bohlen-Janssen et al. (2018a) as follows:

$$ASC_{GTL_k} = 27.376 * \left[\left(\frac{T_{WD} - T_{min}}{30.42 - T_{min}} \right)^{0.266 * \frac{30.42 - T_{min}}{T_{max} - 30.42}} * \left(\frac{T_{max} - T_{WD}}{T_{max} - 30.42} \right)^{0.266} \right] * WD$$

Where:

T_{WD} = mean temperature during the wetness period (in °C)

WD = leaf wetness duration (in h)

Following the results from Montesinos et al. (1995b), the cardinal temperatures T_{min} and T_{max} were fixed at 0 °C and 35 °C, respectively.

Available conidia CON_{AV_k}

As the purple spot lesions produce always conidia (in contrast to ascospores) and the fungus can also survive saprophytically on plant residue, the daily CON_{AV_k} was calculated with the logistic model of the trapped conidia according Bohlen-Janssen et al. (2018b):

$$CON_{AV_k} = \frac{1}{1 + \frac{1-0.001}{0.001} * \exp[-(0.012 * SumT_k)]}$$

Where:

$SumT_k$ = sum of daily mean values of temperature (base $T = 0$ °C, only on day with $RA > 0.2$ mm), reached on day k starting from the 1st of May

Conidia infection period CIP

The CIP was calculated as described for the ascospore infection period AIP beginning with an hour of rainfall (RA) > 0.2 mm.

Conidia germination CON_{GER_k}

The effect of temperature (T_{WD}) and leaf wetness duration (WD) on CON_{GER_k} was calculated using a combination of a generalized beta function (Bassanezi et al. 1998) with a modified Chapman Richards function with an additional parameter (Payandeh et al. 1980) and all parameter values were derived by Bohlen-Janssen et al. (2018b) as follows:

$$CON_{GER_k} = 100 * \left[\left(\frac{T_{WD} - T_{min}}{23.344 - T_{min}} \right)^{0.105 * \frac{23.344 - T_{min}}{T_{max} - 23.344}} * \left(\frac{T_{max} - T_{WD}}{T_{max} - 23.344} \right)^{0.105} \right] * [1 - \exp(-(-0.144 + 0.078 * T_{WD}) * WD)]^{6.554}$$

Where:

T_{WD} = mean temperature during the dew period (in °C)

WD = leaf wetness duration (in h)

The cardinal temperatures T_{min} and T_{max} were fixed at 0 °C and 35 °C, respectively (Montesinos et al. 1995b).

Conidia germ tube length CON_{GTL_k}

The effect of the temperature (T_{WD}) and the leaf wetness duration (WD) on the germ tube length of conidia (CON_{GTL_k}) was modelled with a combined beta-power function and all parameter values were derived by Bohlen-Janssen et al. (2018b) as follows:

$$CON_{GTL_k} = 14.777 * \left[\left(\frac{T_{WD} - T_{min}}{28.68 - T_{min}} \right)^{0.564 * \frac{28.68 - T_{min}}{T_{max} - 28.68}} * \left(\frac{T_{max} - T_{WD}}{T_{max} - 28.68} \right)^{0.564} \right] * WD^{1.369}$$

Where:

T_{WD} = mean temperature during the dew period (in °C)

WD = leaf wetness duration (in h)

Following the results from Montesinos et al. (1995b), the cardinal temperatures T_{min} and T_{max} were fixed at 0 °C and 35 °C, respectively.

Mycelium growth MG_k

For the monocyclic and polycyclic phases, the mycelium growth (MG_k) was modelled using a generalized beta function according to Bohlen-Janssen et al. (2018b) as follows:

$$MG_k = 100 * \left(\frac{T - T_{min}}{24.726 - T_{min}} \right)^{n * \frac{24.726 - T_{min}}{T_{max} - 24.726}} * \left(\frac{T_{max} - T}{T_{max} - 24.726} \right)^{2.028}$$

Where:

T = actual hourly temperature (in °C)

The cardinal temperatures T_{min} and T_{max} were fixed at 0 °C and 35 °C, respectively Montesinos et al. (1995b). Mycelium growth is used as an indirect measurement of the growing of lesions after infection. The daily value of MG_k is the mean value of the hourly-calculated MG for the last 24 hours.

5.3.2. Model validation

A first model validation was done by using disease severity (DS) data of seven years (nine trials), made available by the Plant Protection Service of The Chamber of Agriculture Lower Saxony around Hannover region. The assessed DS are mean values of untreated plots in randomised fungicide trials. Location, trial year, variety, weather station and trial symbols are listed in Table 5.1. For the subjective validation, the simulated visible disease proportions (V) were compared with the data recorded in the field. The simulation is considered as correct when the simulated value of V lies within the confidence interval of the assessed DS . Overestimation is given when the simulated value overrides the upper confidence limit, underestimation when the simulated value is below the lower confidence limit (Racca et al. 2010; Racca et al. 2011).

The statistical validation was done with two parametric tests (regression analysis, hypothesis test) and one non-parametric test (Kolmogorov-Smirnov) (Racca et al. 2011).

Table 5.1 Locations, years, varieties and weather stations used for the model validation

Location	Year	Variety	Weather station	Symbol for Fig. 5.3 to 5.5
Buchholz	2006	Gijnlim	Bergen	A
Buchholz	2008	Gijnlim	Bergen	B
Burgwedel/Fuhrberg	2009	Gijnlim	Hannover	C
Langförden	2010	Steiniva	Cloppenburg	D
Burgwedel/Fuhrberg	2011	Gijnlim	Hannover	E
Burgwedel/Fuhrberg	2012	Gijnlim	Hannover	F
Hannover Ahlem	2014a	Gijnlim	Hannover	G1
Burgwedel/Fuhrberg	2014b	Gijnlim	Hannover	G2
Burgwedel/Fuhrberg	2014c	Gijnlim	Hannover	G3

5.3.3. Weather data

Standard meteorological parameters were used: temperature (T), relative humidity (RH) and rainfall (RA) recorded from a weather station. Area specific interpolated weather data (T , RH) from meteorological stations and radar measurements (RA) provided from the German Meteorological Service (DWD) via www.isip.de, as described by Racca et al.

(2010), were also used as input parameters for the model. To apply the model with non-recorded data of leaf wetness duration (WD) and to avoid mismatch of measurements from different sensors, the leaf wetness was simulated through the vapor deficit pressure calculated with relative humidity (RH) and temperature (Prenger and Ling 2001).

5.3.4. Statistical software

Data preparation and statistical modelling was done with software Microsoft Excel 2016™, XLSTAT Version 2016.05.33324 (Copyright Addinsoft 1995-2016) and SigmaPlot for Windows Version 13.0 (Copyright Systat Software, Inc. 2014).

5.4. Results

5.4.1. Model output

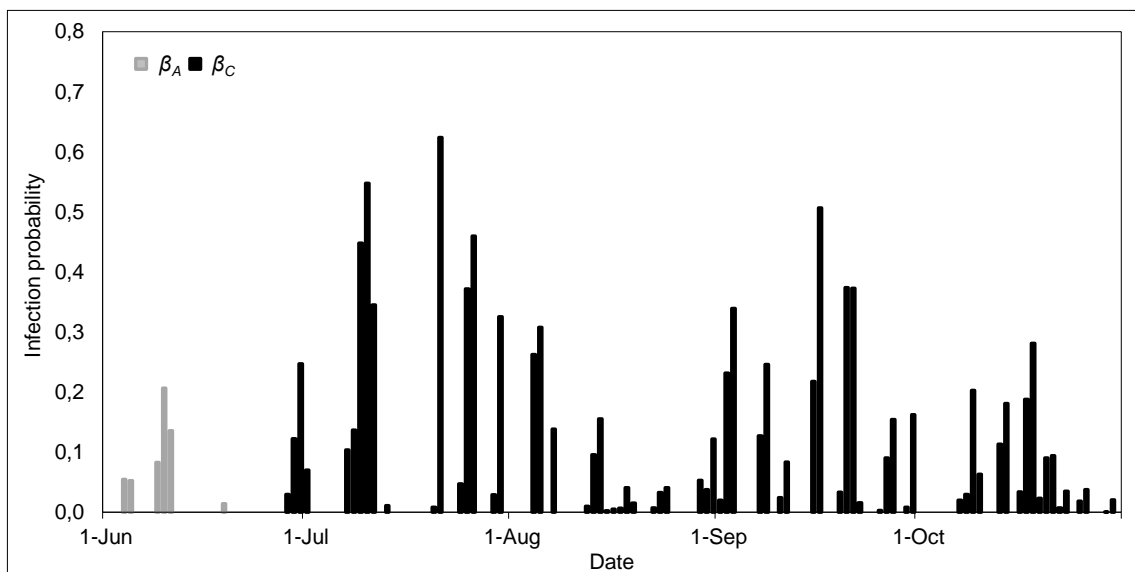


Figure 5.1 Values of infection probabilities β_A and β_C for the weather station Hannover in the period between 1st of June and 31st of October, 2014

As an example, the daily values of β_A and β_C for the weather station Hannover in the period between the 1st of June and the 31st of October 2014 are displayed (Fig. 5.1). Overall, the ascospore infection probability β_A is only relevant up to mid-June and the most severe disease development is outside of the ascospore season, in which only β_C plays a role.

The final model output of the different disease categories using the daily values of β_A and β_C from Fig. 5.1 is illustrated in Fig. 5.2. The total-, visible- and infectious disease proportion are only less in June, slowly rising from mid-July to September. From the 1st of September, this three proportions increases visibly.

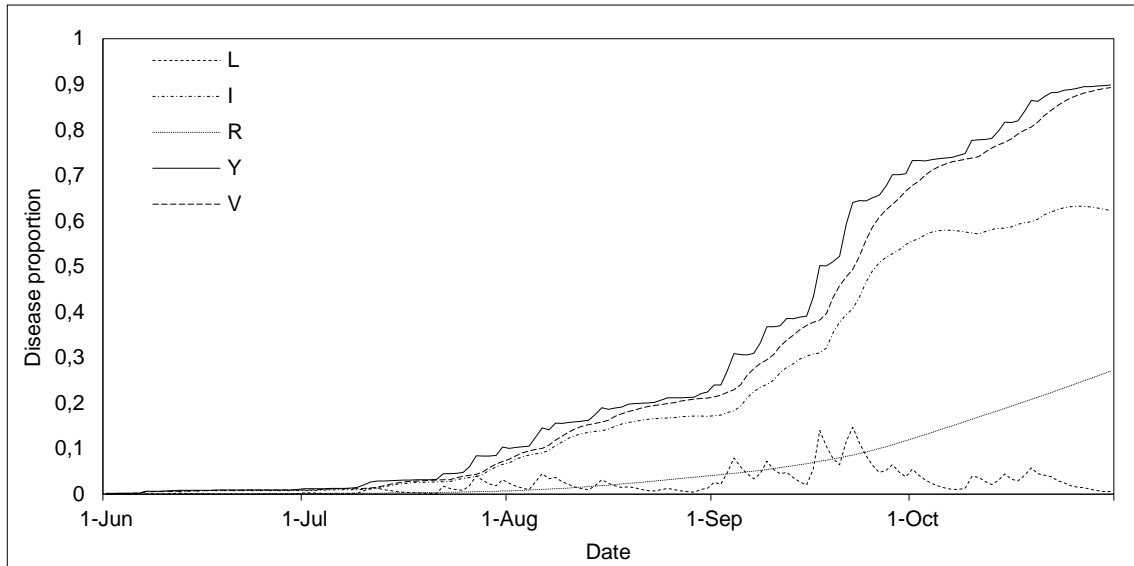


Figure 5.2 SIMSTEM model output of the different disease categories. Weather station Hannover, 2014, period between the 1st of June and the 31st of October. L = latent disease proportion; I = infectious disease proportion; R = removed disease proportion; Y = total disease proportion; V = visible disease proportion

5.4.2. Subjective validation

For the validation, only the simulated visible disease proportion V was considered in relation to the assessed disease severity DS . Compared to the 46 assessment data, 40 simulated disease proportions (87 %) were classified as correct. Only in three cases (6.5 %), the disease proportion was underestimated and in three cases (6.5 %) overestimated (Fig. 5.3 to 5.5). The majority of the simulated V lines was within the confidence interval of the assessed DS (Fig. 5.3 to 5.5). There were some exceptions at the locations A, F and G1. The overestimations in A at the 15th and at the 29th of August are the two first time points of DS . In F, the third time-point (at the 24th of August) was overestimated in comparison to the DS value. In location G1, the epidemic after August 5 was clearly underestimated.

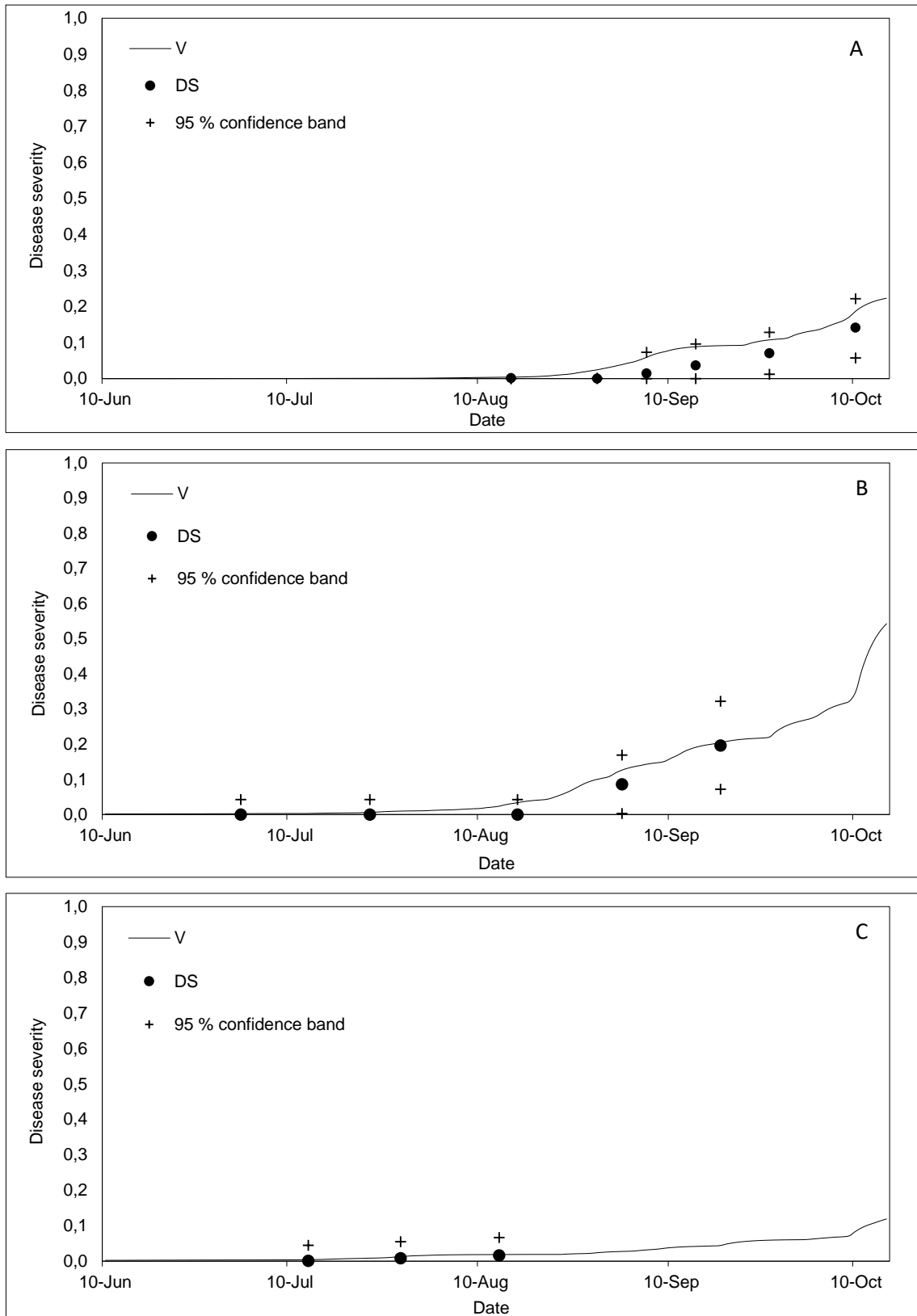


Figure 5.3 Assessed disease severity (*DS*) compared with visible disease proportion simulated by the SIMSTEM model (line = simulated *V*, point = assessed *DS* value with 95 % confidence interval). See Table 5.1 for the location A, B, C and years

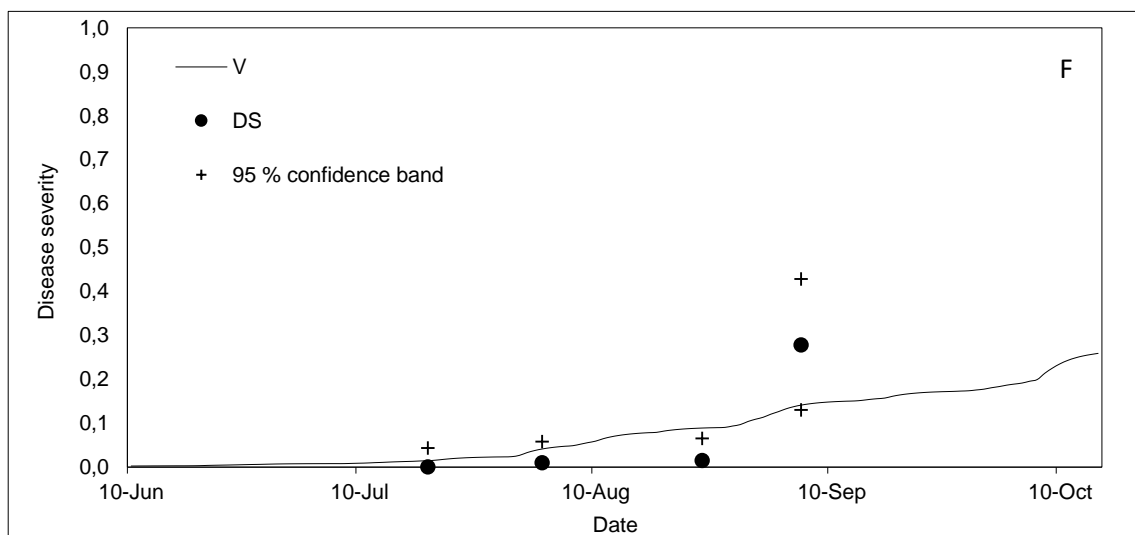
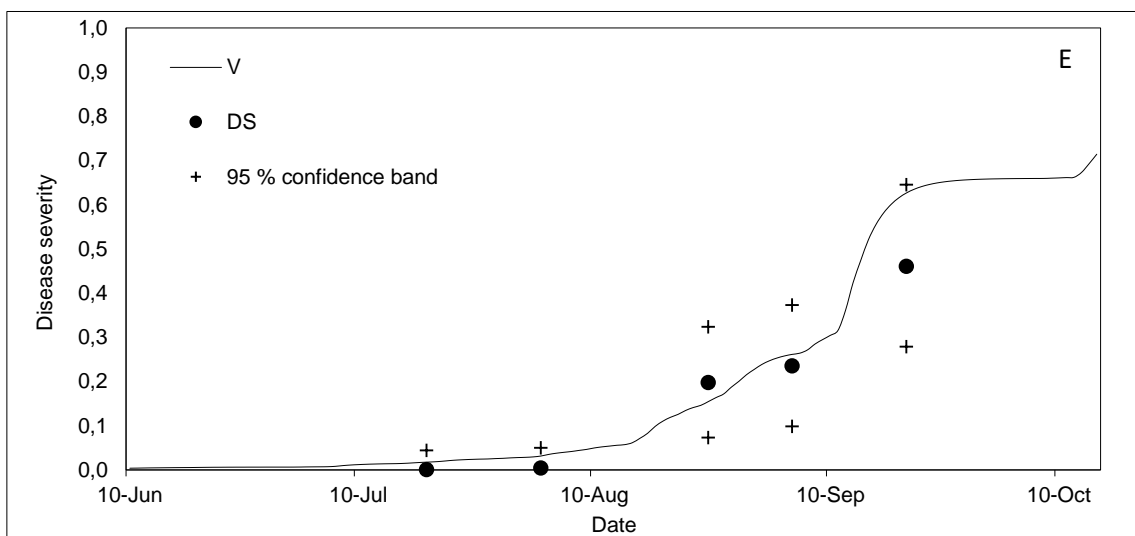
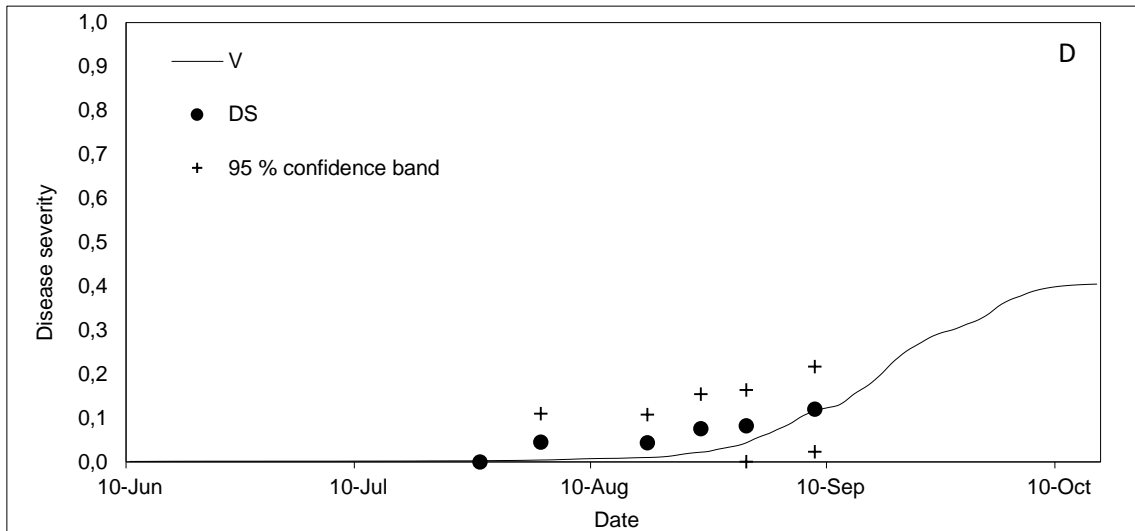


Figure 5.4 Assessed disease severity (*DS*) compared with visible disease proportion simulated by the SIMSTEM model (line = simulated *V*, point = assessed *DS* value with 95 % confidence interval). See Table 5.1 for the location D, E, F and years

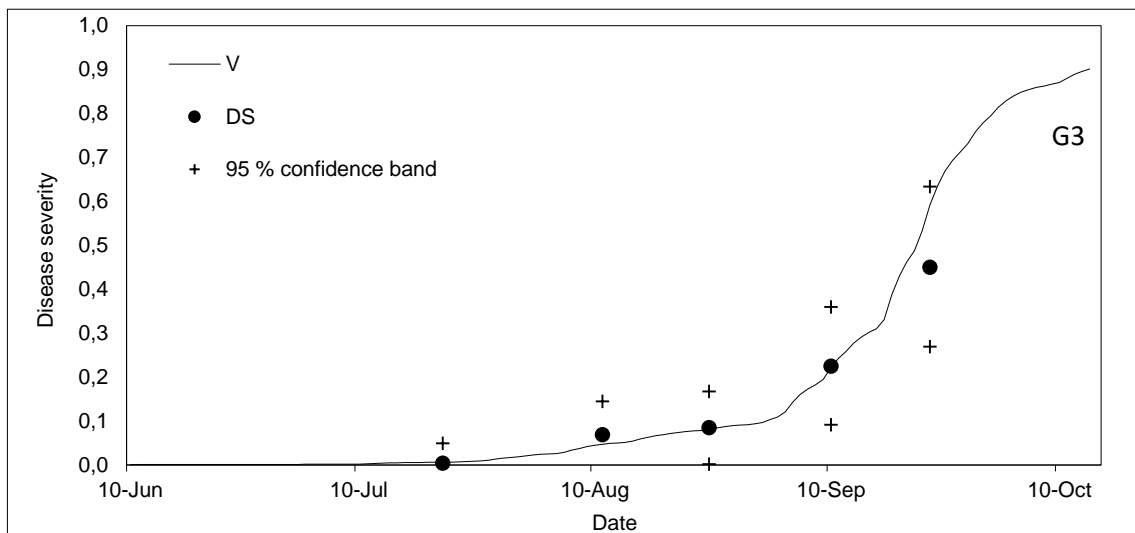
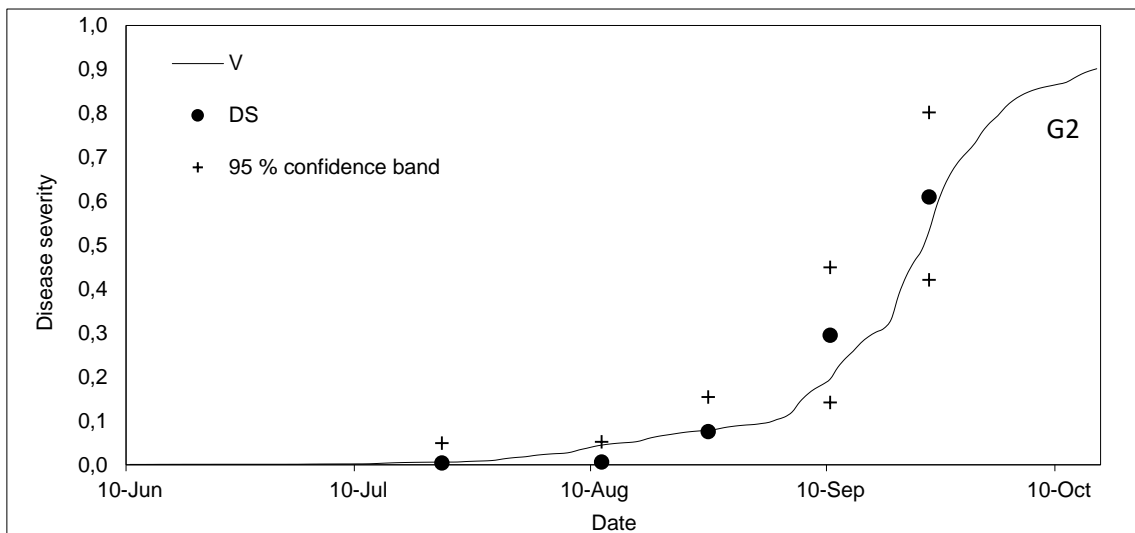
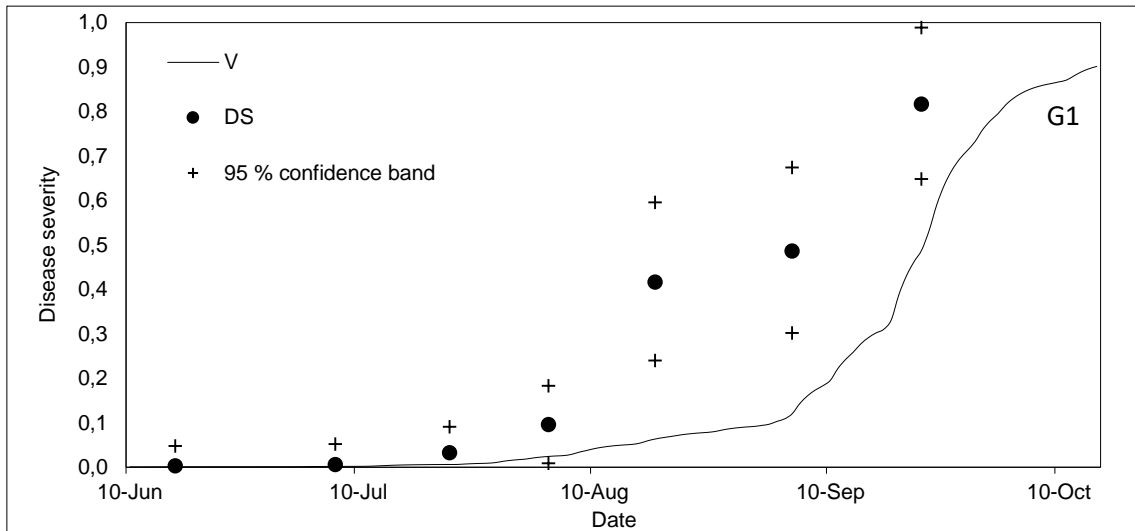


Figure 5.5 Assessed disease severity (*DS*) compared with visible disease proportion simulated by the SIMSTEM model (line = simulated *V*, point = assessed *DS* value with 95 % confidence interval). See Table 5.1 for the location G1, G2, G3 and years

5.4.3. Statistical validation

The statistical validation with two parametric tests (regression analysis, hypothesis test, Table 5.2, Fig. 5.6) and one non-parametric test (Kolmogorov-Smirnov, Table 5.3) gave different results. For the linear regression (Fig. 5.6), the slope value of 0.697 (Table 5.2; $R^2 = 0.71$) shows that the model is significantly underestimating the observations, while the intercept is very close to 0. The high number of non-significant cases of the Kolmogorov-Smirnov test (Table 5.3; n.s. = 75.8) means that the model was considered a statistically accurate simulator of the field data (Teng 1981).

The pronounced underestimation of the model occurred only in trial G1 (Fig. 5.5). In contrast to the other trials, the asparagus was not harvested in this trial so that the plants were longer exposed to infections resulting in higher disease severities. When the data of this extraordinary trial are left out the regression analysis, R^2 increased to 0.89 and the slope was 0.97, which is not different from 1. Consequently, the model can be considered as a statistically accurate simulator of the field data.

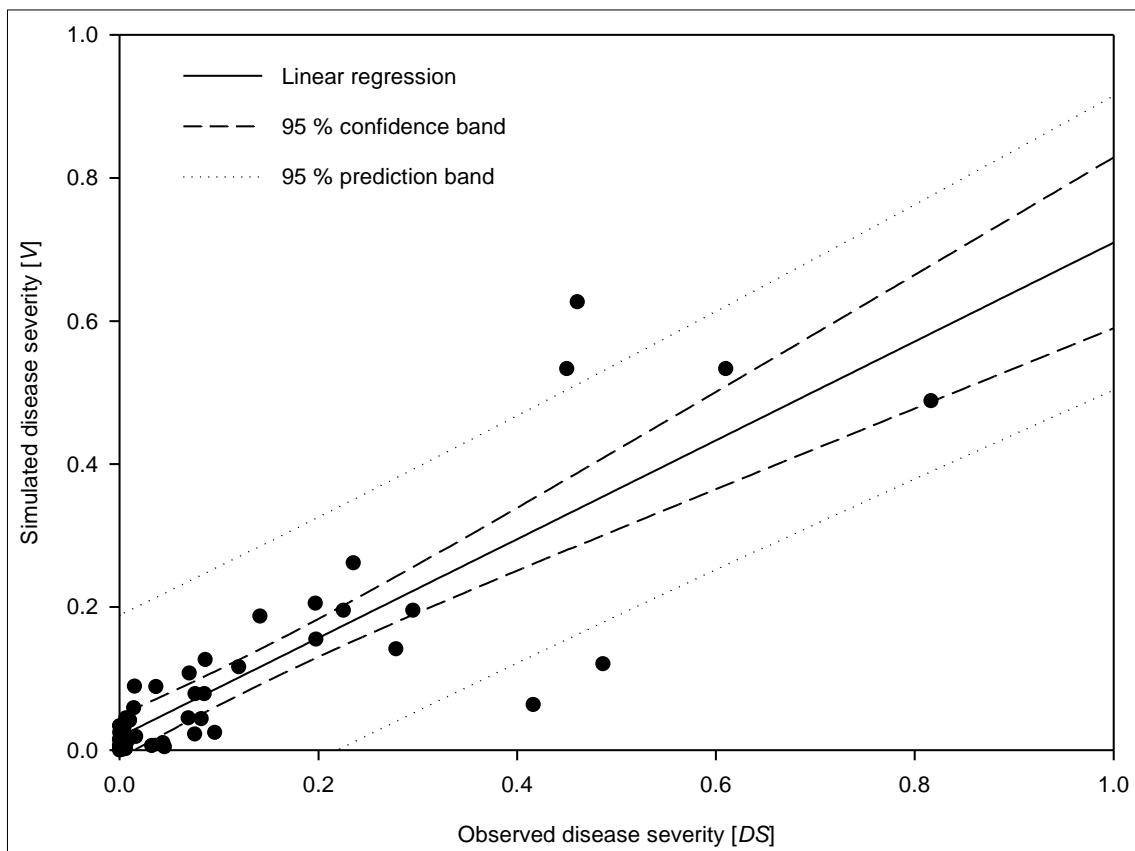


Figure 5.6 Validation of the SIMSTEM model using regression analysis

Table 5.2 Validation of the SIMSTEM model. Hypotheses test of regression parameters: For the intercept, the hypotheses are H_0 , that the intercept = 0 and H_1 , that the intercept \neq 0. For the slope, the hypotheses are H_0 , that the slope = 1 and H_1 , that the slope \neq 1 (Teng 1981)

Source	Value	Standard Error	P	R ²
Intercept	0.019	0.015	0.217	0.71
Slope	0.697	0.066	< 0.001	

Table 5.3 Validation of the SIMSTEM model with non-parametric Kolmogorov-Smirnov test, shares (in %) of the significance ($p < 0.05$)

Location	Year	Observation	n.s.	s.
Buchholz	2006	6	89.3	10.7
Buchholz	2008	5	32.9	67.1
Burgwedel/Fuhrberg	2009	3	99.6	0.4
Langförden	2010	6	32.9	67.1
Burgwedel/Fuhrberg	2011	5	81.9	18.1
Burgwedel/Fuhrberg	2012	4	51.8	48.2
Hannover Ahlem	2014a	7	93.8	6.2
Burgwedel/Fuhrberg	2014b	5	100.0	0.0
Burgwedel/Fuhrberg	2014c	5	100.0	0.0
All	All	46	75.8	24.2

5.4.4. Applying SIMSTEM in practice

SIMSTEM can be used in different ways. First of all, to estimate the beginning of the epidemic. A possible hypothetical threshold for the first appearance of symptoms in the asparagus field could be derived by comparing the assessed data in the very early phase (from 0 to 0.05 *DS*) with the simulated *V* by means of box plot analysis (Fig. 5.7). The threshold for the disease appearance was assessed at the lower quartile of the *V* (0.006), in this case 82 % of the assessed *DS* (disease appearance) were simulated correctly. The equivalent date for $V = 0.006$ is for the average of all seven simulated curves the 15th of July. By practical experiences, this date is appropriate when plant debris were buried and plants were cut until mid-June.

Again, considering a hypothetical threshold for the first treatment, an assessed *DS* from 0.05 to 0.1 of simulated *V* could be chosen between the lower quartile (0.044) and the median (0.079) of *V* by box plot analysis (Fig. 5.8). The equivalent date for $V = 0.044$ is the 18th of August. The dates of the first appearance and the first treatment fit also to the interpolated *DS* data of all nine trials.

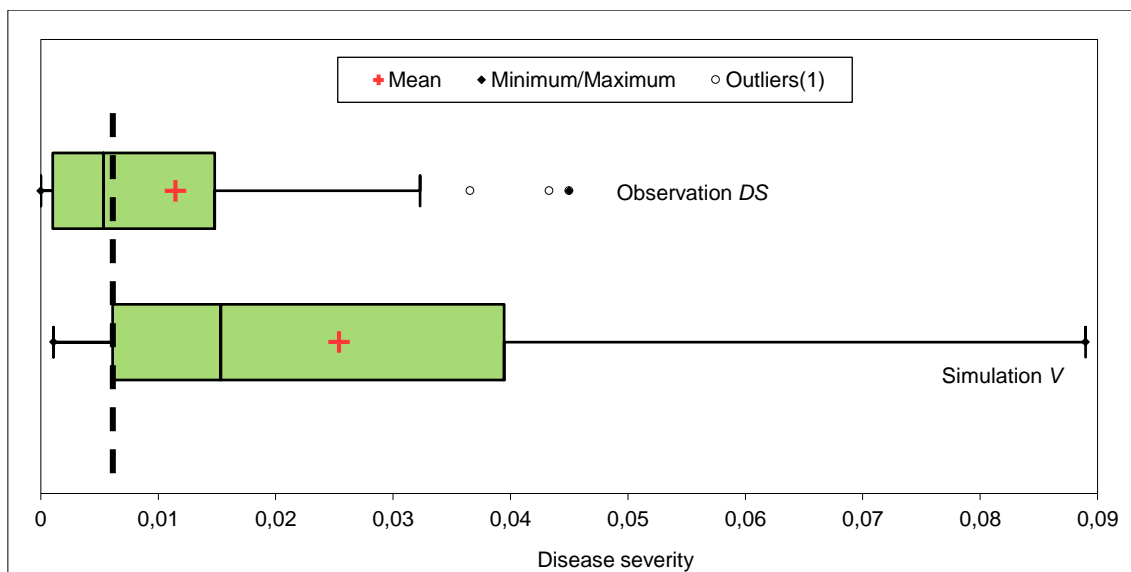


Figure 5.7 Hypothetical threshold for the simulation of the disease appearance in the fields, comparison of assessed *DS* data (0-0.05 *DS*) with simulated *V*

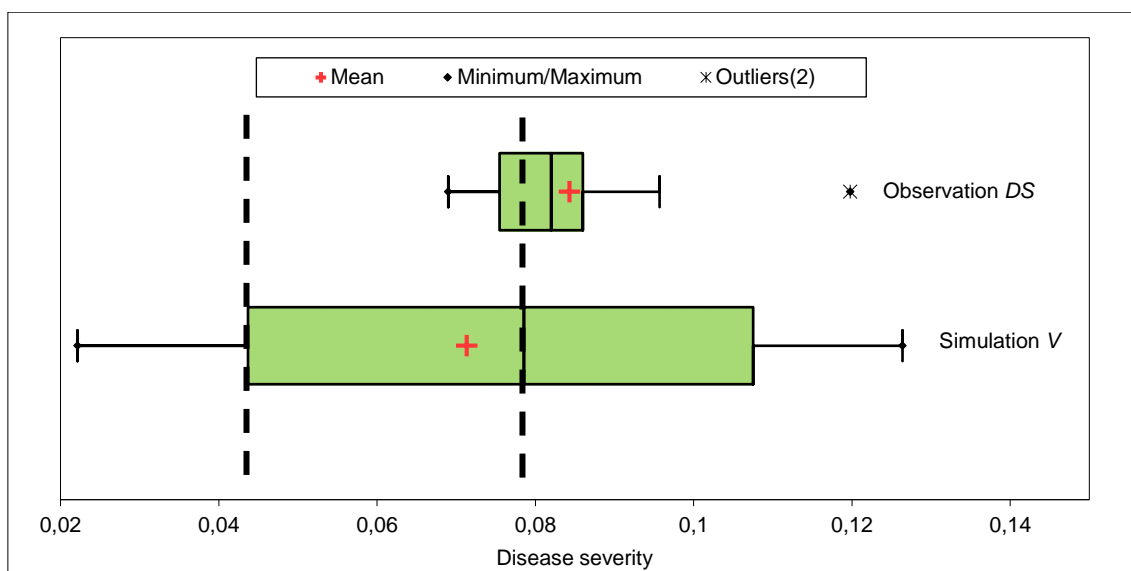


Figure 5.8 Hypothetical threshold for the simulation of the date of the first treatment, comparison of assessed *DS* data (0.05-0.1 *DS*) with simulated *V*

For the practical use by advisors and farmers, it was important to identify not only the disease expressed as *DS*, but also the most favourable infection period or periods with high disease pressure (Gutsche and Kluge 1996; Racca and Jörg 2007). This information could be useful after the first treatment, when little is known about the fungicide efficacy. The following treatments can be timed depending on the disease pressure after the first treatment (Racca et al. 2007; Racca and Tschöpe 2011). To develop a traffic light system,

all simulated disease proportion data V (Fig. 5.3 to Fig. 5.5) were first logit transformed. Since the field assessment are done partly every week with an interval of 7 days, a mean of the last seven days was calculated to simulate relative disease increase (r_L). Then, a simple box plot analysis of r_L was used to determine two risk thresholds based on the median and the upper quartile (Fig. 5.9). Low disease risk: $r_L < 0.042$; medium disease risk: from $0.042 \leq r_L < 0.071$; high disease risk: $r_L > 0.071$.

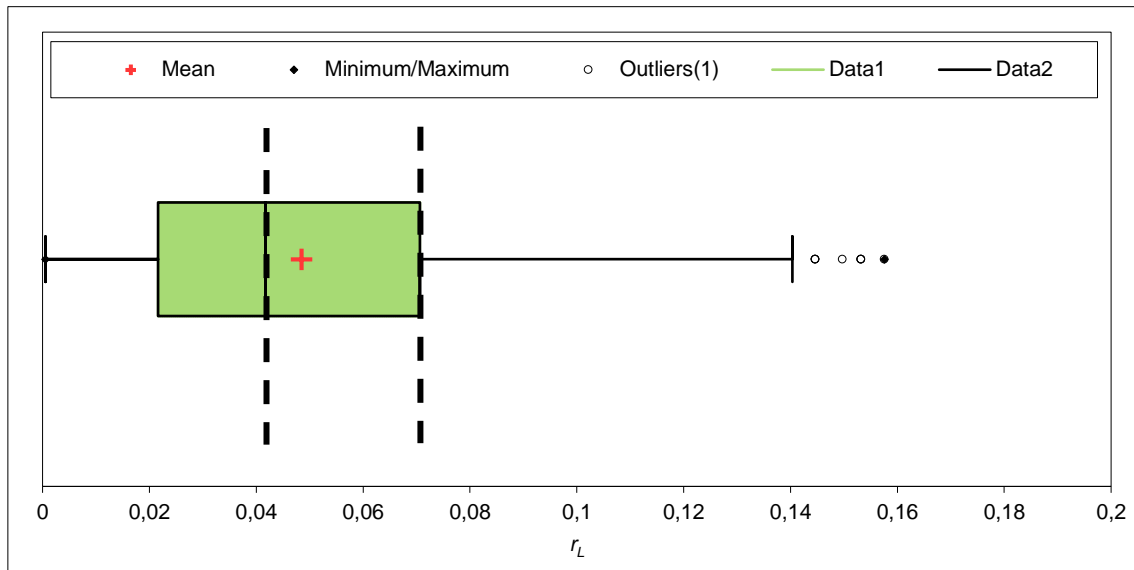


Figure 5.9 Boxplot analysis of the relative disease increase r_L data to determine two risk thresholds for the traffic light system based on the median and the upper quartile

In practice, users of SIMSTEM will be warned of infection periods, based on regional weather data, by means of the traffic light system. For example, red light stands for a forecasted high-risk period. The user is therefore given the opportunity to treat asparagus plants with protective fungicides, at the right time, before imminent infection periods. In Fig. 5.10 to 5.13, four examples of simulating the disease proportion V and the relative disease increase r_L are illustrated with the three risk classes. In Fig. 5.10, weather station Bergen, year 2006, three high disease pressure periods were simulated. The first from the 23rd to the 27th of June, the second from the 3rd to the 11th of August and the third, three weeks long period, from the 21st of August to the 10th of September. Apart from the high-risk periods, there was one separate medium risk period from the 15th to the 20th of July. The influence of r_L on V is less clearly visible in Fig. 5.10 in contrast to the three further examples (Fig. 5.11 to 5.13). In Bergen 2008 (Fig. 5.11) there were three high disease

pressure periods. A first short period from the 25th to the 28th of July, the second period from the 14th to the 18th of August and the third period from the 24th to the 30th of August.

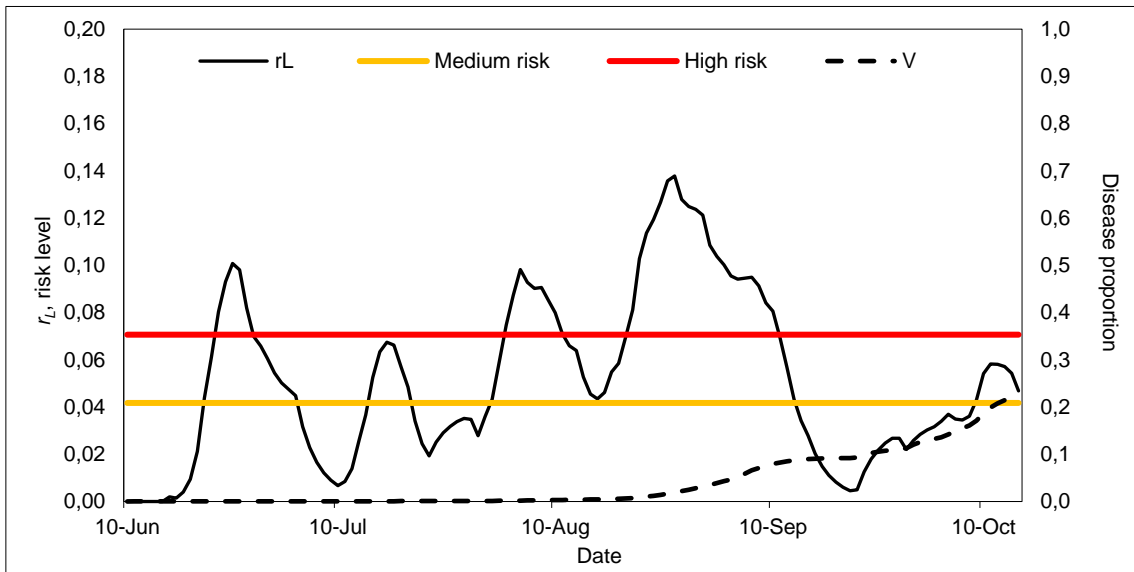


Figure 5.10 Simulation of disease proportion V and relative disease increase r_L for the weather station Bergen, year 2006

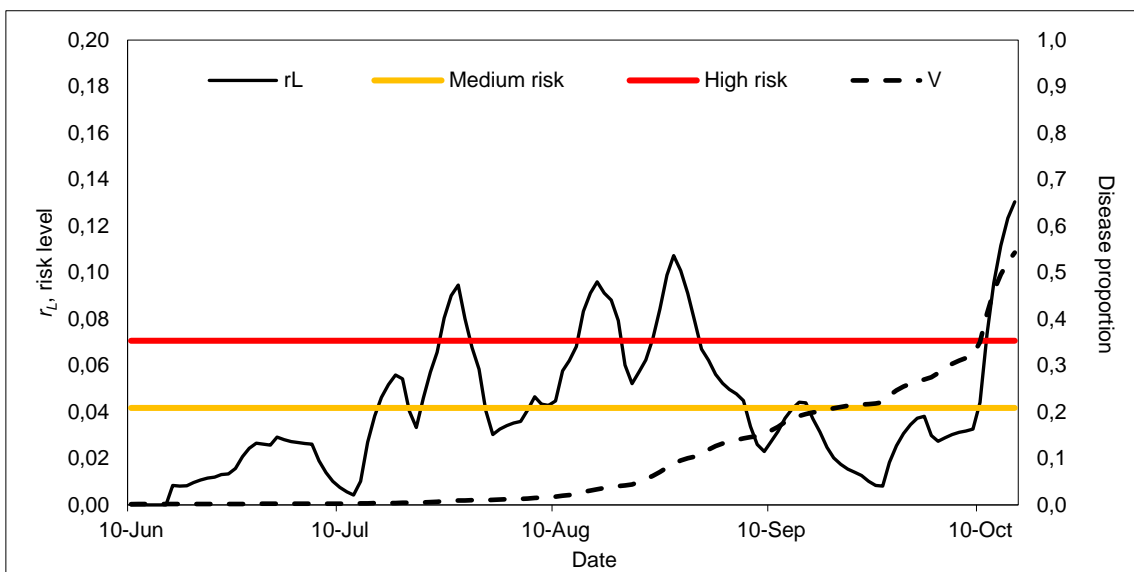


Figure 5.11 Simulation of disease proportion V and relative disease increase r_L for the weather station Bergen, year 2008

The signalization of relevant risk periods for weather station Hannover 2009 was only sporadic (Fig. 5.12). Only two small periods with a high infection risk, at 20th of July and from the 29th to the 31st of July, and medium risk in September, were calculated.

Against all other examples, in Hannover 2014, five high-risk periods were determined (Fig. 5.13). The first from the 13th to the 19th of July, the second from the 28th of July to the 5th of August, the third from the 9th to the 13th of August, the fourth from the 6th to the 16th of September and a fifth late period from the 19th of September to the 7th of October. As the second and the third period and also the fourth and the fifth period are close together, they can be considered as only two long periods. So, three main periods with high infection risk were simulated in Hannover 2014.

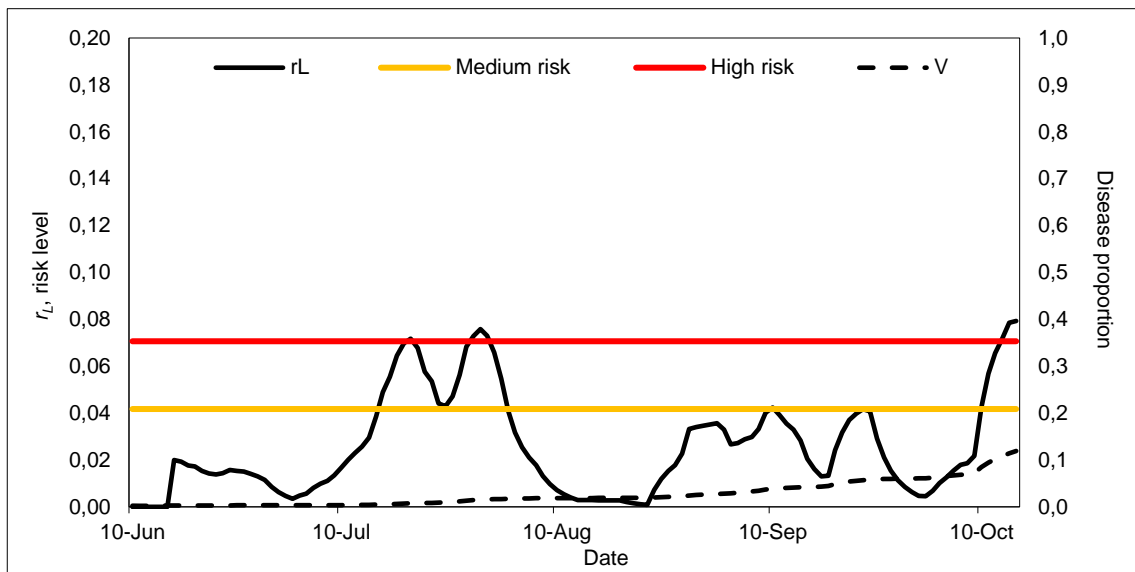


Figure 5.12 Simulation of disease proportion V and relative disease increase r_L for the weather station Hannover, year 2009

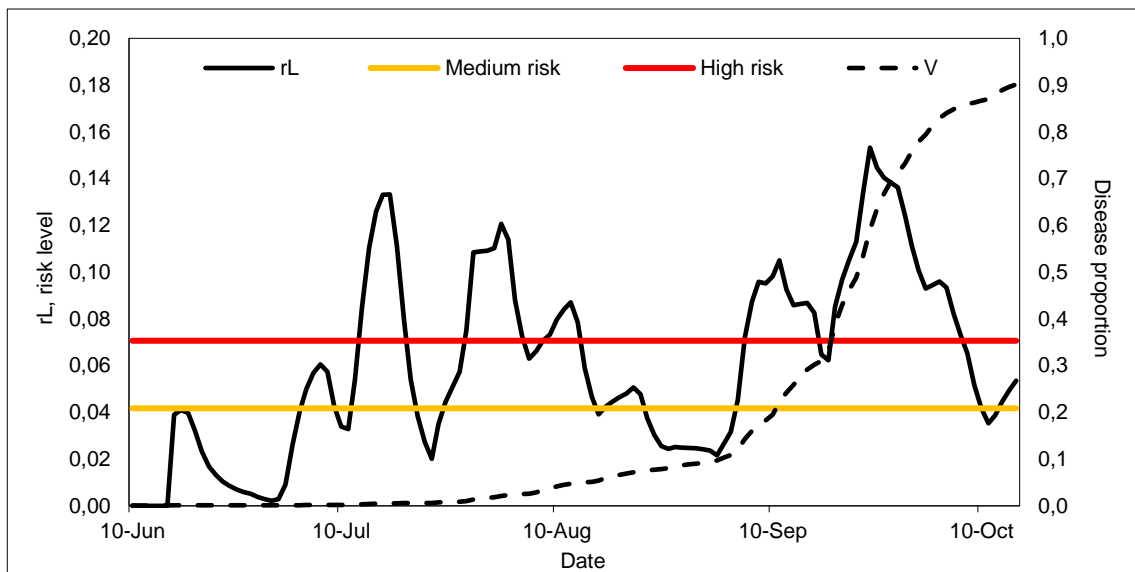


Figure 5.13 Simulation of disease proportion V and relative disease increase r_L for the weather station Hannover, year 2014

5.5. Discussion

In contrast to the BSPcast and TOM-CAST models, SIMSTEM was adapted to the biology of *S. vesicarium* in asparagus (Bohlen-Janssen et al. 2018a; Bohlen-Janssen et al. 2018b). Moreover, the consideration of the germ tube length as a factor for the infection process was new for *S. vesicarium*, and SIMSTEM considers the monocyclic phase too (Bohlen-Janssen et al. 2018a; Bohlen-Janssen et al. 2018b). Therefore, the SIMSTEM algorithm is more complex than that of BSPcast and TOM-CAST. Contrary to the treatment suggestions by the TOM-CAST model (Pitblado 1992), SIMSTEM uses three risk classifications instead of a certain summarised DSV (S)-value (cumulated by daily DSV values from 0 to 4, depending on the daily mean temperature and leaf wetness duration) with a reset of the DSV values after a fungicide treatment.

The date of the first appearance, and especially the proposed initial treatment, is a considerable gain in information. However, the calculated dates are not generally applicable. Taking into account the hypothetical treatment start date (18th of August), only up to two treatments with protective fungicides are theoretically necessary for all high-risk periods (Figs. 5.10 to 5.13). This finding would mean a saving on fungicide applications and operating expenses against a strategy of fewer treatments. The late simulated treatment date is an important theoretical approach; however, repeated trials are needed to test whether the combat of *S. vesicarium* from mid-August would be sufficient in praxis without having yield losses in the following year. The first appearance and the number of treatments are dependent on the date of the harvest's end, and the number of treatments also depends on the duration of the selected fungicide. Various internal infestation tests point out that fungicide treatments starting in mid-August are too late for short-harvested or not harvested young plantings in Northern Germany (Wichura, unpublished data). Furthermore, the latest final treatment recommendation is in Lower Saxony, Germany, currently at the beginning of September, since natural maturity occurs from then on. Therefore, the mathematically derived initial treatment date is partly too late because the initial treatment date was calculated for fully harvested asparagus plantings. Otherwise, the *V* data have clearly demonstrated how late a value of 0.044 (4.4 % disease proportion) is reached in such cultivated asparagus plantings.

Considering the date of the first appearance (15th of July), up to one treatment against the high-risk periods (Figs. 5.10 to 5.13) can be additionally saved. Based on practical experience, the risk of the first appearance depends on the date of the start of the growing

season. From the perspective of the integrated pest management concept, no treatment recommendation should be made before the 15th of July for asparagus plantings in Germany, in which debris were well buried, and plants were cut until about the 24th of June. Otherwise, in young and uncut or short-harvested plantings, infestation can already be measured in June. The plan to ensure more flexibility for the entire forecaster is to include a biofix date in the input mask of SIMSTEM to fix the exact start date of plant growth for each separate asparagus field.

A simple reduction of the number of treatments is not the primary aim of this work; rather, its focus is especially on the fungicide treatments' correct time placement, which was achieved in SIMSTEM by developing the traffic light system. This more conservative treatment strategy, which we recommend, settled between the current practice and the projected start date of treatment. By simulating the disease risk for Bergen in 2006 and 2008, and Hannover in 2009 and 2014, it was demonstrated that only up to three main periods with high infection risk were signalised (Figs. 5.10 to 5.13). Longer periods, such as during September in Bergen in 2006 (Fig. 5.10), must be treated several times, since coatings can be washed off by rain, and the duration of action of the fungicides can be insufficient. Provided that only up to these three periods, and four in Bergen 2006, were classified as being relevant for action, SIMSTEM will need partly fewer fungicide treatments against purple spot, as previously common in practice in Germany. It will also require fewer than the number treatments recommended by the BSPcast and TOM-CAST models, since their suggestions are equivalent to a seven- to 15-day treatment (Llorente et al. 2000; Meyer et al. 2000). Compared to the inaccurate treatment strategy in practice, with SIMSTEM it is now possible to forecast the exact time point of treatment. Also, the treatment suggestions via the traffic light system will later depend on the biofix date. To combat the medium risk periods, similarly frequent applications, as recommended by BSPcast and TOM-CAST, would be necessary. In Hannover in 2009, application could be kept to a minimum (Fig. 5.12) because high- and medium risk-periods were determined in a few cases.

The *T* and *WD* dependent factors' lesion growth and spore formation are possible model parts that have not yet been elaborated, and which might contribute to an improvement of SIMSTEM. Extended investigation and modelling of plant development, incorporated

into an ontogenetic model, would also be useful. Here, the natural senescence of asparagus plants in autumn can be taken into account. In addition, varietal differences in their growth could be incorporated.

Based on observations during this work, fields with a higher basic infestation risk cannot be ruled out. For a separate consideration of these risk fields, the initial condition of the model can be varied, for example, 0.001 as normal risk and 0.005 as high risk. This approach can be used to evaluate particularly sensitive areas, such as young plantings or susceptible varieties, which would lead to a more sensitive approach to the disease. A further option for an extension of the model is the calculation of fungicidal efficiency as a flexible resultant factor on β .

The SIMSTEM model will be available on the agricultural internet platform for integrated plant production ISIP (www.isip.de) after the currently running test phase. SIMSTEM has a special Java-based in- and output mask, which will enable its operation on different types of mobile devices in addition to use on a desktop. The model can be used flexibly because it can forecast the beginning of the epidemic, the first treatment, the disease progression (as a proportion of the diseased leaf area), and signal periods with high disease pressure via a traffic light system. A first validation was promising. Resulting from the ongoing evaluation phase, further adjustments may be made in the future.

Acknowledgements

This study was funded by the German Federal Ministry of Food and Agriculture (BMEL) and the Federal Office for Agriculture and Food (BLE) (grant number 2814702511). We would like to thank Ulrike Weier, Stefan Radtke, Lisa Jettkowski, Sabine Brinkmann, Peter Kronenberger, and Moritz Müller for conducting the cited fungicide trials at Agricultural Chamber Lower Saxony in the past years.

6. General discussion

The objectives of this study were:

- (i) to develop a molecular- and genetics-based method to distinguish *S. vesicarium* from *S. botryosum*;
- (ii) to analyse infected German asparagus samples to identify the prevalent causal agent of purple spot in Germany;
- (iii) to describe and model the monocyclic phase of *S. vesicarium* in asparagus based on biological data from ascospores gathered in laboratory and field trials;
- (iv) to describe and model the polycyclic phase of *S. vesicarium* in asparagus based on biological data from conidia collected in laboratory and field trials; and
- (v) to relate the monocyclic and polycyclic phases in the revised forecasting model SIMSTEM and complete its implementation in www.isip.de.

Before engaging in an extensive literature review and proceeding to the modelling efforts, the identification of the proper pathogen was essential. Considerable previous research has been devoted to the morphological description of *Stemphylium* sp. The drawings, shapes, and length-width ratios (Wiltshire 1938; Neergaard 1945; Simmons 1967; 1969; 1985; Ellis 1971; Singh 1977; Câmara et al. 2002; Inderbitzin et al. 2009; Puig et al. 2015) have been helpful in some instances; however, even when taken together, they are insufficiently specific to identify all of our samples taken from asparagus. Today, a simple PCR reaction can distinguish *S. vesicarium* from *S. botryosum*; identification can also be performed directly from infected asparagus samples with the help of qPCR (Graf et al. 2016). These new options lead to significant time savings and safe distinctions between both species in practice. The high workload with fungal cultures, which was previously necessary for morphological identification, can also be reduced.

In the past, *S. botryosum* was detected in asparagus samples from Germany (Leuprecht 1988; Menzinger and Weber 1990), Japan (Suzui 1973), and Greece (Elena 1996). While the former result from Germany may indicate an evolution in *Stemphylium* over time, improper identification is more likely, justifiable by the clear result in Graf et al. (2016).

Furthermore, Menzinger's and Weber's (1990) images of *S. botryosum* conidia, originating from Germany, seem to match better to *S. vesicarium* (Wiltshire 1938; Simmons 1967; 1969).

The presence of *S. botryosum* in asparagus from Japan (Suzui 1973) has been questioned (Singh 1977; Falloon et al. 1987), and this strain (NBRC 31381/MAFF 305562), which was previously thought to be *S. botryosum* (Suzui 1973), was re-identified as *S. herbarum* by Kurose et al. (2015). In contrast to this finding, Graf et al. (2016) recently identified the strain as *S. vesicarium*. The description of *S. herbarum* in asparagus is atypical; nevertheless, the four-locus phylogeny, proposed by Inderbitzin et al. (2009) and used by Kurose et al. (2015), is generally unable to differentiate between *S. vesicarium*, *S. herbarum*, *S. alfalfa*, *S. tomatonis*, and *S. sedicola* (Inderbitzin et al. 2009). As the cytochrome b region of *S. herbarum*, *S. alfalfa*, *S. tomatonis*, and *S. sedicola* has not yet been sequenced, it is not known whether the sequence of this region can help to differentiate between these species (Graf et al. 2016).

In the history of purple spot pathogen identification, the description of *S. botryosum* in Grecian asparagus is the most interesting. Elena (1996) described the conidia as variously subspherical, oblong, or broadly ovoid, measuring 19-29 μm \times 14-23 μm and with an L/W-ratio of 1.2:1.4 (1.2). This small L/W-ratio matches the forms of *S. botryosum* and *S. globuliferum* (Simmons 1967; 1969). Therefore, either the strain of interest is an *S. vesicarium* strain with an atypically small L/W-ratio or the occurrence of *S. botryosum* in asparagus in Greece cannot yet be conclusively disproven.

In addition to the pathogen identification, it was important to model the essential parts of the monocyclic and polycyclic phases of *S. vesicarium* to develop a new forecast model in asparagus. The first point of investigation was the annual spore flight of the fungus in asparagus plantings. From the outset of the investigation, it was known that *S. vesicarium* presents two different spore types, namely ascospores and conidia, with different seasonality (Falloon and Tate 1986; Hausbeck et al. 1997). The cumulative percentage of trapped ascospores, which was modelled by a Chapman Richards function depending on *SumT* (base 5 °C and $RA > 0.0$), resulted in a better adjustment ($R^2 = 0.93$) than that provided by the cumulative percentage of trapped conidia modelled by a logistic function ($R^2 = 0.81$) depending on *SumT* (base 0 °C and $RA > 0.2$). This is explainable by the larger scatter of the conidial data than that of the ascospore data (Bohlen-Janssen et al. 2018a;

Bohlen-Janssen et al. 2018b). Both models were best adapted to the data and are already used by SIMSTEM.

Ascospore flight in asparagus is often completed before harvesting ends, and a gap can exist from June to July, during which the fungus releases no or few spores (Bohlen-Janssen et al. 2018a; Bohlen-Janssen et al. 2018b). Furthermore, the illustration of both the infection probability and the model output clarifies more clearly that, in the normal case, only the conidia infection probability β_C is responsible for the height of the disease proportion and the loss of an active photosynthesis area (Chapter 5, Fig. 5.1 and 5.2) as well as yield losses in the next harvest season (Menziez et al. 1992).

These findings raise the following question: “how can the disease develop?”, although asparagus plants could often not be infected during the measured ascospore discharge in spring (Bohlen-Janssen et al. 2018a), and conidia could consequently not really be formed on primary lesions. Field observations are partly contradictory because primary infections, according to Falloon and Tate (1986), could be partially observed in the described gap. To properly diagnose other possible sources of purple spot infections in Germany, it is necessary to understand the asparagus production cycle. Once the asparagus plants are completely dead, before the onset of winter, plant debris is crushed into small pieces and mixed into the soil (Brückner et al. 2008). Before and during harvest, asparagus producers work with black and white foils to influence the beginning, duration, and amount of harvest (Brückner et al. 2008). During this time, the plant debris lies flat and partly dry beneath the foil, so the discharge of ripe ascospores cannot have yet occurred. After the harvesting of white asparagus, the foils are removed. The plant debris then lies partially freely on the soil surface, where, shortly after the harvest, rain may induce an extra ascospore flight. This is an assumption based on the field observations in the present project; it still has to be demonstrated because our experiments were not designed to answer this particular question. Previous research has proven that pseudothecia in the upper soil layer do not decompose for up to three months (Johnson 1990; Srivastava et al. 1996); the long viability of pseudothecia would support the above-mentioned theory of ascospore flight after foil removal. Likewise, during mechanical tillage, the plant debris that is buried with mature ascospores may also be brought to the surface of the soil.

Another theoretical approach is that new sprouting spears, which grow through crown-overlying debris and old dead spears, can be infected directly by ascospores produced within this material and not by airborne ascospores. This can also be explained by the

long durability of the plant debris and ascospores in the soil (Johnson 1990; Srivastava et al. 1996). In this particular case, no ascospores would be detectable on our constructed ascospore traps. As a result of these considerations, we conclude that additional ways in which ascospore infections occur should be investigated in future research to further understand the disease and optimise the current forecasting model.

The general influx of ascospores and conidia of other hosts from the area around the asparagus plantation provides an additional possibility for infections and thus the spread and development of purple spot. *S. vesicarium* is known to be a pathogen of pear (Ponti et al. 1982), onion (Shishkoff and Lorbeer 1989), garlic (Aveling 1992), luzerne (Irwin and Bray 1991), alfalfa (Chaisrisook et al. 1995a), and various herbs (Rossi et al. 2005b; Köhl et al. 2009); it is also associated with blossom-end rot in apple (Weber and Dralle 2013). Fifteen genera and 24 species have been identified as hosts for *Stemphylium* species (Farr and Rossman 2015). The wide host range and high degree of differentiation in host specificity among isolates of *S. vesicarium*, for pathogenicity and virulence, have been covered extensively in the literature (Bansal et al. 1992; Montesinos et al. 1995a; Basallote-Ureba et al. 1999; Singh et al. 1999). Early experiments did not prove the pathogenicity of foreign isolates in asparagus (Falloon et al. 1987). Later, necrosis and leaf spots were detected on asparagus after inoculation by conidia from garlic and onion isolates; conidia then developed on the lesions (Basallote-Ureba et al. 1999). In a preliminary experiment (unpublished), lesions were induced on green asparagus spears from apple, pear, and onion isolates; however, conidial formation on these lesions was not observed. Therefore, Koch's postulates (Koch 1912) on proof of the change of the host were not completely fulfilled; however, the formation of lesions and the findings of Basallote-Ureba et al. (1999) demonstrate the importance of further consideration.

Apart from spore flight, several biological processes, which naturally follow after the landing of the spore on the host, were modelled. The primary challenge during the modelling process was the adaptation of the germination data for both phases because clear interactions between temperature and leaf wetness duration could be observed (as can be seen when comparing the single curves in Fig. 3.3 and Fig. 4.3). The shapes of the curves differed with increasing temperature, which means that flexible models must be developed. The behaviour of the two spore types was consequently and successfully modelled using different combined functions (Eq. 3.5 and Eq. 4.6). The optimal temperature for

ascospores was 31.04 °C, while that for conidia was 23.34 °C, i.e., the optimal temperature of ascospore germination is significantly higher than that of conidial germination. Both spore types of *S. vesicarium* germinated rapidly, and the effect of temperature on germination was less after 24 h (Figs. 3.4, Fig. 4.4). The adaptation of the conidia germination data was more accurate ($R^2 = 0.99$) than the adaptation of the ascospore germination data ($R^2 = 0.90$).

The next step in the modelling process was the mathematical adaptation of the germ tube length data. Reasons to examine the germ tube length for both phases included the extremely rapid germination of ascospores and conidia, and the low or non-existent temperature dependence of the germination after 24 h. An unsuccessful experiment, which should have revealed the disease severity of conidia on six-week-old plants, firmly supported the use of germ tube length as a factor for the infection process. The germ tube length had to be adapted differently for each phase (Eq. 3.8 and Eq. 4.8) because the spore types do not behave identically. The selected adjustments fit the biological data well ($R^2 > 0.97$) (Fig. 3.7 and Fig. 4.6). In this case, the optimum temperature for ascospores was 30.42 °C, while that for conidia was 28.68 °C, i.e., the optimal temperatures for both spore types are relatively high and similar (Table 3.6 and Table 4.5). However, such high temperatures were not achieved at times of ascospore release in spring to early summer (Fig. 3.1), this must also be taken into account when interpreting the ascospore germination data.

A comparison of the two graphs of the germ tube length (Fig. 3.7 and Fig. 4.6) revealed that conidial germ tubes are roughly 1.75 times longer than ascospore germ tubes after 24 h of leaf wetness. Due to the different shapes of the two adjustments (Eq. 3.8 and Eq. 4.8), this does not apply to the first hours of leaf wetness. The germ tubes of ascospores grew 1.85 times faster (27.4 $\mu\text{m}/\text{h}$) than those of conidia (14.8 $\mu\text{m}/\text{h}$) after the first hour of wetness. Only after 5 h of leaf wetness did the speed of conidial germ tube growth exceed that of ascospore germ tube growth. Longer germ tubes can be interpreted as higher disease pressure during the infection process because stomata or wounds can be reached faster.

Both life cycle phases of *S. vesicarium* were successfully implemented in the algorithm of SIMSTEM. The current SIMSTEM version has demonstrated its applicability to intensively harvested asparagus plantings, and the first validation was successful. Nevertheless, there are two main points that would significantly improve the model and increase

its practical relevance. On the one hand, it is crucial that the epidemic can be calculated accurately even for plantings with earlier plant growth, for example, if plants were shorter or not harvested. The sooner the harvest ends and the plants are growing with green parts above the soil surface, the longer these plants are exposed to infection by the spores of the fungus. There is also a higher risk for ascospore infections in unharvested young plantings. In the future, a higher flexibility of the model should be ensured by means of a biofix, which allows one to enter a field-specific start date for the beginning of plant growth in the input mask of SIMSTEM. On the other hand, an ontogenetic model, which describes seasonal plant growth from the biofix date onward, might have a significant influence on the calculation of the H-L-I-R epidemic model. The consideration of the natural senescence and a variety difference in plant growth would be a further improvement of the model.

In addition to the mentioned application possibilities, the use of SIMSTEM offers another advantage. Today, when an infection period begins, producers are increasingly challenged to treat all of their fields in time, reinforced by the increasing size of horticulture farms in Germany (Hauschild et al. 2013), which also applies to asparagus producers. As SIMSTEM provides area-specific forecasts of the infection risk by interpolated weather data, the fields can be assessed separately. For example, local rains may affect only some fields; therefore, treating all fields simultaneously within one specific interval may be unnecessary. If this information is known to producers, then machines and employees could be deployed more efficiently. SIMSTEM can currently only forecast periods of high-risk disease pressure three days in advance. As a result, the success of treatments still strongly depends on the speed of fungicide application. Given this consideration, and besides the correct time of application, state-of-the-art application technology remains the decisive factor for disease control.

In summary, all the objectives of this work were achieved. A new differentiation method for *S. vesicarium* and *S. botryosum* was developed as an important basis for the modelling process. The most significant difference between the species is a 3-kb intron, which is present in the cytochrome b region of *S. botryosum* and absent in the cytochrome b region of *S. vesicarium*. The frequency of the species was detected from infected asparagus samples, which identified *S. vesicarium* exclusively. Data from spore flight, germination,

germ tube length, the number of lesions, and mycelium growth suitably provided mathematical descriptions of both phases of purple spot. Both phases were then combined in the algorithm of the new forecasting model SIMSTEM; however, of these two phases, the polycyclic phase was more important. SIMSTEM is a new IPM tool that optimises the time point of fungicide application to combat purple spot in asparagus; it will be available on the agricultural internet platform for integrated plant production ISIP (www.isip.de) after its testing phase is completed.

7. References

- Ahmad, A. (2014). *Stemphylium* grey leaf spot disease of lupins in Western Australia: Doctoral Thesis, The University of Western Australia.
- Ainsworth, C. (2000). Boys and girls come out to play: The molecular biology of dioecious plants. *Annals of Botany*, 86, 211-221.
- Amaro-López, M. A., Zurera-Cosano, G., & Moreno-Rojas, R. (1998). Trends and nutritional significance of mineral content in fresh white asparagus spears. *International Journal of Food Sciences and Nutrition*, 49, 353-363.
- Aveling, T. A. S. (1992). First report of *Stemphylium vesicarium* on garlic in South Africa. *Plant Disease*, 76, 426.
- Bansal, R. K., Menzies, S. A., & Broadhurst, P. G. (1992). Pathogenic variation among strains of *Stemphylium vesicarium* causing leaf spot of asparagus. *New Zealand Journal of Crop and Horticultural Science*, 19, 69-71.
- Basallote-Ureba, M. J., Prados-Ligero, A. M., & Melero-Vara, J. M. (1999). Aetiology of leaf spot of garlic and onion caused by *Stemphylium vesicarium* in Spain. *Plant Pathology*, 48, 139-145.
- Bassanezi, R. B., Amorim, L., Bergamin Filho, A., & Hau, B. (1998). Effects of bean line pattern mosaic virus on the monocyclic components of rust and angular leaf spot of Phaseolus bean at different temperatures. *Plant Pathology*, 47, 289-298.
- Begerow, D., Nilsson, H., Unterseher, M., & Maier, W. (2010). Current state and perspectives of fungal DNA barcoding and rapid identification procedures. *Applied microbiology and biotechnology*, 87, 99-108.
- Benson, B. L. (2009). Update of the world's asparagus production areas, spear utilization and production periods. XII. International asparagus symposium. Lima, 29 october - 1 november 2009.
- Bishop, B.A., Grafius, E., & Osborn, M. (2004). Asparagus miner research 2004. East Lansing, MI, Michigan State University.
- Blancard, D., Piquemal, J.-P., & Gindrat, D. (1984). La Stemphyliose de l'asperge. *Pepinieristes Horticulteurs Maraichers, revue horticole*, 248, 27-30.

- Blok, W. J., & Bollen, G. J. (1995). Fungi on roots and stem bases of asparagus in the Netherlands: Species and pathogenicity. *European Journal of Plant Pathology*, 101, 15-24.
- Bohlen-Janssen, H., Racca, P., Hau, B., & Wichura, A. (2018a). Modelling some aspects of the monocyclic phase of *Stemphylium vesicarium*, the pathogen causing purple spot on asparagus (*Asparagus officinalis* L.). *European Journal of Plant Pathology*, doi.org/10.1007/s10658-018-1455-2
- Bohlen-Janssen, H., Racca, P., Hau, B., & Wichura, A. (2018b). Modelling the effects of temperature and wetness on the polycyclic phase of *Stemphylium vesicarium*, the pathogen causing purple spot on asparagus (*Asparagus officinalis* L.). *J Phytopathol*, doi.org/10.1111/jph.12691
- Bradley, D. J., Gilbert, G. S., & Parker, I. M. (2003). Susceptibility of clover species to fungal infection: The interaction of leaf surface traits and environment. *American Journal of Botany*, 90, 857-864.
- Broome, J. C., English, J. T., Marois, J. J., Latorre, B. A., & Aviles, J. C. (1996). Development of an infection model for *Botrytis* bunch rot of grapes based on wetness duration and temperature. *Phytopathology*, 85, 97-102.
- Brückner, B., Geyer, M., & Ziegler, J. (2008). Spargelanbau: Grundlagen für eine erfolgreiche Produktion und Vermarktung. Stuttgart (Hohenheim), Ulmer.
- Burth, U., & Freier, B. (1996). Zur Entwicklung von Inhalt und Begriff des integrierten Pflanzenschutzes. *Nachrichtenblatt des deutschen Pflanzenschutzdienstes*, 48, 10-13.
- Câmara, M. P., O'Neill, N. R., & van Berkum, P. (2002). Phylogeny of *Stemphylium* spp. based on ITS and glyceraldehyde-3-phosphate dehydrogenase gene sequences. *Mycologia*, 94, 660-672.
- Carisse, O., & Kushalappa, A. C. (1990). Development of an infection model for *Cercospora carotae* on carrot based on temperature and leaf wetness duration. *Phytopathology*, 80, 1233-1238.
- Carson, R. (1962). *Silent Spring*. Boston, Houghton Mifflin Co.
- Chaisrisook, C., Skinner, D. Z., & Stuteville, D. L. (1995a). Molecular genetic relationships of five *Stemphylium* species pathogenic to alfalfa. *Sydowia*, 47, 1-9.

- Chaisrisook, C., Stuteville, D. L., & Skinner, D. Z. (1995b). Five *Stemphylium* spp. pathogenic to alfalfa: Occurrence in the United States and time requirements for ascospore production. *Plant Disease*, 79, 369-372.
- Chase, M. W., Reveal, J. L., & Fay, M. F. (2009). A subfamilial classification for the expanded asparagalean families Amaryllidaceae, Asparagaceae and Xanthorrhoeaceae. *Botanical Journal of the Linnean Society*, 161, 132-136.
- Cheah, L.-H., & Davis, R. D. (2002). New diseases of asparagus - a threat to New Zealand's biosecurity. *New Zealand Plant Protection*, 55, 49-52.
- Clifford, H. T., & Conran, J. G. (1987). 2. Asparagus, 3. Protasparagus, 4. Myrsiphyllum. In: A. S. George (eds.), *Flora of Australia*. Canberra, pp. 159-164.
- Cohen, S. I., & Heald, F. D. (1941). A wilt and root rot of asparagus caused by *Fusarium oxysporum* Schlecht. *Plant Dis. Repr.*, 25, 503-509.
- Cook, M. T. (1923). Dwarf asparagus. *Phytopathology*, 13, 284.
- Crüger, G. (1991). Pflanzenschutz im Gemüsebau, 3. neubearbeitete und erw. Aufl. Stuttgart, Ulmer.
- Cunnington, J. H., & Irvine, G. (2005). Purple spot of asparagus caused by *Stemphylium vesicarium* in Victoria. *Australasian Plant Pathology*, 34, 421-422.
- Damicone, J. P., Manning, W., & Ferro, D. N. (1987). Influence of management practices on severity of stem and crown rot, incidence of asparagus miner, and yield of asparagus grown from transplants. *Plant Disease*, 71, 81-84.
- Dent, D., & Elliott, N. C. (1995). Integrated pest management. London, New York, Chapman & Hall.
- Dix, N. J., & Webster, J. (1995). Fungal ecology. London, Chapman & Hall.
- Dufault, R. J. (1995). Harvest pressures affect forced summer asparagus yield in coastal South Carolina. *Journal of the*, 120, 14-20.
- Dufault, R. J. (1999). Mother stalk culture does not improve plant survival or yield of spring and summer-forced asparagus in South Carolina. *HortScience*, 34, 225-228.
- Dufault, R. J., & Ward, B. (2005). Impact of cutting pressure on yield, quality, root carbohydrates, and survival of spring-harvested or summer-forced asparagus. *HortScience*, 40, 1327-1332.

- Eichhorn, J., Ziegler, J., Laun, N., Keil, B., Racca, P., & Kleinhenz, B., et al. (2010). *Stemphylium*-Prognose mit TomCast. *Julius-Kühn-Archiv*, 428, 426.
- Elena, K. (1996). First report of *Stemphylium botryosum* causing *Stemphylium* leaf spot of asparagus in Greece. *Plant Disease*, 80, 342.
- Ellis, M. B. (1971). Dematiaceous Hyphomycetes. Kew, Surrey, UK, Commonwealth Mycological Institute.
- Elmer, W. H. (1996). Epidemiology and Management of the Diseases Causal to Asparagus Decline. *Plant Disease*, 80, 117-125.
- Endo, R. M., & Burkholder, E. C. (1971). The association of *Fusarium moniliforme* with the crown rot complex of asparagus. *Phytopathology*, 61,
- Faccioli, G. (1965). Further researches on a virus isolated from *Asparagus officinalis* L. *Phytopathologia Mediterranea*, 4, 163-167.
- Falloon, P. G., Falloon, L. M., & Grogan, R. G. (1984). Purple spot and *Stemphylium* leaf spot of asparagus. *California Agriculture*, 38, 21.
- Falloon, P. G., Falloon, L. M., & Grogan, R. G. (1987). Etiology and epidemiology of *Stemphylium* leaf spot and purple spot of asparagus in California. *Phytopathology*, 77, 407-413.
- Falloon, P. G., & Tate, K. G. (1986). Major diseases of asparagus in New Zealand. *Proceedings of the New Zealand Agronomy Society*, 16, 17-28.
- Farr, D. F. & Rossman, A. Y. Fungal databases, systematic mycology and microbiology laboratory, ARS, USDA,. <http://nt.ars-grin.gov/fungalatabases/fungushost/FungusHost.cfm> (Accessed 14 Juli 2015).
- Feller, C., Richter, E., Smolders, T., & Wichura, A. (2012). Phenological growth stages of edible asparagus (*Asparagus officinalis*): codification and description according to the BBCH scale. *Annals of Applied Biology*, 160, 174-180.
- Fujisawa, I. (1986). Asparagus virus. III: A new member of potexvirus from asparagus. *Japanese Journal of Phytopathology*, 52, 193-200.
- Gadoury, D. M., MacHardy, W. E., & Hu, C. (1984). Effects of temperature during ascus formation and frequency of ascospore discharge on pseudothecial development of *Venturia inaequalis*. *Plant Disease*, 68, 223-225.

- Germer, S., Holland, M. J., & Higuchi, R. (2000). High-throughput SNP allele frequency determination in pooled DNA samples by kinetic PCR. *Genome Research*, 10, 258-266.
- Gindrat, D., Varady C., & Neury, G. (1984). Asperge: un enouvelle maladie du feuillage, provoquee par un *Stemphylium*. *Revue Suisse Viticulture, Arboriculture et Horticulture*, 16, 81-85.
- Gompertz, B. (1828). On the nature of the function expressive of the law of human mortality, and on a new mode of determining the value of life contingencies. *Philosophical Transactions of the Royal Society*, 115, 513-585.
- Gossmann, M., Beran, F., Bedlan, G., Plenk, A., Hamedinger, S., & Ohlinger, R., et al. (2008). Investigation on asparagus spears during the main harvest by *Fusarium* spp.-infections and contamination by Fumonisin B1. *Mycotoxin research*, 24, 88-97.
- Gossmann, M., Büttner, C., & Bedlan, G. ((2001). Untersuchungen von Spargel (*Asparagus officinalis* L.) aus Jung- und Ertragsanlagen in Deutschland und Österreich auf Infektionen mit *Fusarium*-Arten. *Pflanzenschutzberichte*, 59, 45-54.
- Gossmann, M., Kleta, S., Humpf, H.-U., & Büttner, C. (2005). Untersuchungen zum endophytischen Befall von *Fusarium proliferatum* (Matsushima) Nirenberg in geernteten Stangen von Spargel (*Asparagus officinalis* L.). *Gesunde Pflanzen*, 57, 53-58.
- Graf, S., Bohlen-Janssen, H., Miessner, S., Wichura, A., & Stammler, G. (2016). Differentiation of *Stemphylium vesicarium* from *Stemphylium botryosum* as causal agent of the purple spot disease on asparagus in Germany. *European Journal of Plant Pathology*, 144, 411-418. doi.org/10.1007/s10658-015-0777-6
- Granke, L. L., & Hausbeck, M. K. (2010). Influence of environment on airborne spore concentrations and severity of asparagus purple spot. *Plant Disease*, 94, 843-850.
- Granke, L. L., & Hausbeck, M. K. (2012). Relationships between airborne *Pleospora herbarum* and *Alternaria* sp. spores in no-till asparagus fields. *Acta Horticulturae*, 950, 285-292.
- Grasso, V., Sierotzki, H., Garibaldi, A., & Gisi, U. (2006). Relatedness among agronomically important rusts based on mitochondrial cytochrome b gene and ribosomal ITS sequences. *Journal of Phytopathology*, 154, 110-118.

- Greiner, H. D. (1980). Untersuchungen über Virus und *Fusarium* an Spargel (*Asparagus officinalis* L.) im nordbadischen Anbaugebiet unter besonderer Berücksichtigung einer Virus-Pilz-Wechselwirkung., Dissertation Universität Hohenheim.
- Grogan, R. G., & Kimble, K. A. (1959). The association of *Fusarium* wilt with the asparagus decline and replant problem in California. *Phytopathology*, 49, 122-125.
- Gutsche, V., & Kluge, E. (1983). Phyteb-Prognose, ein neues Verfahren zur Prognose des Krautfäuleerstauftrittens (*Phytophthora infestans* Mont. De Bary). *Nachrichtenblatt Pflanzenschutz DDR*, 37, 45-48.
- Gutsche, V., & Kluge, E. (1996). The epidemic models for *Phytophthora infestans* and *Pseudocercospora herpotrichoides* and their regional adaptation in Germany. *EPPO Bulletin*, 26, 441-446.
- Halstead, B. D. (1898). The asparagus rust: Its treatment and natural enemies. *NJ Agr. Exp. Sta.*, Bull. 129, 20.
- Hartmann, H. D. (1989). Spargel: Grundlagen für den Anbau; 49 Tab. Stuttgart, Ulmer.
- Hau, B. (1988). Ein erweitertes analytisches Modell für Epidemien von Pflanzenkrankheiten, Habilitationsschrift, Justus-Liebig-Universität, Gießen.
- Hausbeck, M. K., Hartwell, J., & Byrne, J. M. (1997). Epidemiology of *Stemphylium* leaf spot and purple spot in no-till asparagus. *Acta Horticulturae*, 479, 205-210.
- Hauschild, W., Cieplik, U., & Breitenfeld, J. (2013). Erhebungen zum Gemüseanbau in Deutschland neu konzipiert.: Teil II: Ergebnisse der Erhebung 2012. *Statistische Monatshefte Rheinland-Pfalz*, 11, 1057-1067.
- Hawksworth, D. L., Crous, P. W., Redhead, S. A., Reynolds, D. R., Samson, R. A., & Seifert, K. A., et al. (2011). The Amsterdam declaration on fungal nomenclature. *IMA fungus*, 2, 105-112.
- Hein, A. (1960). Über das Vorkommen einer Virose an Spargel. *Z. f. Pfl. Krankheiten*, 67, 217-219.
- Hein, A. (1963). Virose an Spargel. *Mitt. Biol. Bundesanst. Land-Forstwirtschaft. Berlin-Dahlem*, 108, 70-74.
- Hein, A. (1969). Über Viruserkrankungen des Spargels (*Asparagus officinalis* L.): Spargelvirus 1. *Z. Pflanzenkrankh. Pflanzenschutz*, 76, 395-406.

- Hodupp, R. M. (1983). Investigations of factors which contribute to asparagus (*Asparagus officinalis* L.) decline in Michigan: M.S. thesis. Michigan, Michigan State University.
- Inderbitzin, P., Mehta, Y. R., & Berbee, M. L. (2009). *Pleospora* species with *Stemphylium* anamorphs: A four locus phylogeny resolves new lineages yet does not distinguish among species in the *Pleospora herbarum* clade. *Mycologia*, 101, 329-339.
- Irwin, J. A.G., & Bray, R. A. (1991). Variation in virulence within the cool temperature biotype of *Stemphylium vesicarium* (Wallr.) Simmons, a lucerne leaf spot pathogen. *Australian Journal of Experimental Agriculture*, 31, 793-795.
- Johnson, D. A. (1990). Effect of crop debris management on severity of *Stemphylium* purple spot of asparagus. *Plant Disease*, 74, 413-415.
- Johnson, D. A., & Lunden, J. D. (1984). First report of purple spot (*Stemphylium vesicarium*) of asparagus in Washington. *Plant Disease*, 68, 1099.
- Johnson, D. A., & Lunden, J. D. (1986). Effects of wounding and wetting duration on infection of asparagus by *Stemphylium vesicarium*. *Plant Disease*, 70, 419-420.
- Johnston, S. A., Springer, J. K., & Lewis, G. D. (1979). *Fusarium moniliforme* as a cause of stem and crown rot of asparagus and its association with asparagus decline. *Phytopathology*, 69, 778-780.
- Jörg, E., Kleinhenz, B., Racca, P., & Rossi, V. (1999). Prognose der *Cercospora* Blattfleckenkrankheit mit dem Modell CERCOESY. *Zuckerrübe*, 48, 174-176.
- Kleinhenz, B., & Jörg, E. (1998). Integrierter Pflanzenschutz - Rechnergestützte Entscheidungshilfen. *Schriftenreihe des Bundesministeriums für Ernährung, Landwirtschaft und Forsten, Reihe A: Angewandte Wissenschaft, Heft 473*.
- Koch, R. (1912). Complete Works, Vol. I. George Thieme, Leipzig, pp. 650-660. Leipzig.
- Köhl, J., Groenenboom-de Haas, B., Goossen-van de Geijn, H., Speksnijder, A., Kastelein, P., & Hoog, S. de, et al. (2009). Pathogenicity of *Stemphylium vesicarium* from different hosts causing brown spot in pear. *European Journal of Plant Pathology*, 124, 151-162.

- Krug, H. (1999b). Seasonal growth and development of asparagus (*Asparagus officinalis* L.) V. Fern "ripenig" and crown activity in open fields. *Gartenbauwissenschaft*, 64, 165-172.
- Krug, H. (1999a). Seasonal growth and development of asparagus (*Asparagus officinalis* L.). IV. Crown activity as a function of incubation temperature and temperature gradient. *Gartenbauwissenschaft*, 64, 84-88.
- Krug, H. (1996). Seasonal growth and development of asparagus (*Asparagus officinalis* L.) I. Temperature experiments in controlled environments. *Gartenbauwissenschaft*, 61, 18-25.
- Krug, H. (1998). Seasonal growth and development of asparagus (*Asparagus officinalis* L.) II. Influence of drought on crown activity. *Gartenbauwissenschaft*, 63, 71-78.
- Kurose, D., Misawa, T., Suzui, T., Ichikawa, K., Kisaki, G., & Hoang, L., et al. (2015). Taxonomic re-examination of several Japanese *Stemphylium* strains based on morphological and molecular phylogenetic analyses. *Journal of General Plant Pathology*, 81, 358-367.
- Lacy, M. L. (1982). Purple spot: A new disease of young asparagus spears caused by *Stemphylium vesicarium*. *Plant Disease*, 66, 1198-1200.
- Lalancette, N., Ellis, M. A., & Madden, L. V. (1988). Development of an infection efficiency model for *Plasmopara viticola* on American grape based on temperature and duration of leaf wetness. *Phytopathology*, 78, 794-800.
- Leach, C. M. (1962). Sporulation of diverse species of fungi under near-ultraviolet radiation. *Canadian Journal of Botany*, 40, 151-161.
- Leach, C. M. (1967). Interaction of near-ultraviolet light and, temperature on sporulation of the fungi *Alternaria*, *Cercospora*, *Fusarium*, *Helminthosporium*, and *Stemphylium*. *Canadian Journal of Botany*, 45, 1999-2016.
- Leach, C. M., & Aragaki, M. (1970). Effects of temperature on conidium characteristics of *Ulocladium chartarum* and *Stemphylium floridanum*. *Mycologia*, 62, 1071.
- Lee, Y. O., Kanno, A., & Kameya, T. (1996). The physical map of the chloroplast DNA from *Asparagus officinalis* L. *TAG. Theoretical and applied genetics. Theoretische und angewandte Genetik*, 92, 10-14.

- LeSage, L., Dobesberger, E. J., & Majka, C. G. (2008). Introduced leaf beetles of the maritime provinces, 6: The common asparagus beetle, *Crioceris asparagi* (Linnaeus), and the twelve-spotted asparagus beetle, *Crioceris duodecimpunctata* (Linnaeus) (Coleoptera: Chrysomelidae). *Proceedings of the Entomological Society of Washington*, 110, 602-621.
- Leuprecht, B. (1988). *Stemphylium*, eine wichtige Krankheit an Spargel. *Gemüse*, 24, 235-236.
- Leuprecht, B. (1990). *Stemphylium botryosum* Wallr. on *asparagus*. *Gesunde Pflanzen*, 42, 187-191.
- Llorente, I., & Montesinos, E. (2004). Development and field evaluation of a model to estimate the maturity of pseudothecia of *Pleospora allii* on pear. *Plant Disease*, 88, 215-219.
- Llorente, I., & Montesinos, E. (2006). Brown spot of pear: an emerging disease of economic importance in Europe. *Plant Disease*, 92, 99-104.
- Llorente, I., Moragrega, C., Ruz, L., & Montesinos, E. (2012). An update on control of brown spot of pear. *Trees*, 26, 239-245.
- Llorente, I., Vilardell, A., & Montesinos, E. (2006). Infection potential of *Pleospora allii* and evaluation of methods for reduction of the overwintering inoculum of brown spot of pear. *Plant Disease*, 90, 1511-1516.
- Llorente, I., Vilardell, A., Vilardell, P., & Montesinos, E. (2008). Evaluation of new methods in integrated control of brown spot of pear (*Stemphylium vesicarium*, teleomorph *Pleospora allii*). *Acta Horticulturae*, 800, 825-832.
- Llorente, I., Vilardell, P., Bugiani, R., Gherardi, I., & Montesinos, E. (2000). Evaluation of BSPcast disease warning system in reduced fungicide use programs for management of brown spot of pear. *Plant Disease*, 84, 631-637.
- Llorente, I., Villardell, P., & Montesinos, E. (2011). Evaluation of a revision of the BSPcast decision support system for control of brown spot of pear. *Phytopathologia Mediterranea*, 50, 139-149.
- Logrieco, A., Doko, B., Moretti, A., Frisullo, S., & Visconti, A. (1998). Occurrence of Fumonisin B 1 and B 2 in *Fusarium proliferatum* infected asparagus plants. *Journal of Agricultural and Food Chemistry*, 46, 5201-5204.

- Madden, L., Pennypacker, S. P., & MacNab, A. A. (1978). FAST, a forecast system for *Alternaria solani* on tomato. *Phytopathology*, 68, 1354-1358.
- Madden, L. V., Hughes, G., & van den Bosch, F. (2007). The study of plant disease epidemics. St. Paul, Minn., The American Phytopathological Society.
- Menzies, S. A. (1980). Disease and decline problems in asparagus, *Proceedings of seminar on asparagus*. Hamilton, New Zealand Ministry of Agriculture and Fisheries. (pp. 65-68).
- Menzies, S. A., Bansal, R. K., & Broadhurst, P. G. (1991). Effect of environmental factors on severity of *Stemphylium* leaf spot on asparagus. *New Zealand Journal of Crop and Horticultural Science*, 19, 135-141.
- Menzies, S. A., Broadhurst, P. G., & Triggs, C. M. (1992). *Stemphylium* disease of asparagus (*Asparagus officinalis* L.) in New Zealand. *New Zealand Journal of Crop and Horticultural Science*, 20, 427-433.
- Menzinger, W., & Weber, D. (1990). Der Pilz *Stemphylium botryosum* Wallr. am Spargel. *Gemuese*, 26, 16-18.
- Meyer, M. P., Hausbeck, M. K., & Podolsky, R. (2000). Optimal fungicide management of purple spot of asparagus and impact on yield. *Plant Disease*, 84, 525-530.
- Miessner, S., & Stammler, G. (2010). *Monilinia laxa*, *M. fructigena* and *M. fructicola* risk estimation of resistance to QoI fungicides and identification of species with cytb gene sequences. *Journal of Plant Diseases and Protection*, 117, 162-167.
- Montesinos, E., Moragrega, C., Llorente, I., & Vilardell, P. (1995a). Susceptibility of selected European pear cultivars to infection by *Stemphylium vesicarium* and influence of leaf and fruit age. *Plant Disease*, 79, 471-473.
- Montesinos, E., Moragrega, C., Llorente, I., Vilardell, P., Bonaterra, A., & Ponti, I., et al. (1995b). Development and evaluation of an infection model for *Stemphylium vesicarium* on pear based on temperature and wetness duration. *Phytopathology*, 85, 586-592.
- Montesinos, E., & Vilardell, P. (1992). Evaluation of FAST as a forecasting system for scheduling fungicide sprays for control of *Stemphylium vesicarium* on pear. *Plant Disease*, 76, 1221-1226.

- Neergaard, P. (1945). Danish species of *Alternaria* and *Stemphylium*: Taxonomy, parasitism, economical significance. Copenhagen and Humphrey Millford, Oxford, U.P., London, Einar Munksgaard.
- Neubauer, C. (1997). *Stemphylium* an Spargel. *Gemüse*, 7, 421-424.
- Neubauer, C. (1998). Epidemiologie und Schadrelevanz von *Stemphylium botryosum* Wallr. an Spargel. *Gesunde Pflanzen*, 50, 251-256.
- Otto, G. (2009). Die endotrophe Mykorrhiza – eine mögliche Ursache für das Phänomen des „Johannistriebes“ von Apfelgehölzen? *Journal für Kulturpflanzen*, 61, 254-259.
- Paludan, N. (1964). Virussygddomme hos *Asparagus officinalis*. *Maanedsovers. Plantesygd.*, 407, 11-16.
- Paschold, P. J., Artelt, B., & Hermann, G. (2002). Influence of harvest duration on yield and quality of asparagus. *Acta Horticulturae*, 589, 65-71.
- Payandeh, B., Wallace, D. R., & MacLeod, D. M. (1980). An empirical regression function suitable for modelling spore germination subject to temperature threshold. *Canadian Journal of Botany*, 58, 936-941.
- Perkins, J. H. (1982). Insects, experts, and the insecticide crisis: The quest for new pest management strategies. New York, Plenum Press.
- Pitblado, R. E. (1992). The development and implementation of TOM-CAST: A weather-timed fungicide spray program for field tomatoes. Ontario, Canada, Ministry of Agriculture and Food.
- Ponti, I., Cavani, P., & Brunelli, A. (1982). ‘‘Maculatura bruna’’ delle pere: eziologia e difesa. *Inform. Fitopat.*, 32, 35-40.
- Posnette, A. F. (1969). Nematode-transmitted viruses in asparagus. *Journal of Horticultural Science*, 44, 403-406.
- Prados-Ligero, A. M., González-Andújar, J. L., Melero-Vara, J. M., & Basallote-Ureba, M. J. (1998). Development of *Pleospora allii* on garlic debris infected by *Stemphylium vesicarium*. *European Journal of Plant Pathology*, 104, 861-870.
- Prados-Ligero, A. M., Melero-Vara J. M., Corpas-Hervias C., & Basallote-Ureba M. J. (2003). Relationships between weather variables, airborne spore concentrations and

- severity of leaf blight of garlic caused by *Stemphylium vesicarium* in Spain. *European Journal of Plant Pathology*, 109, 301-310.
- Prenger, J. J. & Ling, P. P. (2001) Greenhouse condensation control - Understanding and using Vapor Pressure Deficit (VPD): Extension factsheet, Wooster, Ohio State University (15 Mai 2017).
- Puig, M., Ruz, L., Montesinos, E., Moragrega, C., & Llorente, I. (2015). Combined morphological and molecular approach for identification of *Stemphylium vesicarium* inoculum in pear orchards. *Fungal biology*, 119, 136-144.
- Putnam, A. R., & Lacy, M. L. (1977). Asparagus management with no-tillage. MI State Univ. Agric. Exp. Sta. Res. Rep.
- Racca, P., & Jörg, E. (2007). CERCBET 3 - A forecaster for epidemic development of *Cercospora beticola*. *EPPO Bulletin*, 37, 344-349.
- Racca, P., Jörg, E., Mittler, S., & Petersen, J. (2002). CERCBET 3 - ein flexibles Modell zur Prognose von Bekämpfungsschwellenüberschreitungen bei *Cercospora beticola*. *Mitteilungen aus der Biologischen Bundesanstalt für Land- und Forstwirtschaft*, 390, 218-219.
- Racca, P., Kleinhenz, B., & Jörg, E. (2007). SIMPEROTA 1/3 - a decision support system for blue mould disease of tobacco. *OEPP/EPPO* 388-373.
- Racca, P., Kleinhenz, B., Zeuner, T., Keil, B., Tschöpe, B., & Jung, J. (2011). Decision support systems in agriculture: Administration of meteorological data, use of Geographic Information Systems (GIS) and validation methods in crop protection warning service. In: C. Jao (eds.), *Efficient decision support systems - Practice and challenges from current to future*, InTech. Rijeka, pp. 331-351.
- Racca, P., & Tschöpe, B. (2011). SIMCOL - A decision support system for integrated control of anthracnose on blue lupin. *Journal für Kulturpflanzen*, 63, 411-422.
- Racca, P., Zeuner, T., Jung, J., & Kleinhenz, B. (2010). Model validation and use of geographic information systems in crop protection warning service. In: E.-C. Oerke, R. Gerhards, G. Menz and R. A. Sikora (eds.), *Precision Crop Protection – the Challenge and Use*, Springer Netherlands, pp. 259-276.
- Richards, F. J. (1959). A flexible growth function for empirical use. *Journal of Experimental Botany*, 10, 290-301.

- Robb, A. R. (1984). Physiology of asparagus (*Asparagus officinalis*) as related to the production of the crop. *New Zealand Journal of Experimental Agriculture*, 12, 251-260.
- Rossi, V., Bugiani, R., Giosué, S., & Natali, P. (2005). Patterns of airborne conidia of *Stemphylium vesicarium*, the causal agent of brown spot disease of pears, in relation to weather conditions. *Aerobiologia*, 21, 203-216.
- Rossi, V., Giosue, S., & Bugiani, R. (2003). Influence of air temperature on the release of ascospores of *Venturia inaequalis*. *Journal of Phytopathology*, 151, 50-58.
- Rossi, V., Patteri, E., & Bugiani, R. (2008). Sources and seasonal dynamics of inoculum for brown spot disease of pear. *European Journal of Plant Pathology*, 121, 147-159.
- Rossi, V., Patteri, E., & Giosué, S. (2006). Temperature and humidity requirements for germination and infection by ascospores of *Pleospora alii*, the teleomorph of *Stemphylium vesicarium*. *IOBC/wprs Bulletin* 223-230.
- Rossi, V., Patteri, E., Giosué, S., & Bugiani, R. (2005b). Growth and sporulation of *Stemphylium vesicarium*, the causal agent of brown spot of pear, on herb plants of orchard lawns. *European Journal of Plant Pathology*, 111, 361-370.
- Rossmann, A. Y., Crous, P. W., Hyde, K. D., Hawksworth, D. L., Aptroot, A., & Bezerra, J. L., et al. (2015). Recommended names for pleomorphic genera in Dothideomycetes. *IMA fungus*, 6, 507-523.
- Schmitt, J., Kleinhenz, B., Werthmüller, J., & Racca, P. (2016). Prognosemodell zur Berechnung primärer Infektionen von *Venturia inaequalis*. *Julius-Kühn-Archiv*, 454, 295-296.
- Schoch, C. L., Seifert, K. A., Huhndorf, S., Robert, V., Spouge, J. L., & Levesque, C. A., et al. (2012). Nuclear ribosomal internal transcribed spacer (ITS) region as a universal DNA barcode marker for fungi. *Proceedings of the National Academy of Sciences of the United States of America*, 109, 6241-6246.
- Seefelder, W., Gossmann, M., & Humpf, H.-U. (2002). Analysis of Fumonisin B1 in *Fusarium proliferatum* - Infected asparagus spears and garlic bulbs from Germany by liquid chromatography–Electrospray Ionization Mass Spectrometry. *Journal of Agricultural and Food Chemistry*, 50, 2778-2781.

- Shelton, D. R., & Lacy, M. L. (1980). Effect of harvest duration on yield and on depletion of storage carbohydrates in asparagus roots. *Journal of the American Society for Horticultural Science*, 105, 332-335.
- Shenoy, B. D., Jeewon, R., & Hyde, K. D. (2007). Impact of DNA sequence-data on the taxonomy of anamorphic fungi. *Fungal Diversity*, 26, 1-54.
- Shishkoff, N., & Lorbeer, J. W. (1989). Etiology of *Stemphylium* leaf blight of onion. *Phytopathology*, 79, 301-304.
- Sierotzki, H., Frey, R., Wullschleger, J., Palermo, S., Karlin, S., & Godwin, J., et al. (2007). Cytochrome b gene sequence and structure of *Pyrenophora teres* and *P. tritici-repentis* and implications for QoI resistance. *Pest management science*, 63, 225-233.
- Simmons, E. G. (1967). Typification of *Alternaria*, *Stemphylium*, and *Ulocladium*. *Mycologia*, 59, 67-92.
- Simmons, E. G. (1969). Perfect states of *Stemphylium*. *Mycologia*, 61, 1-26.
- Simmons, E. G. (1985). Perfect states of *Stemphylium*. II. *Sydowia*, 38, 284-293.
- Singh, G. (1977). Plant pathogenic species of *Stemphylium* wallr. in New Zealand: A thesis presented in partial fulfilment of the requirements for the degree of Doctor of Philosophy at Massey University.
- Singh, P., Bugiani, R., Cavanni, P., Nakajima, H., Kodama, M., & Otani, H., et al. (1999). Purification and biological characterization of host-specific SV-toxins from *Stemphylium vesicarium* causing brown spot of european pear. *Phytopathology*, 89, 947-953.
- Spiess, A.-N., & Neumeyer, N. (2010). An evaluation of R2 as an inadequate measure for nonlinear models in pharmacological and biochemical research: A Monte Carlo approach. *BMC pharmacology*, 10, 6.
- Srivastava, A. K., Borse, V. A., Gupta, R. P., & Srivastava, P. K. (1996). Mode of perpetuation and role of nature in spread of *Stemphylium* blight and purple blotch diseases of onion. A short note. *Newsletter Natl. Hort. Res. And Dev. Foundation*, 16, 9-11.

- Stammler, G., Schutte, G. C., Speakman, J., Miessner, S., & Crous, P. W. (2013). *Phyllosticta* species on citrus: Risk estimation of resistance to QoI fungicides and identification of species with cytochrome b gene sequences. *Crop Protection*, 48, 6-12.
- StBA (Statistisches Bundesamt) (Hrsg.) (2015). Gemüseerhebung 2014: Anbau und Ernte von Gemüse und Erdbeeren. (= Fachserie 3 Reihe 3.1.3). Wiesbaden.
- Stoetzel, M. B. (1990). Aphids (Homoptera: Aphididae) colonizing leaves of asparagus in the United States. *Journal of Economic Entomology*, 83, 1994-2002.
- Stone, G. E., & Chapman, G. H. (1908). Report of the botanist. *MA Agr. Exp. Sta.*, 20, 127.
- Sun, T., & Powers, J. R. (2007). Chapter 12: Antioxidants and antioxidant activities of vegetables. In: F. Shahidi and C.-T. Ho (eds.), *In: Antioxidant Measurement and Applications*, American Chemical Society Symposium Series. Washington, DC, pp. 160-183.
- Suzui, T. (1973). *Stemphylium* leaf spot (*Stemphylium botryosum* Wallr.) on asparagus plants. *Annals of the Phytopathological Society of Japan*, 39, 364-366.
- Teng, P. S. (1981). Validation of computer models of plant disease epidemics: A review of philosophy and methodology. *Journal of Plant Diseases and Protection*, 88, 49-63.
- Thompson, A. H., & Uys, M. D. R. (1992). *Stemphylium vesicarium* on asparagus: a first report from South Africa. *Phytophylactica*, 24, 351-353.
- Tomassoli, L., Tiberini, A., & Vetten, H.-J. (2012). Viruses of asparagus. *Advances in virus research*, 84, 345-365.
- Trail, F. (2007). Fungal cannons: Explosive spore discharge in the Ascomycota. *FEMS microbiology letters*, 276, 12-18.
- Trapero-Casas, A., & Kaiser, W. J. (1992). Development of *Didymella rabiei*, the teleomorph of *Ascochyta rabiei*, on chickpea straw. *Phytopathology*, 82, 1261-1266.
- Vogel, G. (1996). Handbuch des speziellen Gemüsebaues. Stuttgart (Hohenheim), Ulmer.
- von Bertalanffy, L. (1957). Quantitative laws in metabolism and growth. *The Quarterly Review of Biology*, 32, 217-231.

- Wallroth, K. F. W. (1833). *Flora Cryptogamica Germaniae: Algas et fungos. II. Norimbergae, DE, Schragius.*
- Wang, Y., Geng, Y., Pei, Y. F., & Zhang, X. G. (2010). Molecular and morphological description of two new species of *Stemphylium* from China and France. *Mycologia*, 102, 708-717.
- Weber, R. W. S., & Dralle, N. (2013). Fungi associated with blossom-end rot of apples in Germany. *European Journal of Horticultural Science*, 78, 97-105.
- Weber, Z., KostECKI, M., BARGEN, S., GOSSMANN, M., WASKIEWICZ, A., & BOCIANOWSKI, J., et al. (2006). *Fusarium* species colonizing spears and forming mycotoxins in field samples of asparagus from Germany and Poland. *Journal of Phytopathology*, 154, 209-216.
- Weinheimer, S. (2008). Einfluss eines differenzierten Wasserangebotes auf Wurzelwachstum und Reservekohlenhydrathaushalt von Bleichspargel (*Asparagus officinalis* L.): Dissertation Humboldt-Universität zu Berlin.
- Weissenfels, M., & Schmelzer, K. (1976). Untersuchungen über das Schadausmaß durch Viren am Spargel (*Asparagus officinalis* L.). *Archives Of Phytopathology And Plant Protection*, 12, 67-73.
- White, T. J., Bruns, T., Lee, S., & Taylor, J. (1990). Amplification and direct sequencing of fungal ribosomal RNA genes for phylogenetics. In: Innis, M.A., D.H. Gelfand, J.J. Sninsky, and T.J. White (eds.), *PCR Protocols: A Guide to Methods and Applications*, Academic Press, Inc. New York, USA, pp. 315-322.
- Wijayawardene, N. N., Crous, P. W., Kirk, P. M., Hawksworth, D. L., Boonmee, S., & Braun, U., et al. (2014). Naming and outline of Dothideomycetes-2014 including proposals for the protection or suppression of generic names. *Fungal Diversity*, 69, 1-55.
- Wilson, D. R., Sinton, S. M., Butler, R. C., Drost, D. T., Paschold, P. J., & van Kruistum, G., et al. (2008). Carbohydrates and yield physiology of asparagus - A global overview. *Acta Horticulturae*, 776, 413-428.
- Wilson, D. R., Sinton, S. M., & Wright, C. E. (1999). Influence of time of spear harvest on root system resources during the annual growth cycle of asparagus. *Acta Horticulturae*, 479, 313-320.

- Wiltshire, S. P. (1938). The original and modern conceptions of *Stemphylium*. *Transactions of the British Mycological Society*, 21, 211-236.
- Yang, H. J. (1982). Autotoxicity of *Asparagus officinalis* L. *Journal of the American Society for Horticultural Science*, 107, 860-862.
- Zapf, S., Klappach, K., Pfenning, J., & Ernst, M. K. (2011). Erarbeitung eines Testverfahrens zur Bestimmung der Protektiv- und Kurativleistung von Fungiziden bei der Bekämpfung des Erregers der *Stemphylium*-Laubkrankheit *Stemphylium botryosum* in der Spargelkultur (*Asparagus officinalis* L.). *Gesunde Pflanzen*, 63, 167-174.

Acknowledgement

Am Ende möchte ich mich bei all den Leuten bedanken, ohne die diese Arbeit nicht möglich gewesen wäre. Insbesondere:

Prof. Dr. Bernhard Hau für die fachkundige Betreuung und die Hilfe im Rahmen der Modellierung, der Prognose und des Publikationsprozesses. Ihre wegweisenden und eleganten Lösungsansätze haben wesentlich zur Qualität dieser Arbeit beigetragen. Ganz besonders hervorzuheben ist, dass Sie mich auch nach Ihrem Eintritt in den Ruhestand so intensiv betreut haben.

Dr. Alexandra Wichura für das in mich gesetzte Vertrauen, die fachkundige Betreuung und die Möglichkeit der Versuchsdurchführungen und Nutzung der Labore am Pflanzenschutzamt Hannover (LWK Niedersachsen). Sie haben mich stets gefördert und Ihr kompetenter Rat kam mir in jeder Phase dieser Arbeit sehr zugute.

Dr. Paolo Racca für die große Hilfe im Rahmen der Modellierung und Prognose, sowie das offene Ohr bei jeder noch so kleinen Frage.

Prof. Dr. Roland W. S. Weber, Dr. Gerd Stammler, Dr. Karl-Heinz Pastrik und besonders **Sarah Graf** für die Unterstützung im Rahmen der Erregeridentifikation.

Dr. Norbert Laun, Simon Deyerling und **Marion Himmel** für die Unterstützung bei der Sammlung von Pflanzenproben und der Kontrolle von Sporenfallen.

Darüber hinaus bedanke ich mich bei allen beteiligten Arbeitskollegen der Landwirtschaftskammer Niedersachsen für die gute Zusammenarbeit und die angenehme und kollegiale Arbeitsatmosphäre. **Sabine Brinkmann, Lisa Jettkowski, Nils Kraushaar, Peter Kronenberger, Moritz Müller, Stefan Radtke, Dieter Weber** und **Ulrike Weier** für die herausragende Teamarbeit und die umfangreiche Hilfe bei allen Feld-, Gewächshaus- und Laborversuchen.

Meiner Frau **Justyna Bohlen-Janßen**, meinen Eltern **Elke** und **Gerd Bohlen-Janßen** und meiner Schwester **Kathrin Zentner** für das in mich gesetzte Vertrauen und jegliche Unterstützung. Meinen Freunden für die vielen schönen Momente und gemeinsamen Erlebnisse.

Curriculum Vitae

Personal details

Name: Henrik Enno Bohlen-Janßen
Birthday: October 12, 1985
Place of birth: Hannover / Germany

Academic education

2013 - 2018 Ph.D. studies in horticultural sciences at the Leibniz University Hannover. Graduation: Dr. rer. hort.
2011 - 2013 Studies of horticultural sciences at the Leibniz University Hannover. Graduation: M. Sc.
2006 - 2010 Studies of horticulture at the University of Applied Sciences Osnabrück. Graduation: B. Sc.

Work history

2013 - 2016 Research assistant at the Plant Protection Service of the Chamber of Agriculture Lower Saxony in Hannover.

In the project “Prognosis of *Stemphylium*” within the association project “Improved control options of *Stemphylium* on asparagus through an optimised scheduling of fungicide application and an improved application technology”

Practical training

2009 Data collection for bachelor’s thesis and insights into plant protection at the Fruit-Growing Centre in Jork

Education

2005 - 2006 Justus-von-Liebig school in Hannover.
Graduation: Entrance qualification for studies at Universities of Applied Sciences
2000 - 2002 Dietrich Bonhoeffer secondary school in Hannover.
Graduation: Secondary school certificate

Vocational training

2002 - 2005 Graduated education in gardening and landscaping

Publications

Bohlen-Janssen, H., Racca, P., Hau, B. and Wichura, A. (2018). Modelling some aspects of the monocyclic phase of *Stemphylium vesicarium*, the pathogen causing purple spot on asparagus (*Asparagus officinalis* L.). *European Journal of Plant Pathology*, doi.org/10.1007/s10658-018-1455-2

Bohlen-Janssen, H., Racca, P., Hau, B. and Wichura, A. (2018). Modelling the effects of temperature and wetness on the polycyclic phase of *Stemphylium vesicarium*, the pathogen causing purple spot on asparagus (*Asparagus officinalis* L.). *Journal of Phytopathology*, doi.org/10.1111/jph.12691

Bohlen-Janssen, H., Racca, P. and Wichura, A. (2016) Biology and modelling of *Stemphylium vesicarium* in asparagus. *Julius-Kühn-Archiv*, 454:548

Graf, S., Bohlen-Janssen, H., Miessner, S., Wichura, A. and Stammler, G. (2016) Differentiation of *Stemphylium vesicarium* from *Stemphylium botryosum* as causal agent of the purple spot disease on asparagus in Germany. *European Journal of Plant Pathology*, 144:411-418. doi.org/10.1007/s10658-015-0777-6

Presentations

- | | |
|------------|---|
| 09/19/2013 | 19. Versuchs- und Informationsausschuss. Hannover |
| 11/06/2013 | Profi-Tag Spargel. Hannover |
| 02/21/2014 | Seminar zum Spargelanbau. Braunschweig |
| 02/26/2014 | Seminar zum Spargelanbau. Nienburg |
| 09/09/2014 | 72. Sitzung AK Spargel, Bundesfachg. Gemüsebau Schif-ferstadt |
| 02/10/2015 | Seminar zum Spargelanbau. Langförden |
| 10/29/2015 | 20. Versuchs- und Informationsausschuss. Ellerhoop |
| 12/01/2015 | 36. Straelener Spargeltag. Straelen |
| 01/25/2016 | 25. Grünberger Spargelseminar. Grünberg |
| 01/30/2016 | Pfälzer Spargeltag 2016. Neustadt an der Weinstraße |
| 02/02/2016 | 23. Freckenhorster Spargeltage. Freckenhorst |
| 02/17/2016 | Seminar zum Spargelanbau. Hannover |